Summary of results from heavy-ion collisions with emphasis on the recent pA data

Constantin Loizides
(LBNL)

17 September 2015

35th International Symposium on Physics in Collision (PIC 2015)

Ultra-relativistic heavy-ion collisions

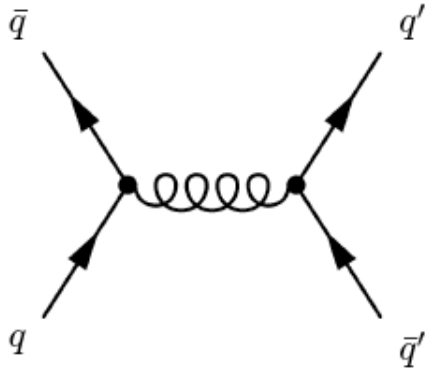

>10 GeV/c

Momentum transfer

0.2 GeV/c

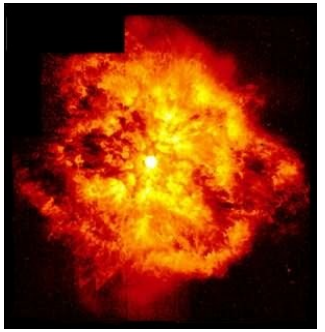

Nebula M1-67
(see hubblesite.org)

Study bulk QCD matter at high T

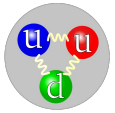

~1fm

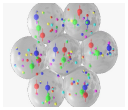

~10fm

Transverse size of collision region

Energy density vs temperature

Fodor et al., JHEP 11 (2010) 077

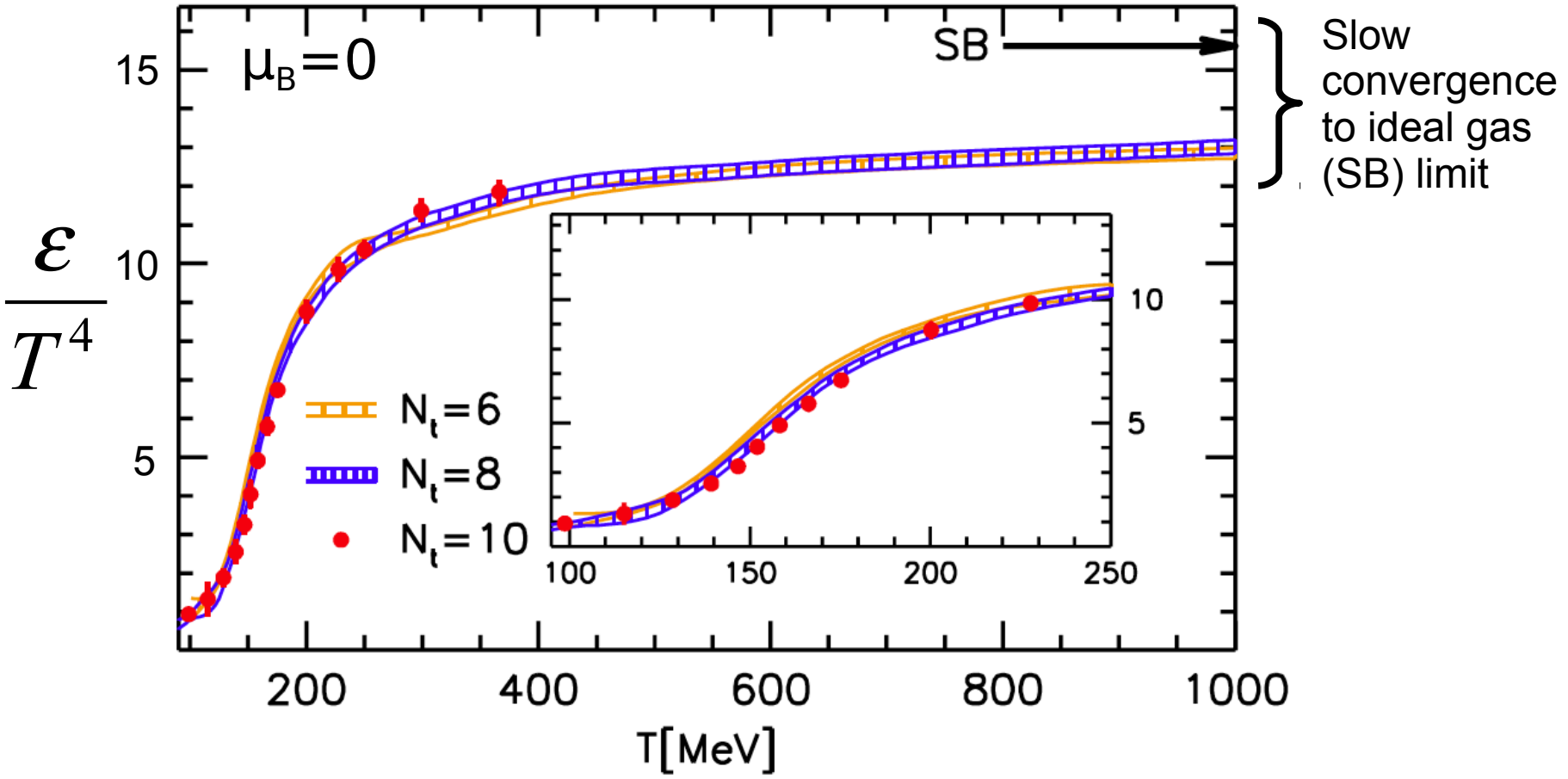

Slow convergence to ideal gas (SB) limit

Rapid cross-over transition between 140 and 200 MeV, and energy densities between 0.2 and 1.8 GeV/fm^3

(often characterized by $T_c \approx 170$ MeV and $\varepsilon_c \approx 1$ GeV/fm^3)

Control parameters: Collision energy

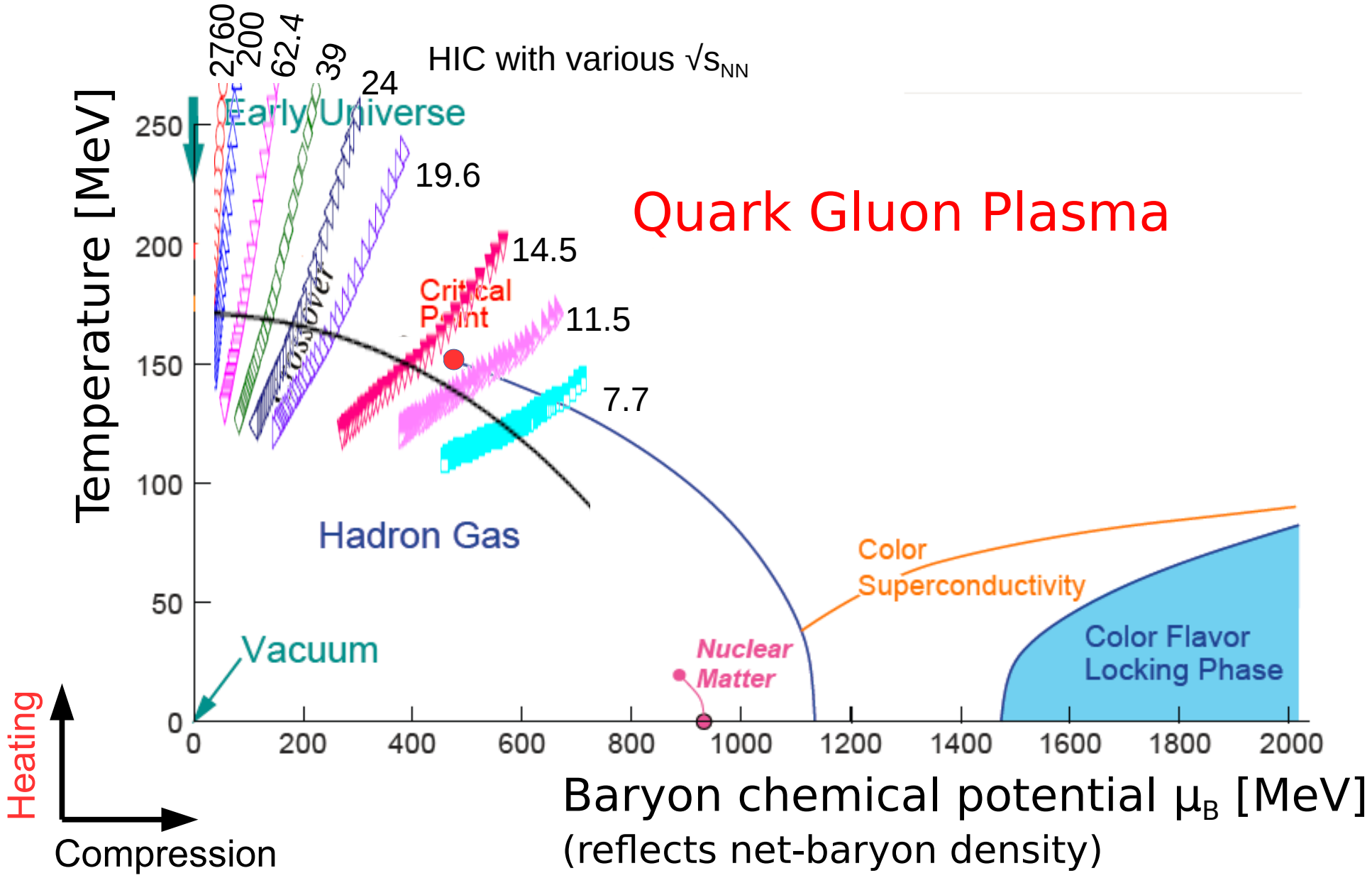

Control parameters: Collision centrality

Nuclear cross-section classes
(by slicing in bins of multiplicity)

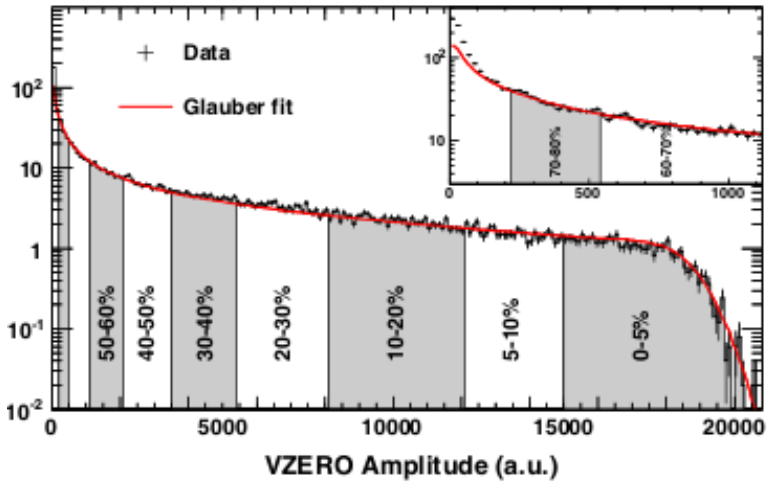

Glauber model

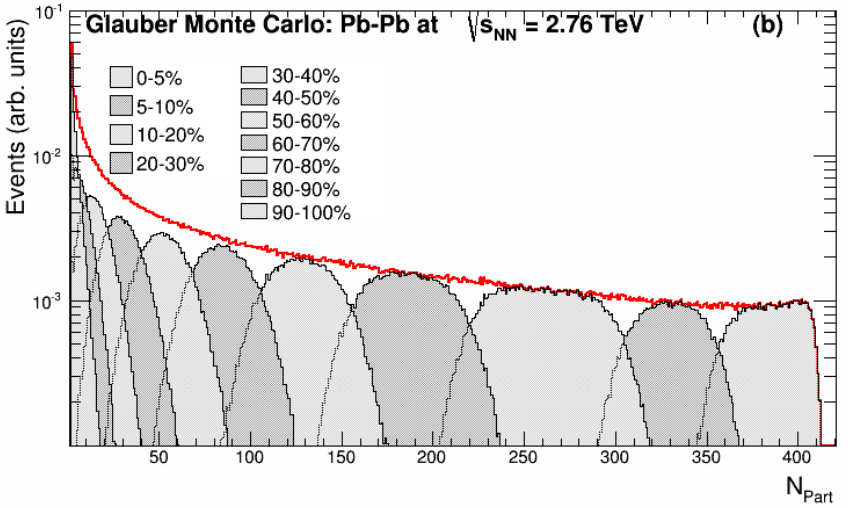

Via model

Cross-section percentile (in %) ⟷ Number of participants

(average monotonously rel. to impact parameter)

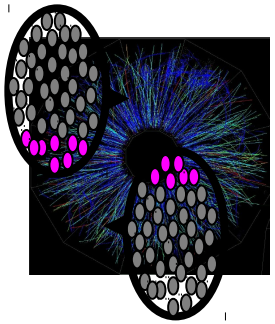

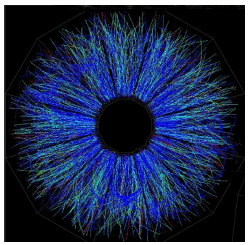

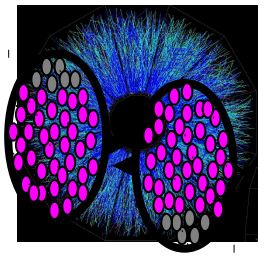

Collision energy

Collision centrality

arXiv:1301.4361

Control parameters: Collision systems

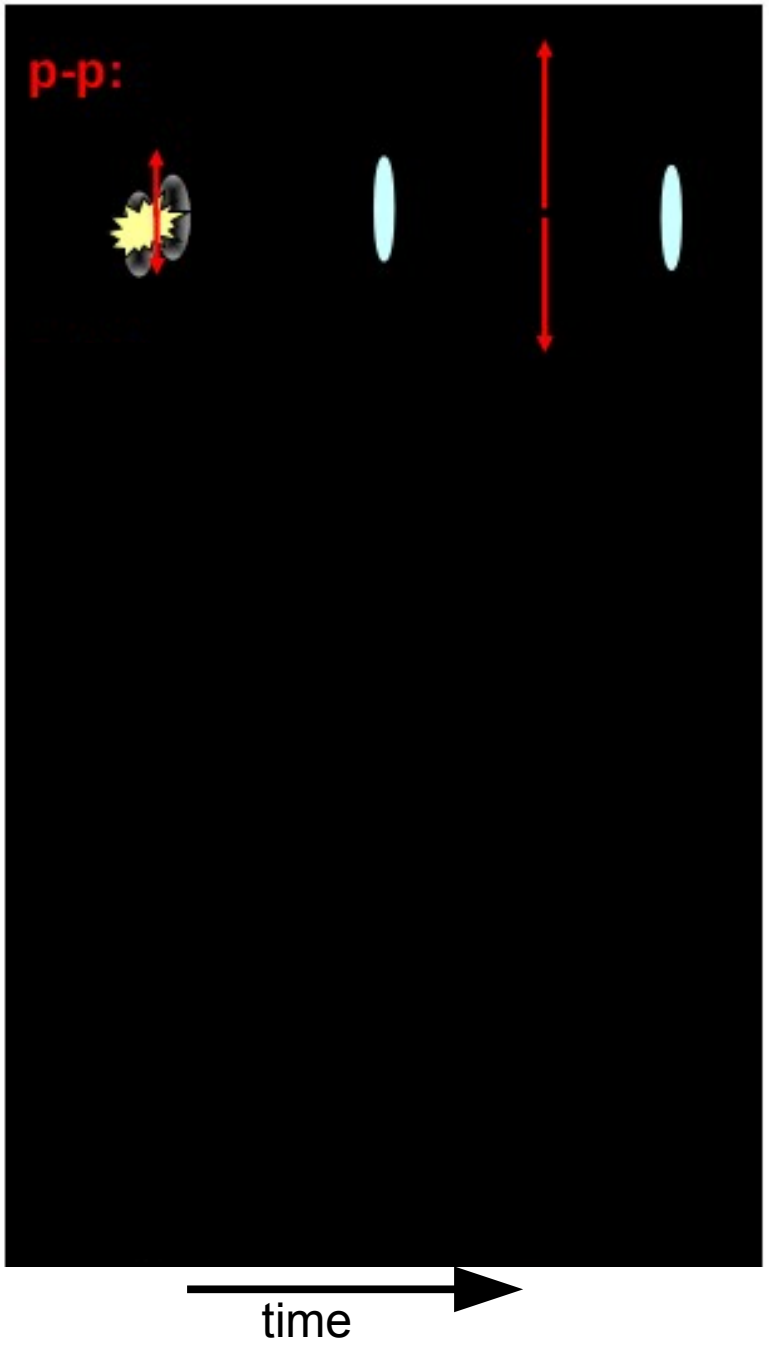

p-p = "QCD vacuum" (reference)

SM of heavy-ion reaction dynamics

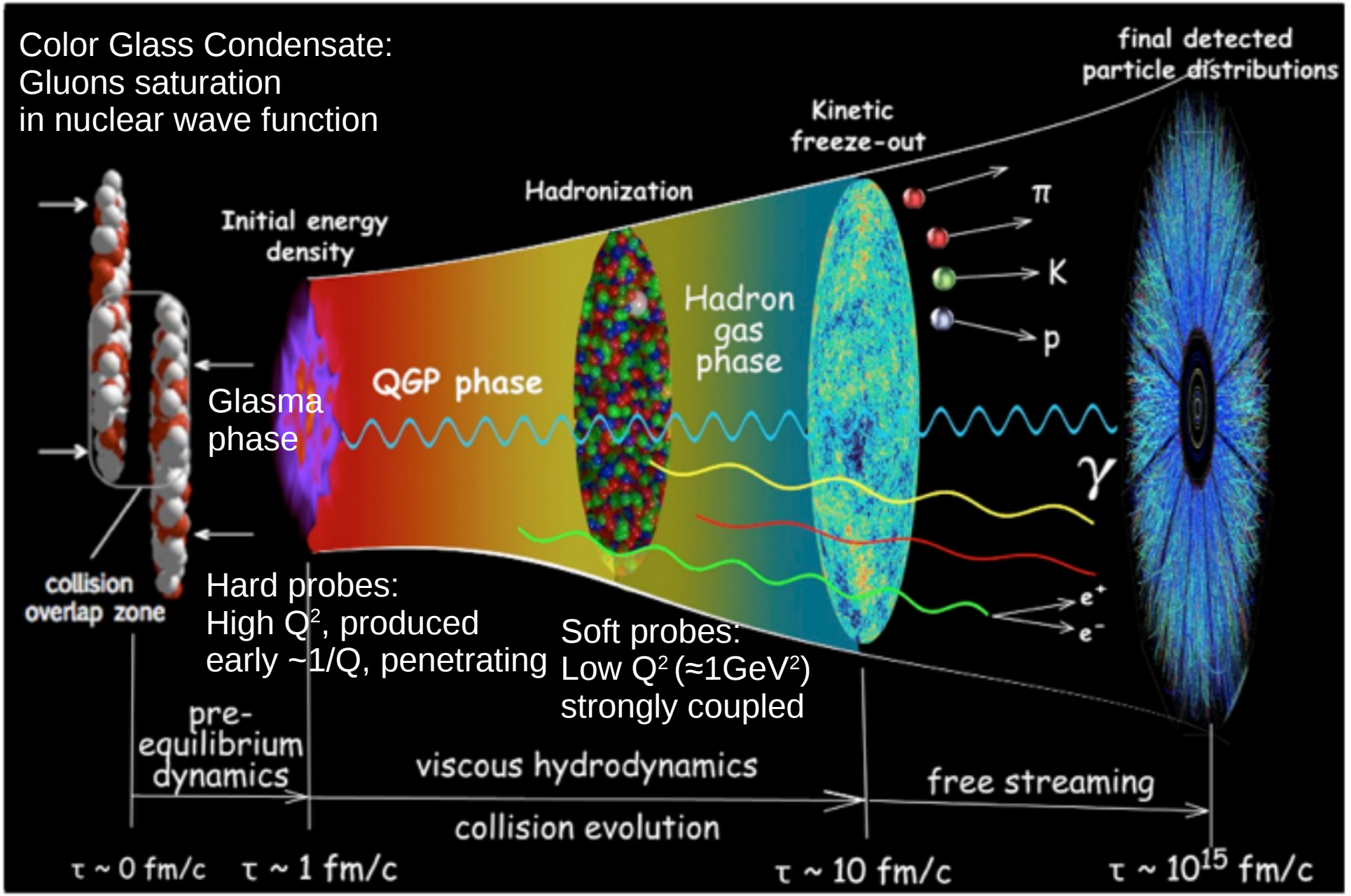

(adapted from C.Shen)

Soft probes

Energy dependence of transverse energy

PRL 109 (2012) 152303

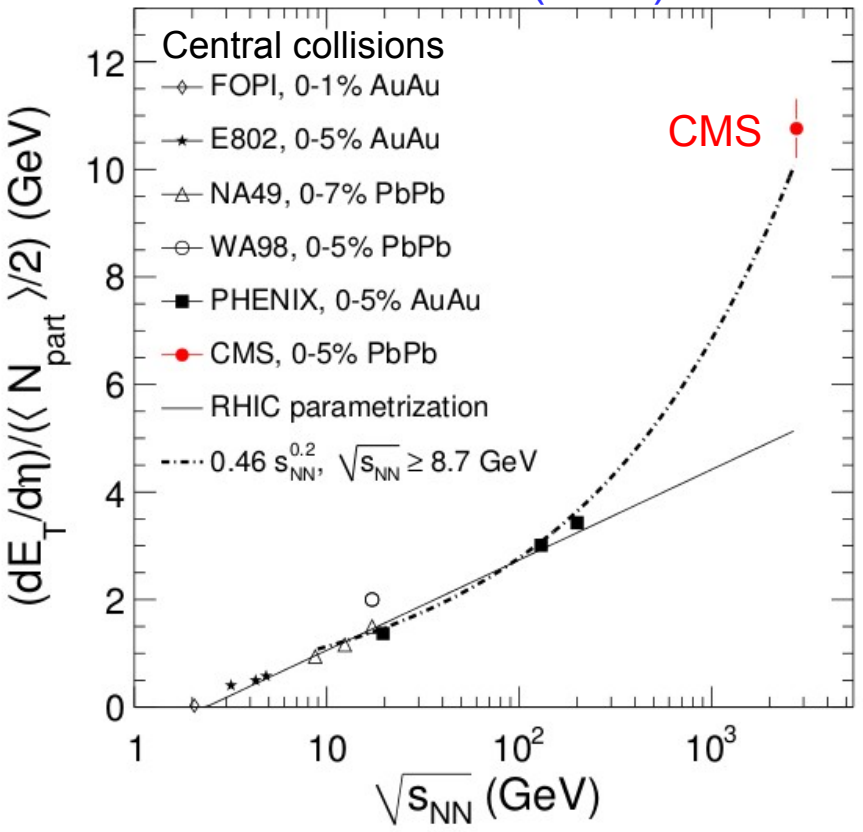

Bjorken estimate:

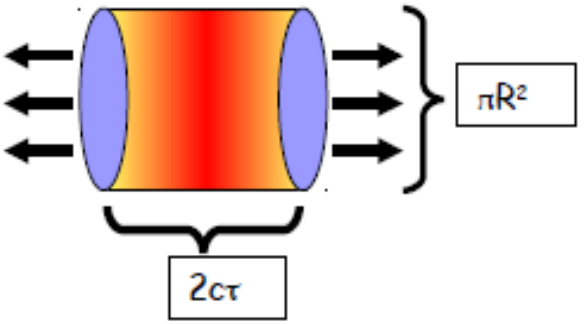

$$\langle \varepsilon \rangle (\tau) = \frac{1}{\tau \, \pi R^2} \frac{\mathrm{d}E_\mathrm{T}}{\mathrm{d}y}$$

Bjorken, PRD 27 (1983) 140

- System undergoes rapid evolution
  - Using 1 fm/c as an upper limit for the time needed to “thermalization”
  - Leads to densities above the transition region (also for AGS)

$$\varepsilon_\mathrm{BJ} = 1.5\,\mathrm{GeV/fm^3} \text{ for } \sqrt{s_\mathrm{NN}} = 5\,\mathrm{GeV}$$
$$\varepsilon_\mathrm{BJ} = 2.9\,\mathrm{GeV/fm^3} \text{ for } \sqrt{s_\mathrm{NN}} = 17\,\mathrm{GeV}$$
$$\varepsilon_\mathrm{BJ} = 5.4\,\mathrm{GeV/fm^3} \text{ for } \sqrt{s_\mathrm{NN}} = 200\,\mathrm{GeV}$$
$$\varepsilon_\mathrm{BJ} = 15\,\mathrm{GeV/fm^3} \text{ for } \sqrt{s_\mathrm{NN}} = 2.76\,\mathrm{TeV}$$

10 Centrality dependence of dN/dη

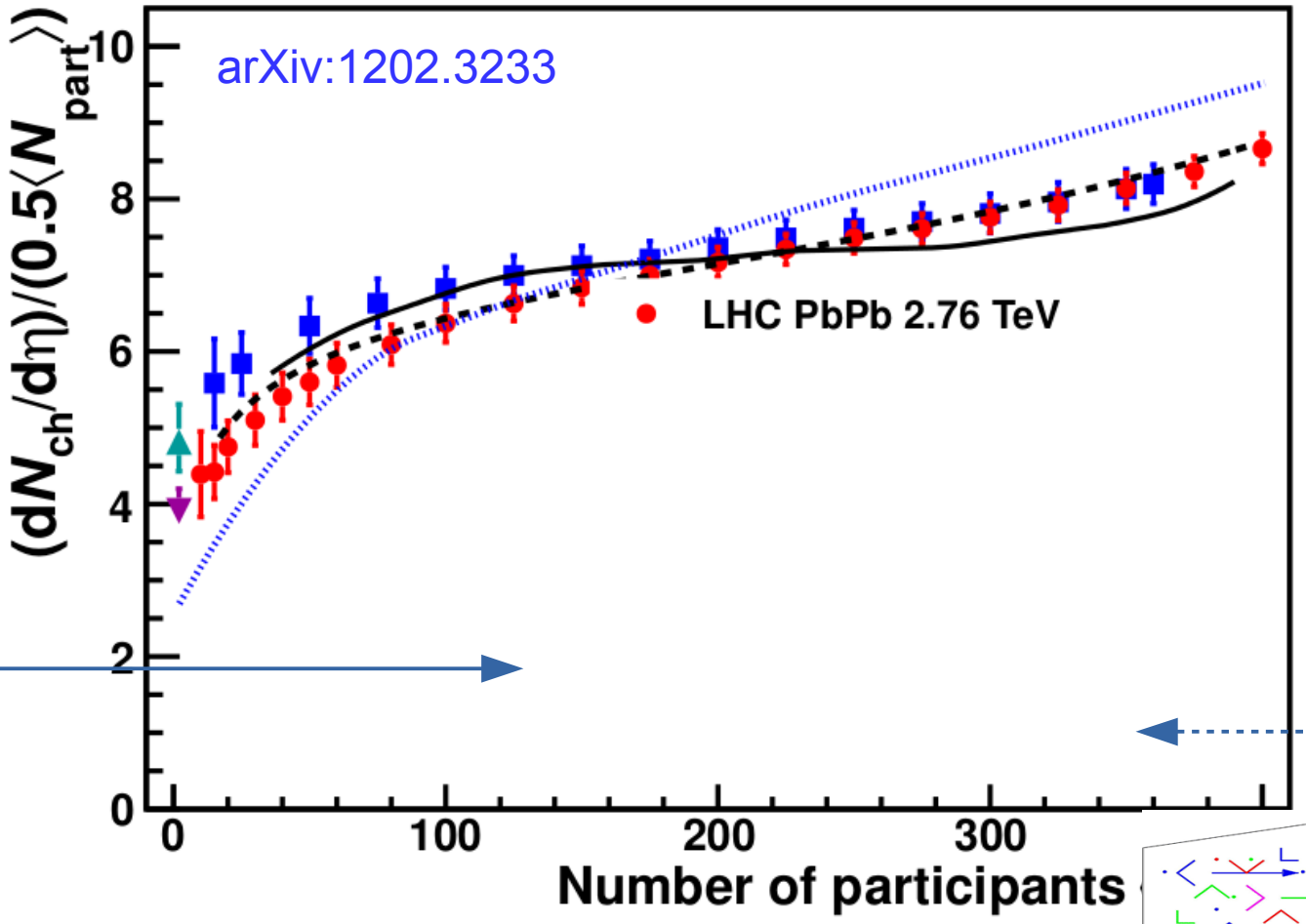

Glauber IC

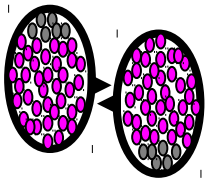

CGC IC

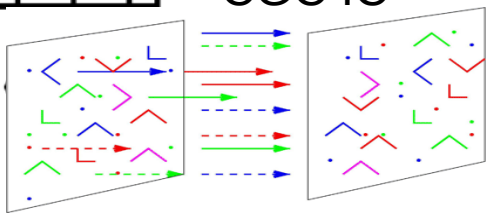

Glauber IC
Two-component model

$$\frac{dN}{d\eta} = \frac{dN}{d\eta^{pp}}\left((1-x)N_{coll} + x\frac{N_{part}}{2}\right)$$

PRC 70 021902 (2004)

Factorization in energy and centrality.
Shape is strikingly similar to RHIC

Two-component models need to incorporate strong nuclear modification. Saturation mod. naturally imply $\frac{dN}{d\eta} \propto N_{part}^{\alpha}\sqrt{s}^{\lambda}$

CGC IC
Color glass condensate

$$\frac{dN}{d\eta} \propto N_{part}^{\alpha}\sqrt{s}^{\lambda}$$

PRL 94 022002 (2005)

11 Initial temperature at RHIC

Direct photons: No charge, no color, ie. they do not interact further
Use (at low p_T) to extract temperature of the system.

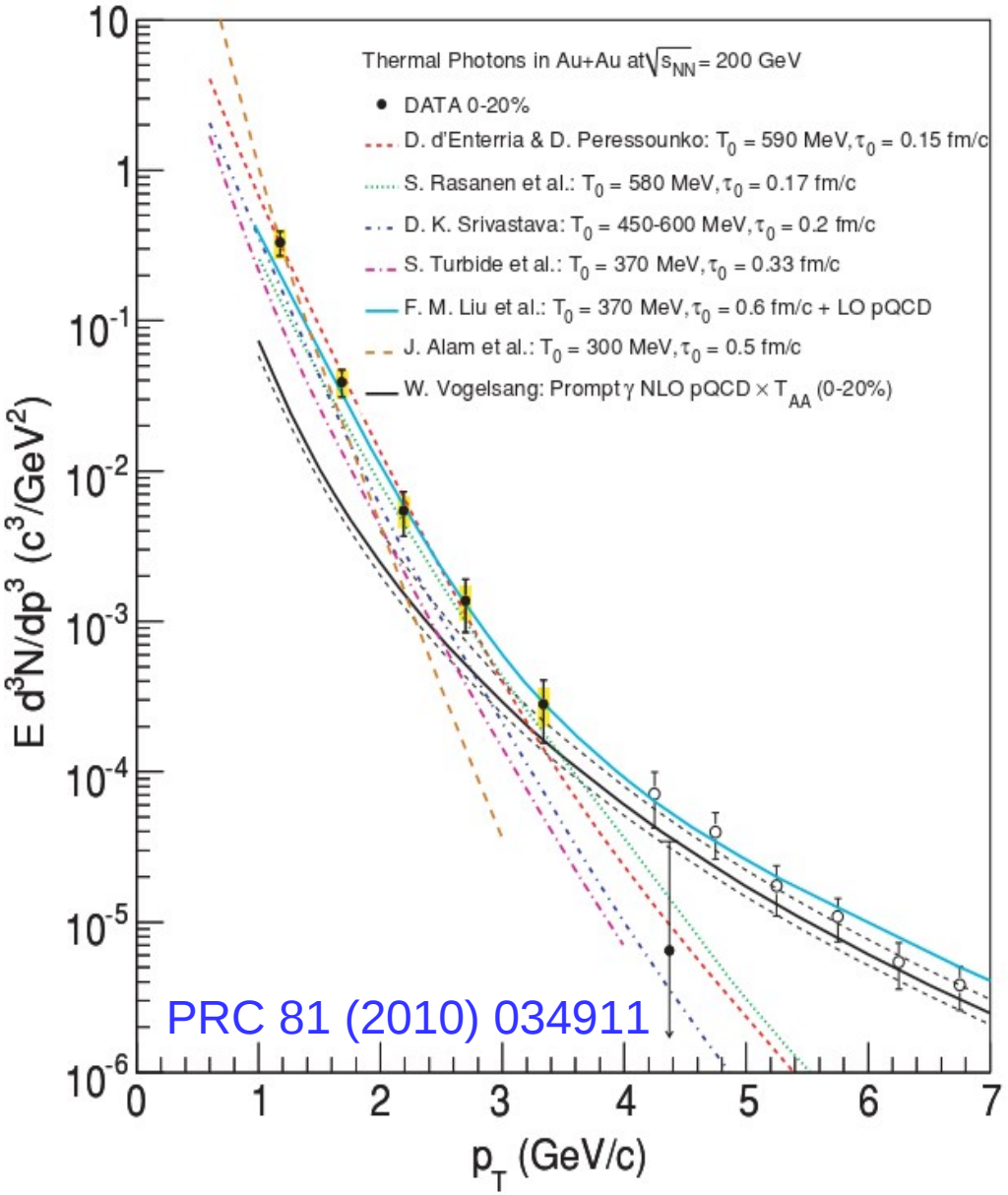

- Different measurements performed using real and virtual photons
  - E.g. via double ratio

$$\gamma^{\mathrm{dir}} = (1 - 1/R)\,\gamma^{\mathrm{inc}}$$
$$R = \left(\gamma/\pi^0\right)_{\mathrm{inc}} / \left(\gamma/\pi^0\right)_{\mathrm{mc}}$$

- Exponential (thermal) shape with inverse slope of T~220 MeV in excess region
- No excess seen in d+A (or pp)
- Calculations give
  - T_{init} = 300-600 MeV (>2T_c)

12 Initial temperature at LHC

$$R = \left(\gamma/\pi^0\right)_{\mathrm{inc}} / \left(\gamma/\pi^0\right)_{\mathrm{mc}}$$

$$\gamma^{\mathrm{dir}} = (1 - 1/R)\,\gamma^{\mathrm{inc}}$$

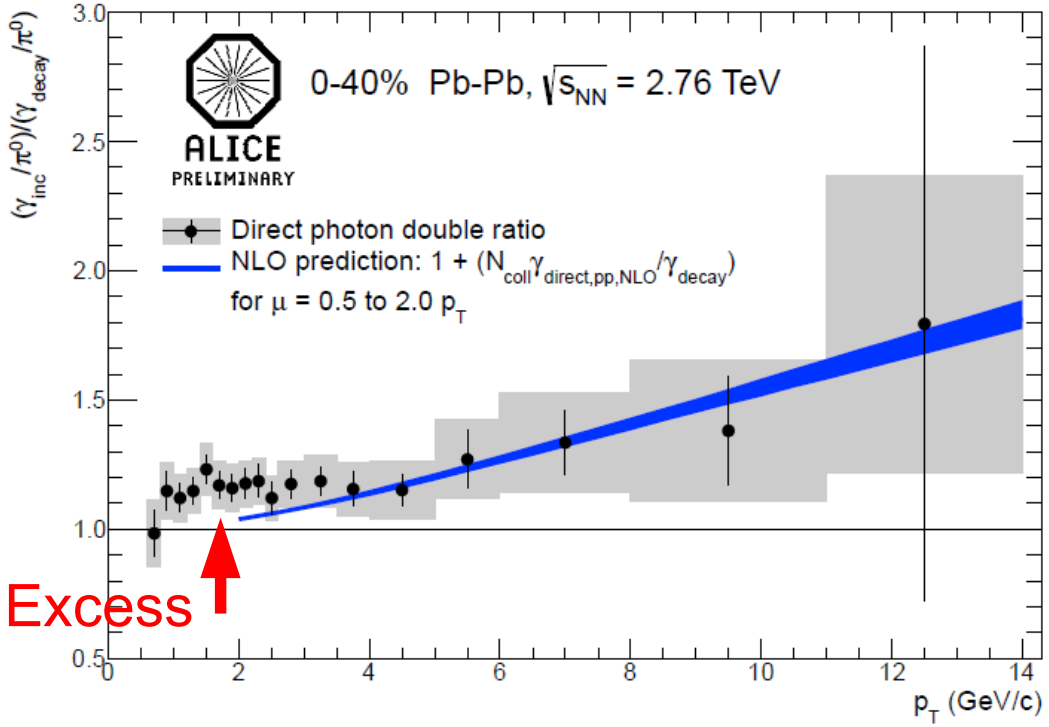

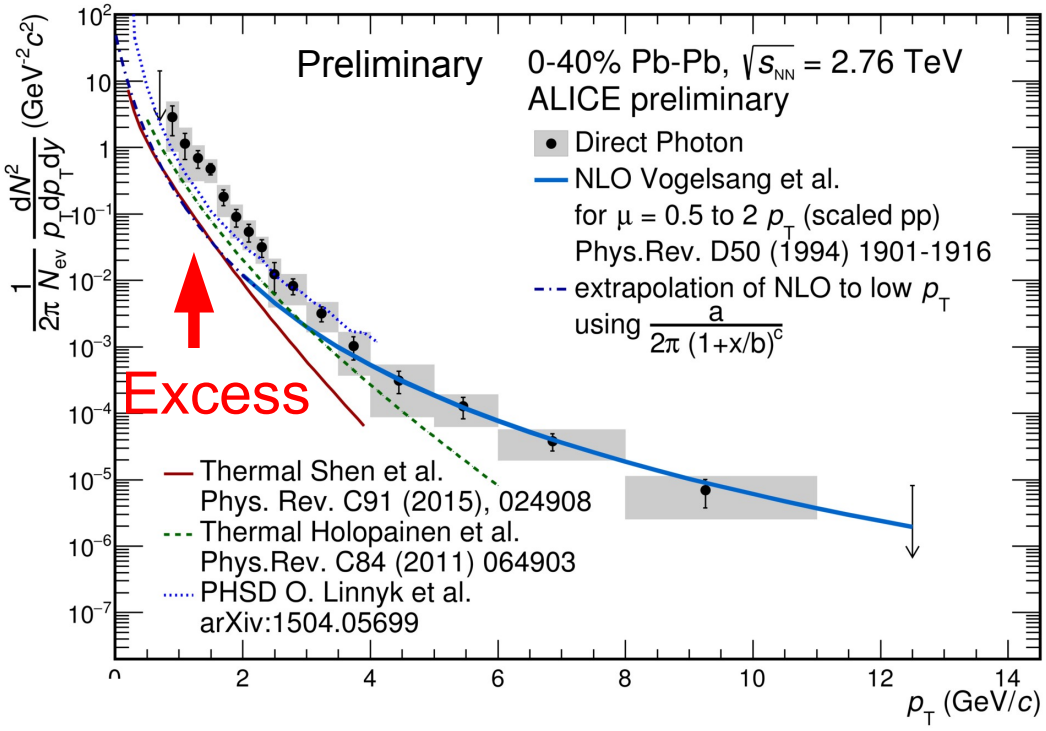

- Measure R = $(\gamma/\pi^0)_{inc}$ / $(\gamma/\pi^0)_{mc}$
- Uncertainties (exactly or partially) cancel in the ratio
  - Normalization
  - Photon reconstruction efficiency

- Inverse slope: T=304±51 MeV
  - About 35% larger than at RHIC
  - Model calculations with T_{init}>400 MeV, but undershoot the data

(final results expected on arXiv by end of Sep)

13 Initial and final anisotropy (~2000)

Time

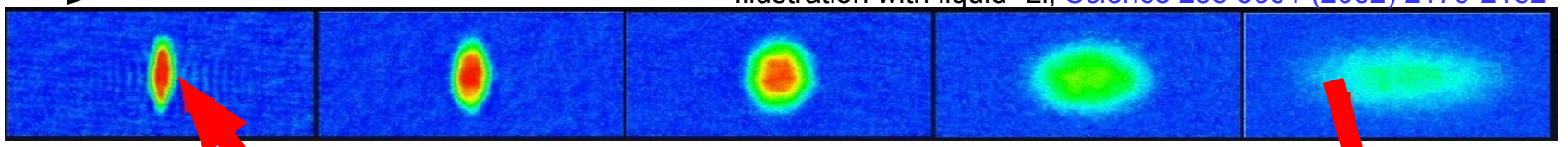

Illustration with liquid ^{6}Li, Science 298 5601 (2002) 2179-2182

(process is self quenching)

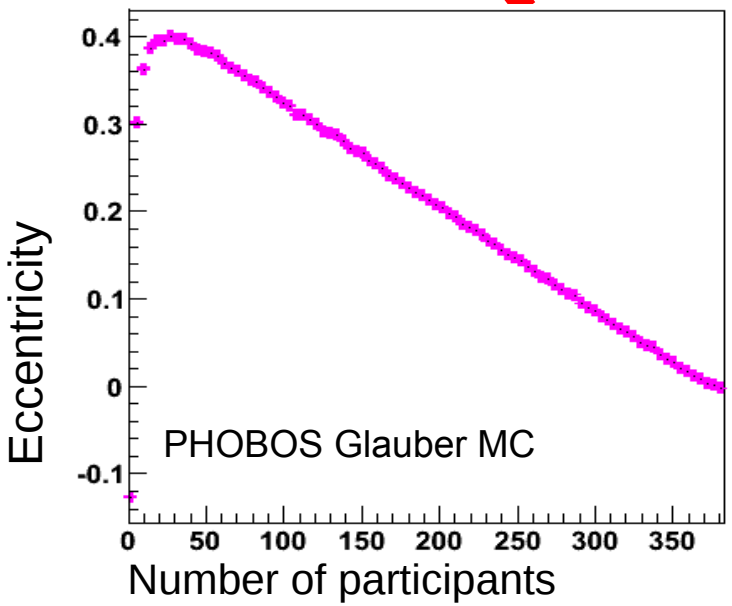

STAR, PRL 86 (2001) 402

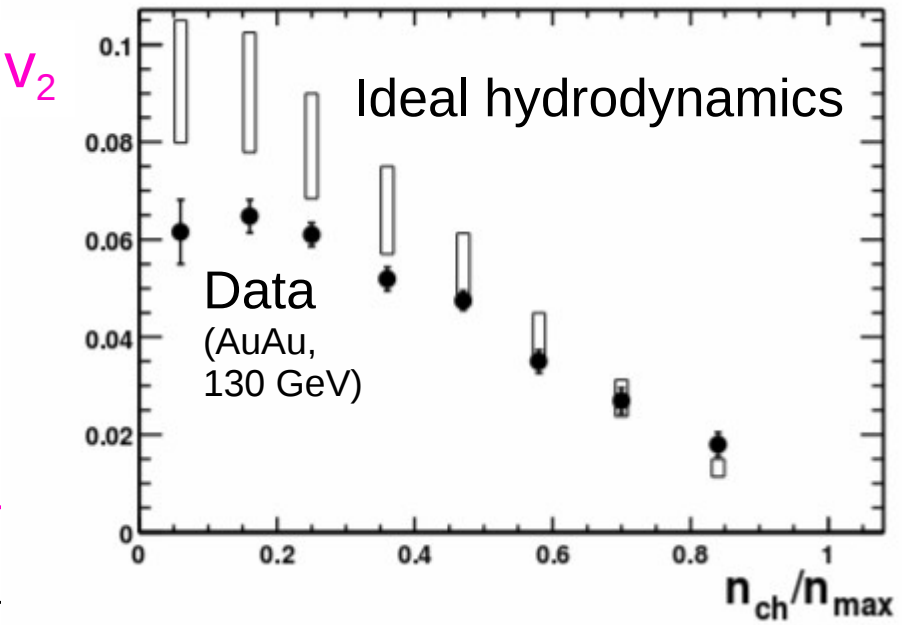

$$v_2 \propto \varepsilon \frac{dN/d}{S}$$ (expect)

Initial spatial anisotropy: Eccentricity

$$\epsilon_{\text{std}} = \frac{\sigma_y^2 - \sigma_x^2}{\sigma_y^2 + \sigma_x^2}$$

If interactions present early (induces long-range Δη correlations)

Momentum space anisotropy: Elliptic flow

$$v_2 = \langle \cos(2\varphi - 2\Psi_R) \rangle$$

14 Initial and final anisotropy (~2010)

Initial spatial anisotropy not smooth, fluctuates event-by-event and contains other higher harmonics / symmetry planes

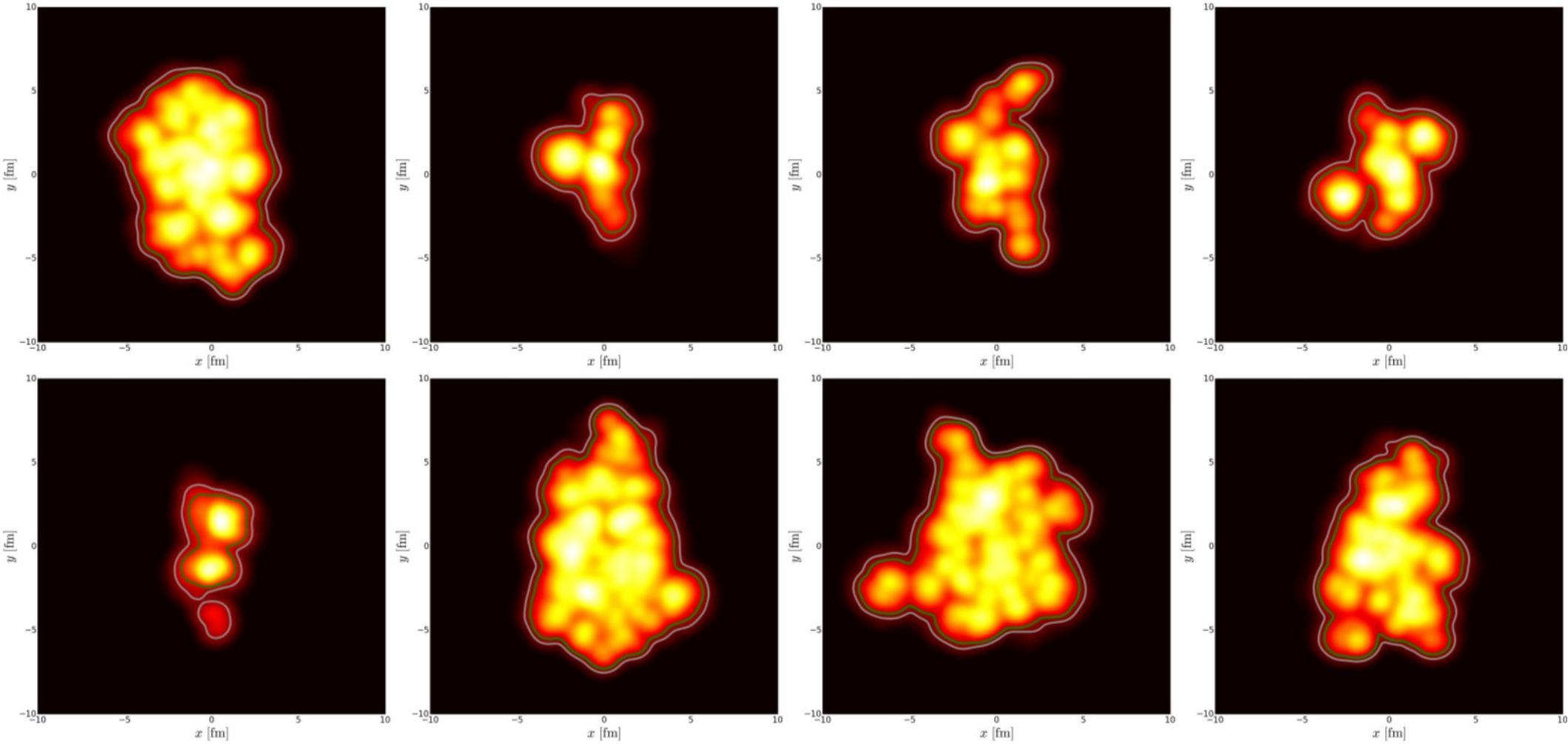

Temperature profiles in transverse plane from hydrodynamical calculation (H. Niemi)

Two-particle correlations

$$\Delta\varphi = \varphi_1 - \varphi_2$$
$$\Delta\eta = \eta_1 - \eta_2$$

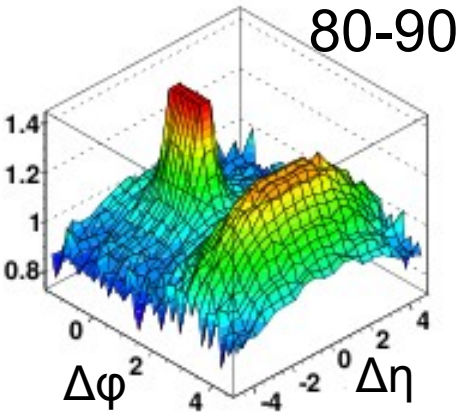

ATLAS
$2<p_T^{trig}, p_T^{assoc}<3$ GeV/c

PRC 86 (2012) 014907

Analysis of do

$V_{n\Delta}$

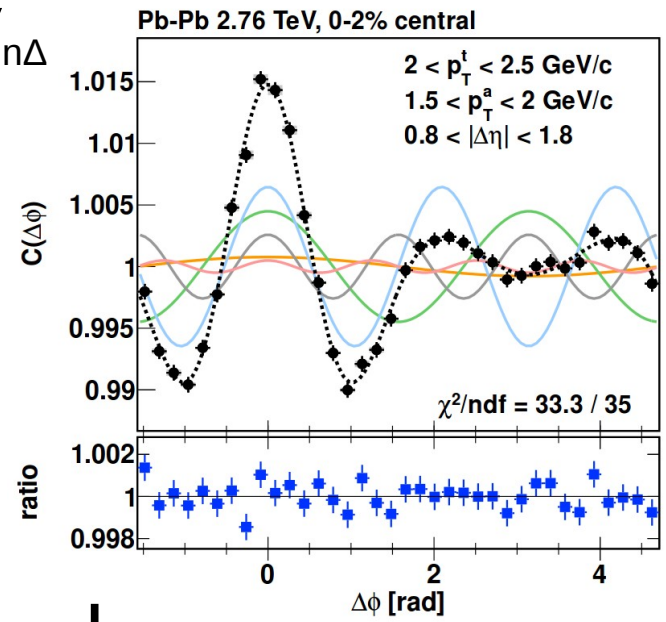

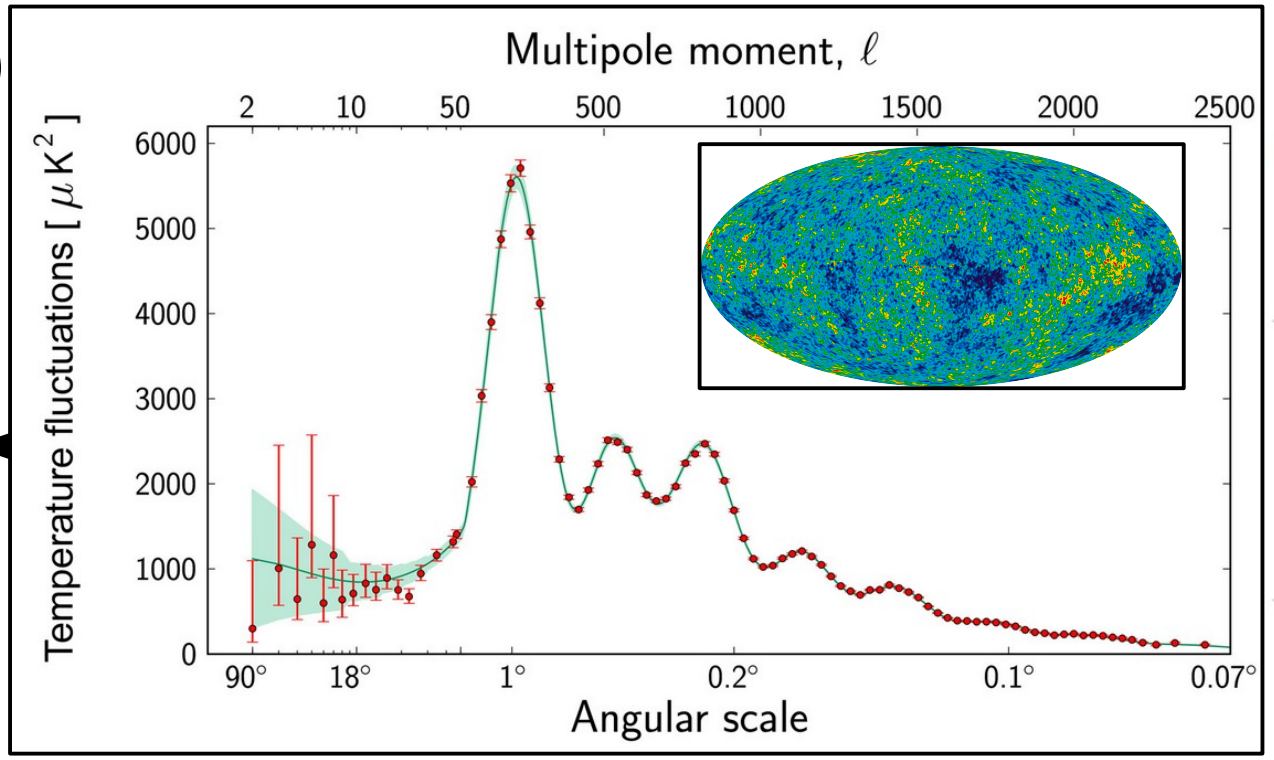

Extract $v_n(p_T)$ using factorization ansatz(*) from global fit

$$V_{n\Delta}(p_{\mathrm{T}}^t, p_{\mathrm{T}}^a) = v_n(p_{\mathrm{T}}^t) v_n^a(p_{\mathrm{T}})$$

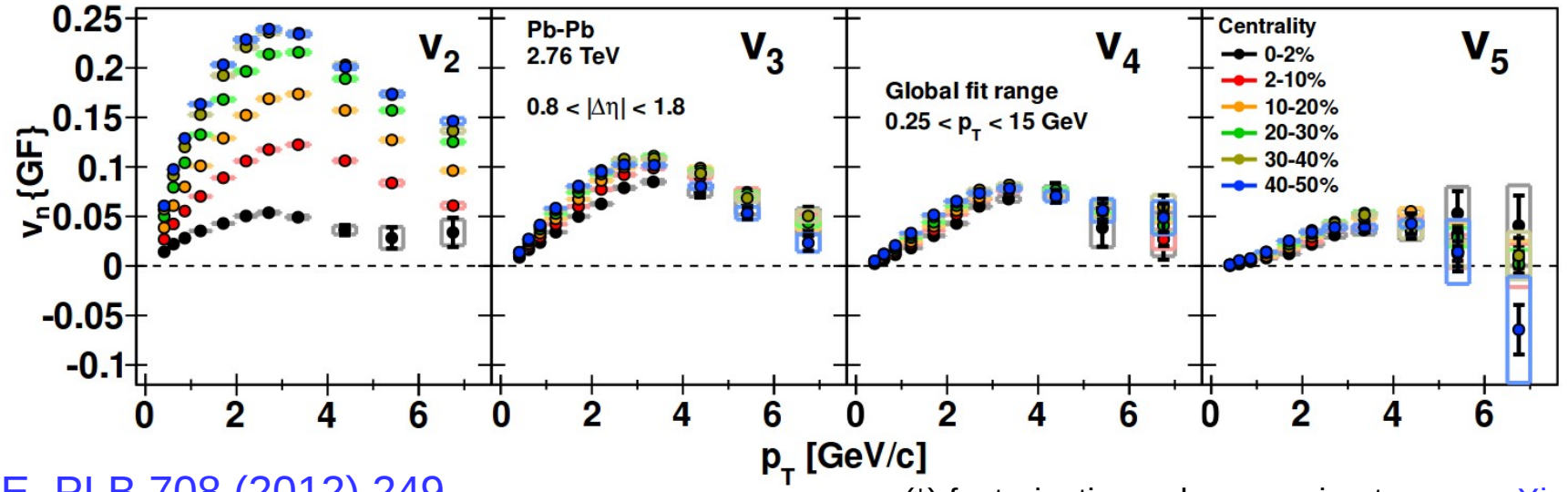

ALICE, PLB 708 (2012) 249

(*) factorization only approximate, see arXiv:1503.01692

Hydrodynamical model calculations

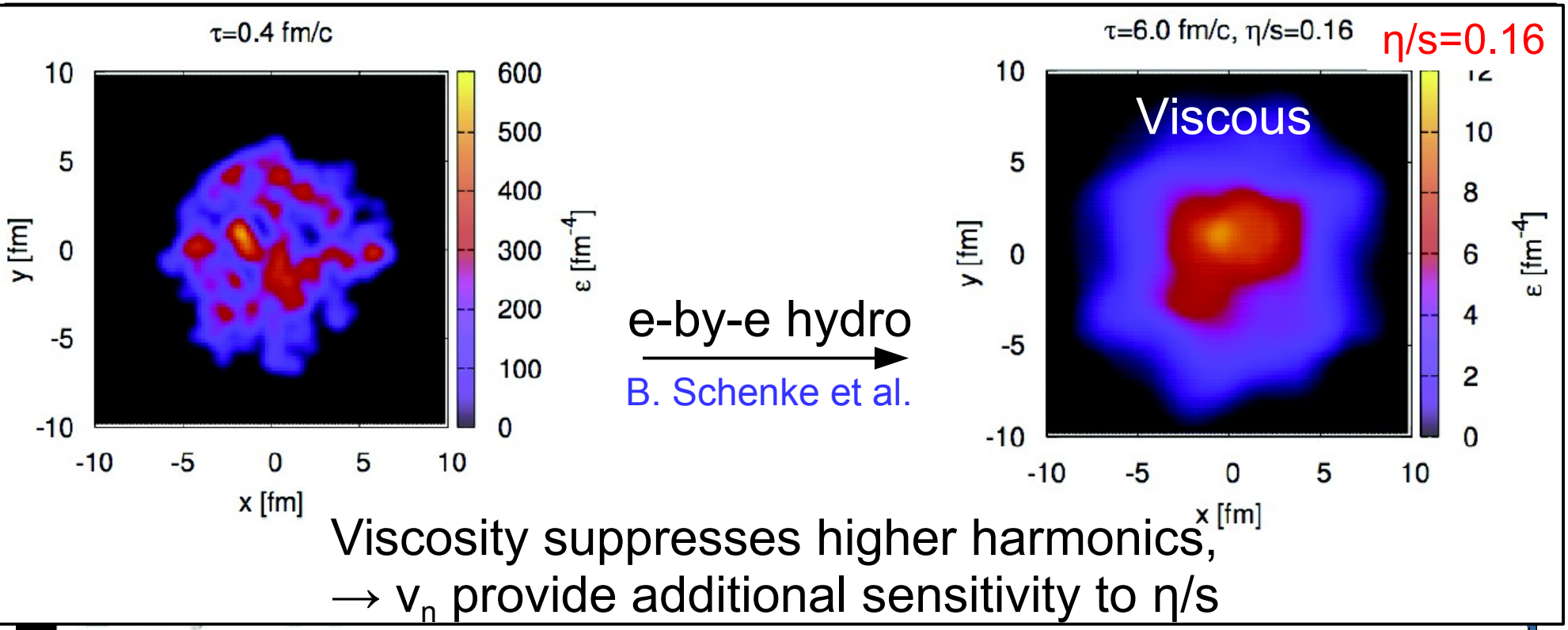

Viscosity suppresses higher harmonics,
→ v_n provide additional sensitivity to η/s

+ initial conditions

+ freeze-out conditions

+ Equation of State

Today even second order calculations (full Israel-Stewart) calculations are done.

Extraction of η/s from model calculations

RHIC

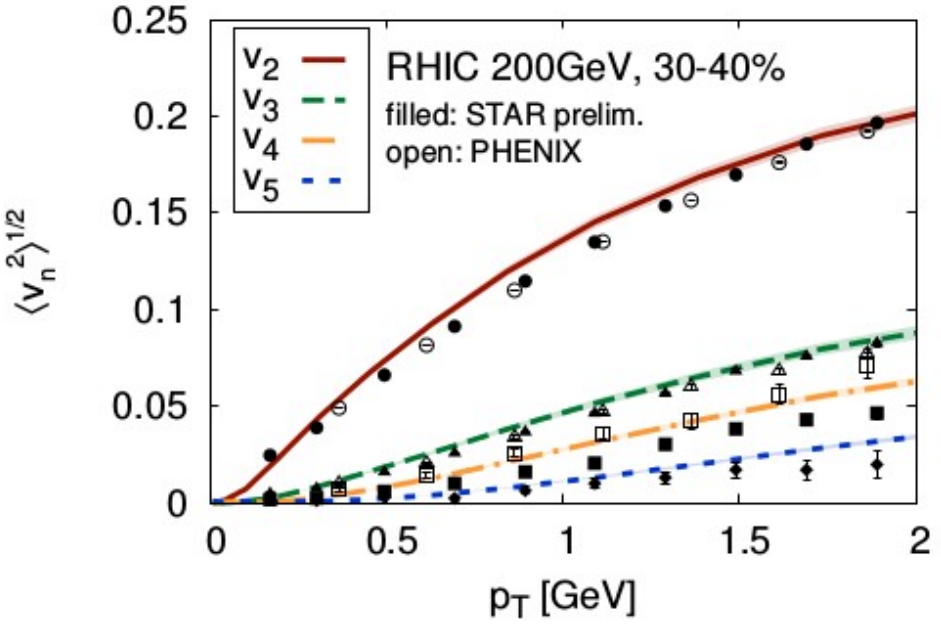

LHC

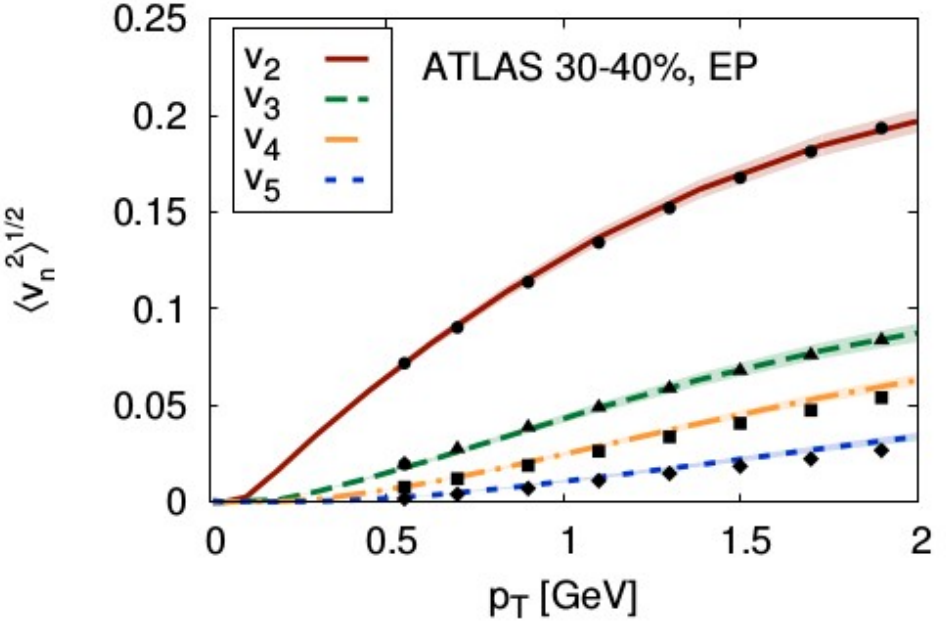

$\eta/s \approx 0.12$ at $\sqrt{s} = 0.2$ TeV

$\eta/s \approx 0.2$ at $\sqrt{s} = 2.76$ TeV

Model (IP-Glasma+viscous hydro) extracts larger η/s for LHC
(uncertainty on η/s about O(100%) from initial state, but largely correlated)

KSS bound

$\eta/s > 1/4\pi \sim 0.08$

Schenke et al., PRL 110 (2013) 012302

Event-by-event fluctuations

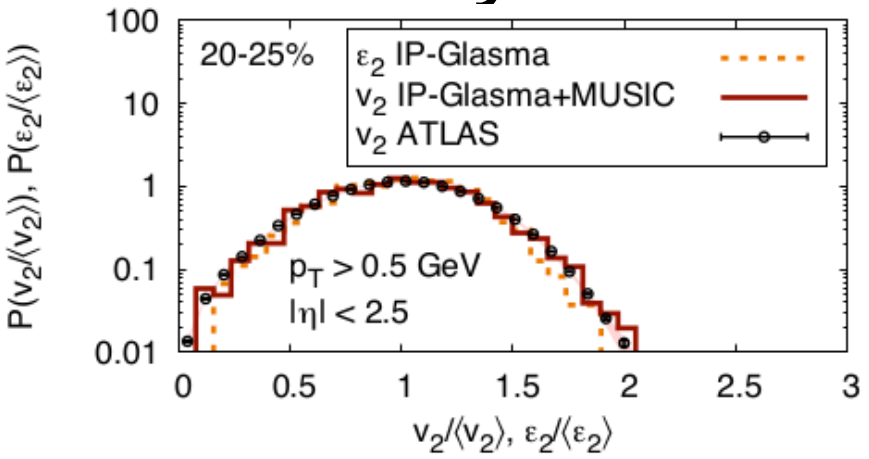

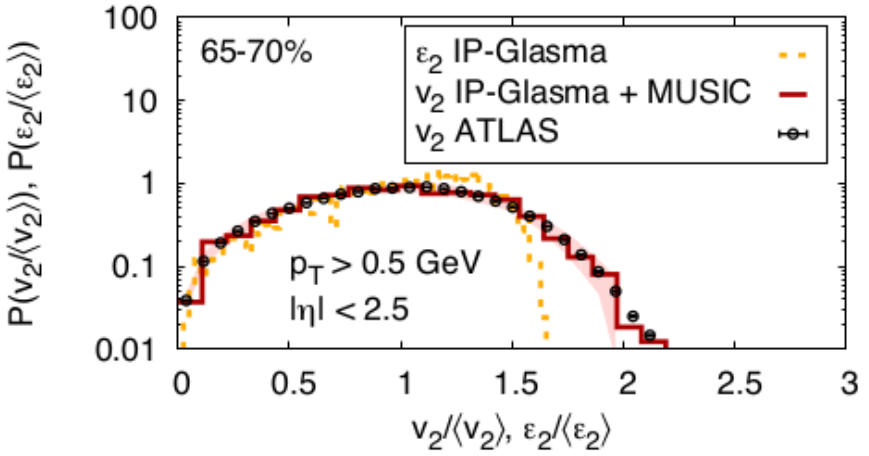

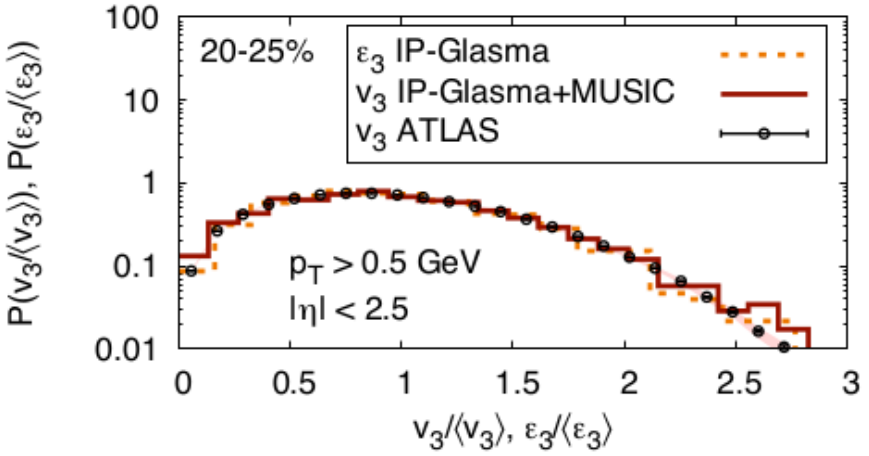

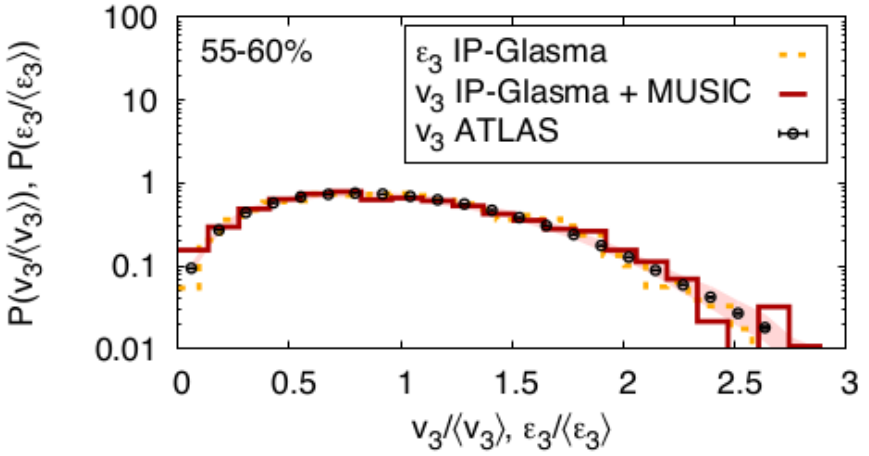

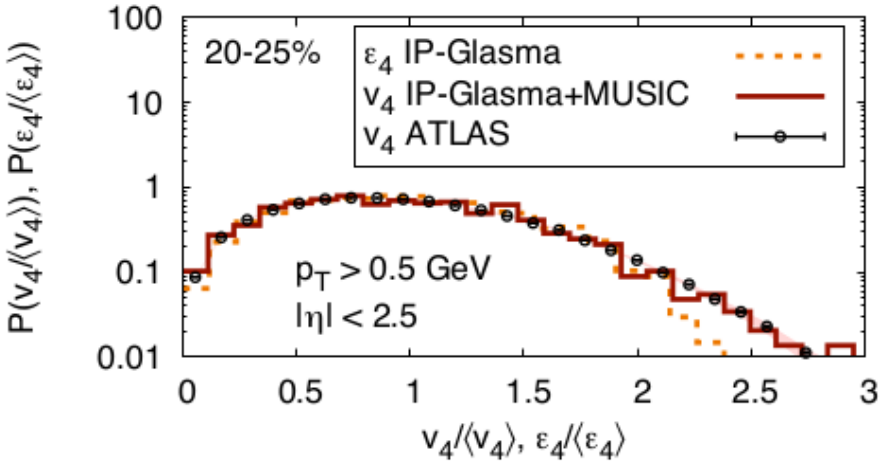

Hydrodynamical calculations can describe event-by-event fluctuations

ATLAS, JHEP 11 (2013) 183
Schenke et al., PRL 110 (2013) 012302

Identified-particle elliptic flow

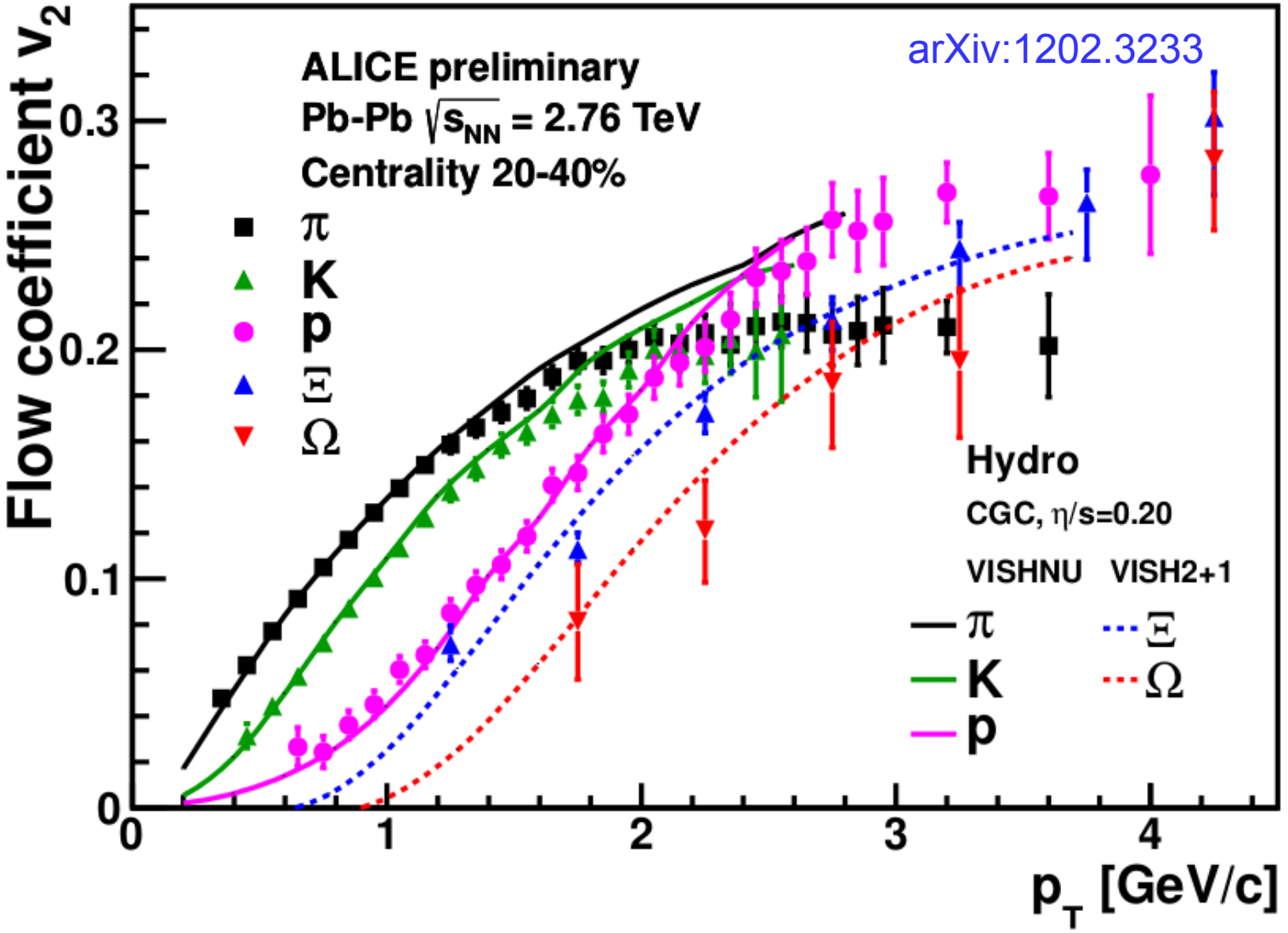

Characteristic particle-mass dependence can be described by hydrodynamical model calculation (taking into account hadronic phase)

Identified-particle triangular flow

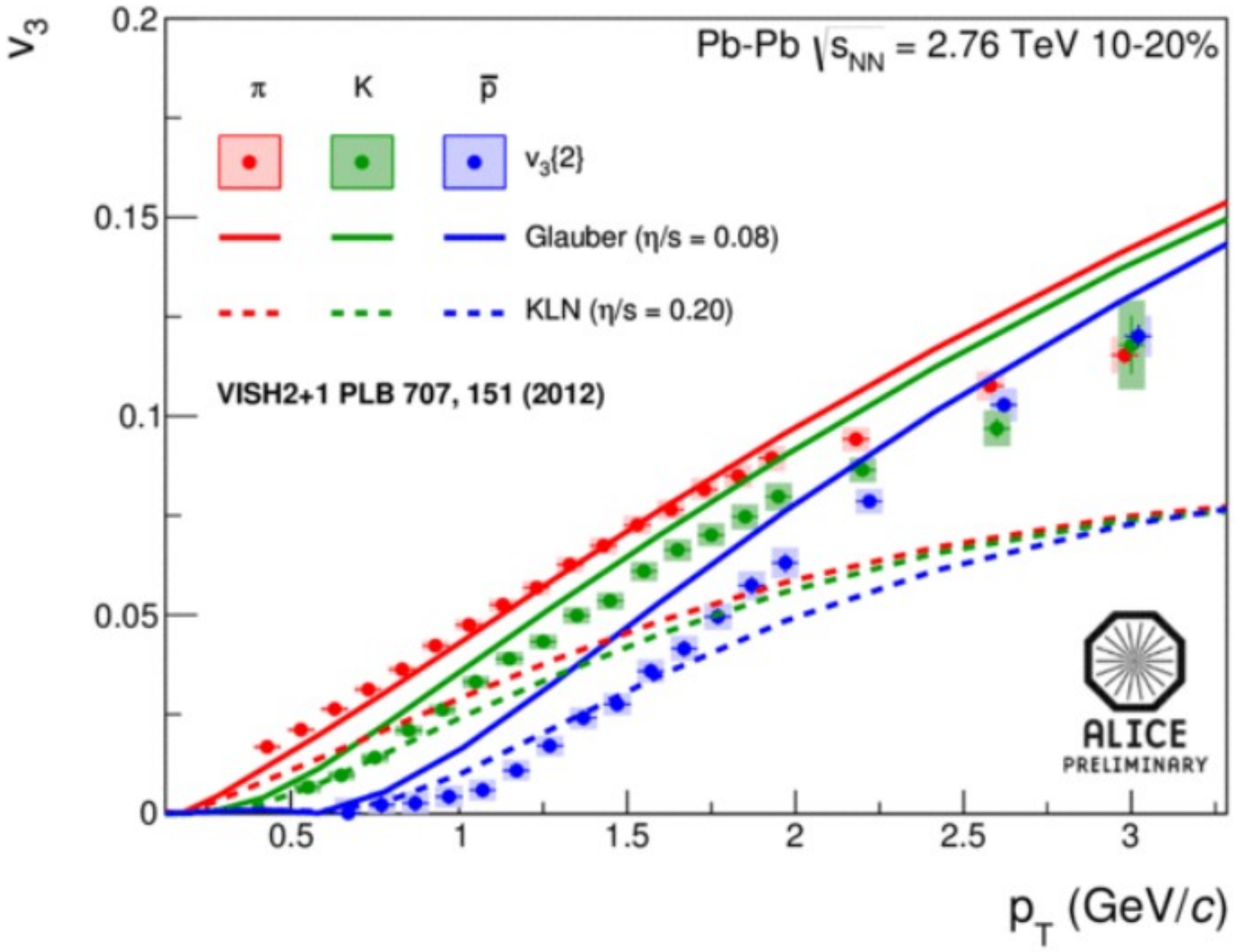

Similar characteristics as elliptic flow and provides additional constraints on η/s

Hard probes

Nuclear modification factor at RHIC

$$R_{\mathrm{AA}} = \frac{\mathrm{d}N_{AA}/\mathrm{d}p_{\mathrm{T}}}{N_{\mathrm{coll}}\,\mathrm{d}N_{pp}/\mathrm{d}p_{\mathrm{T}}}$$

PRC75 (2007) 024909

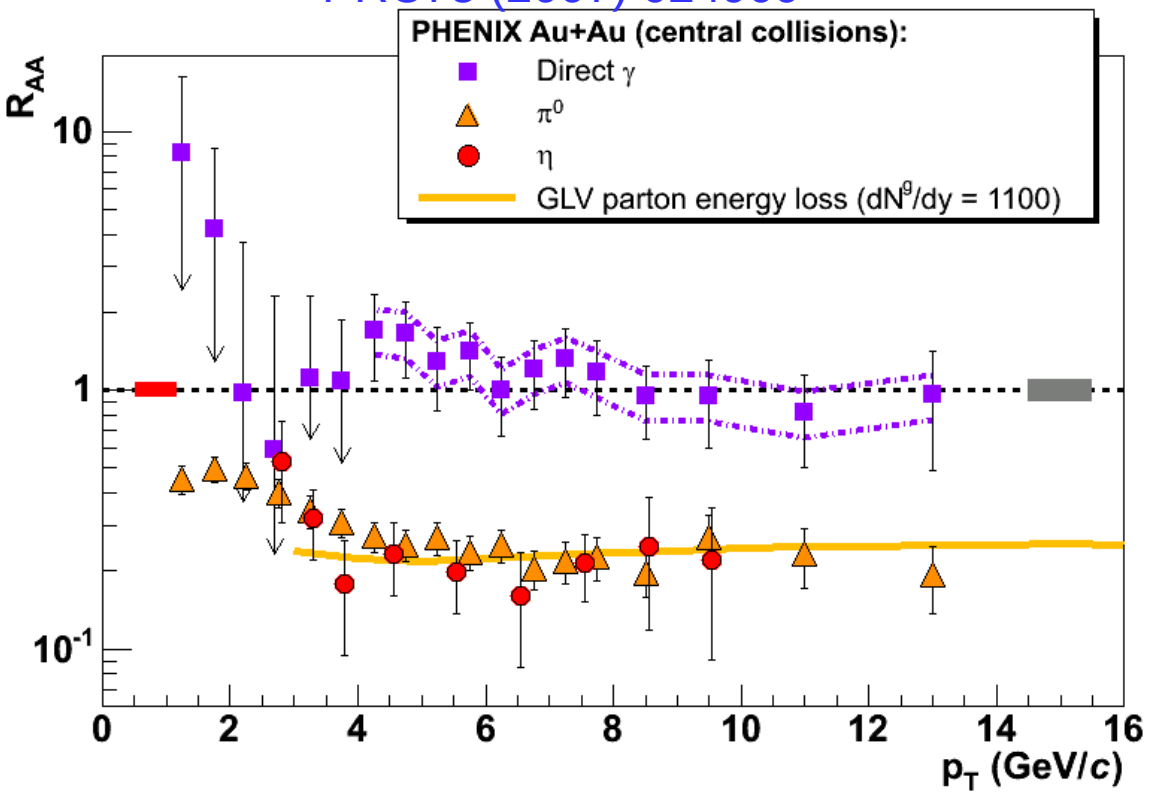

PRL 91 (2003) vol 7

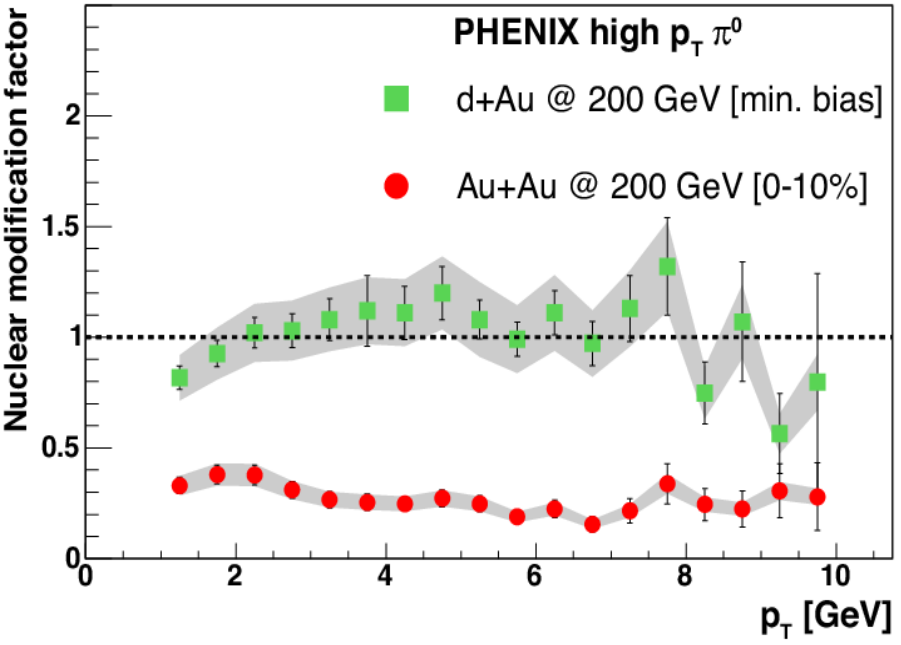

Strong high p_T suppression, consistent with parton energy loss in QGP

Absence of suppression in d+Au control at midrapidty!

Nuclear modification factor at LHC

$$R_{\mathrm{AA}} = \frac{\mathrm{d}N_{AA}/\mathrm{d}p_{\mathrm{T}}}{N_{\mathrm{coll}}\,\mathrm{d}N_{pp}/\mathrm{d}p_{\mathrm{T}}}$$

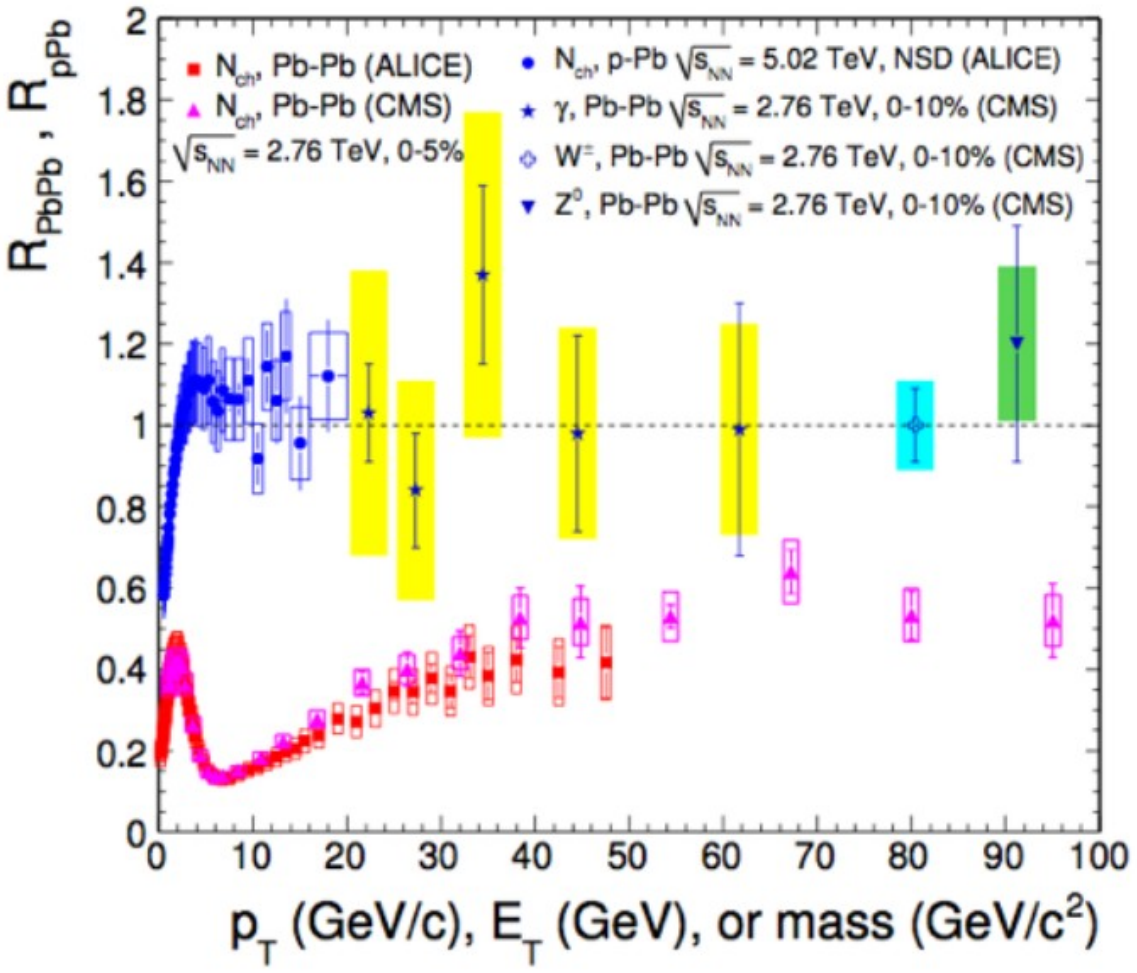

Similar conclusions from measurements at LHC

Parton energy loss aka jet quenching

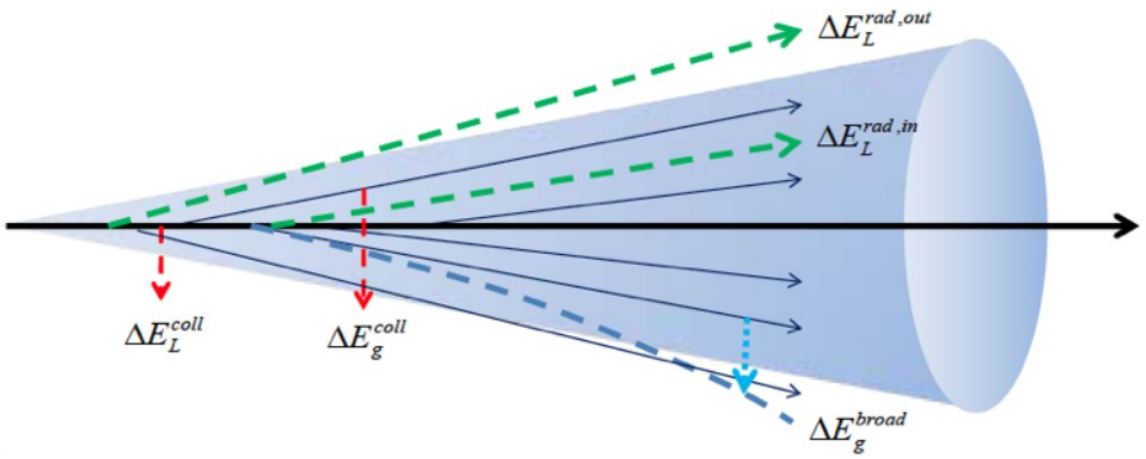

$$\left.\frac{\mathrm{d}E}{\mathrm{d}x}\right|_{\mathrm{coll}} = -C_2\hat{e}$$

$$\left.\frac{\mathrm{d}E}{\mathrm{d}x}\right|_{\mathrm{rad}} = -C_2\hat{q}L$$

Resolution scale of medium

$$\Lambda_{\mathrm{med}} = 1/\sqrt{\hat{q}L}$$

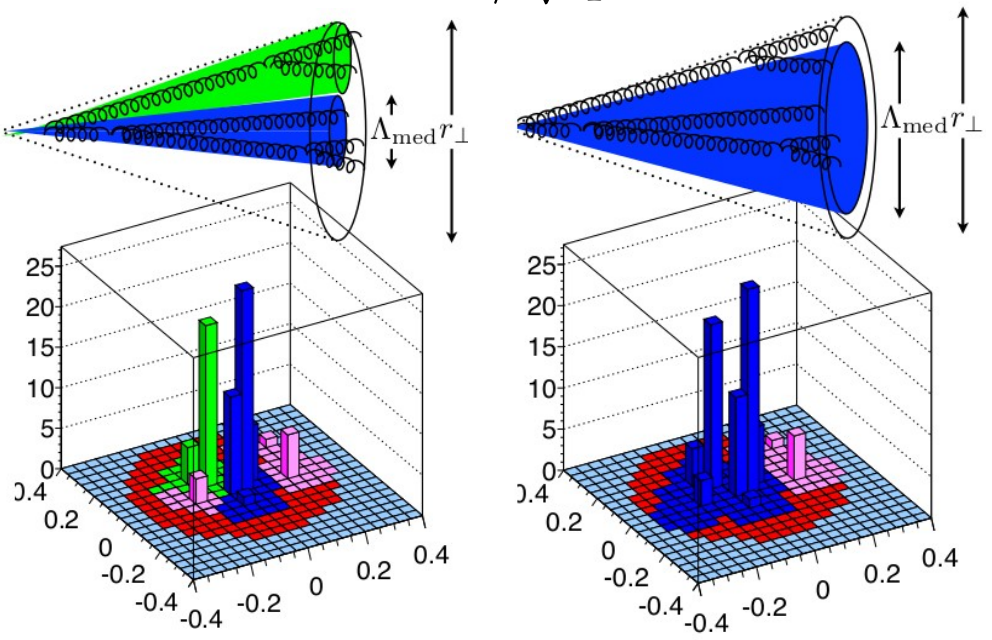

arXiv:1210.7765

Jet suppression

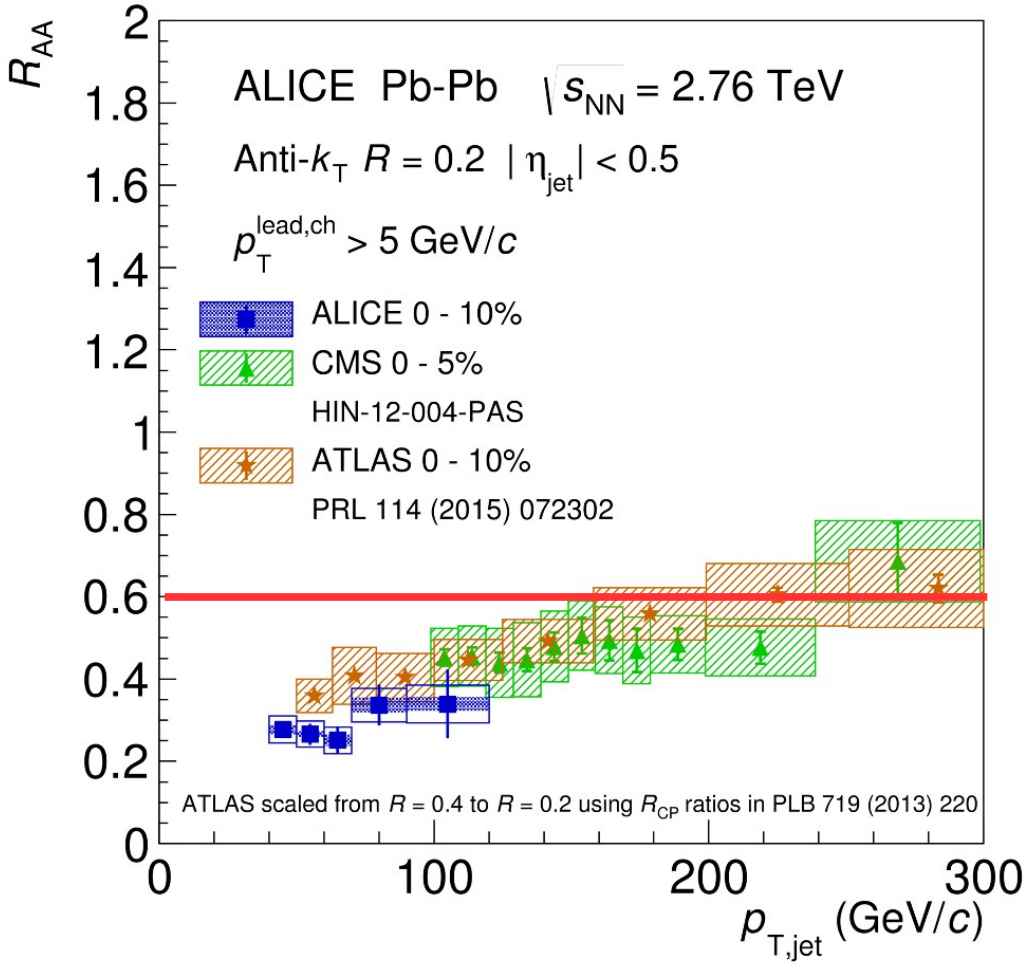

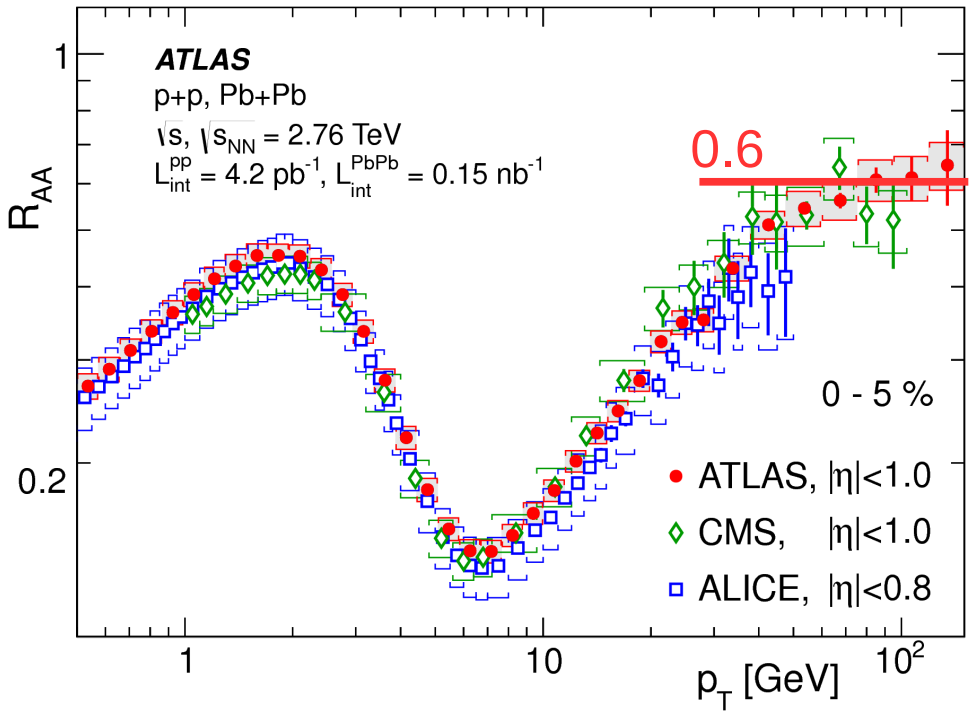

ALI-DER-92552

At high p_T similar suppression of jets as of hadrons:
Indicative of coherent energy loss of jet core

Dijet asymmetry and jet fragmentation

Mueller and Qin, arXiv:1012.5280

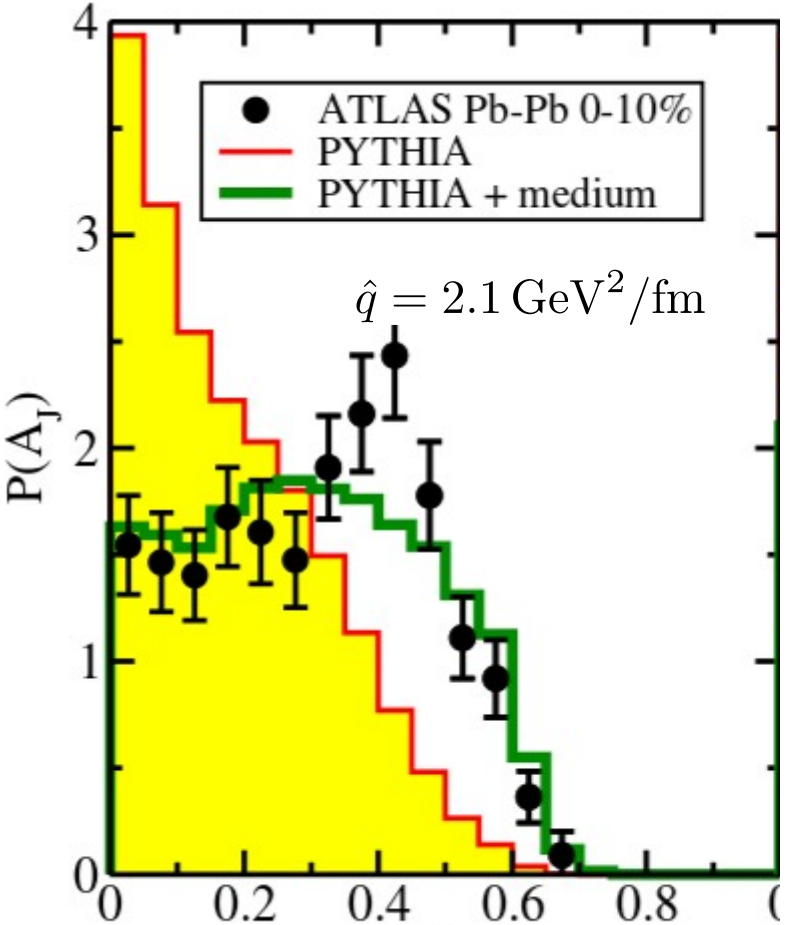

$$A_{\mathrm{J}} = \frac{E_{\mathrm{T1}} - E_{\mathrm{T2}}}{E_{\mathrm{T1}} + E_{\mathrm{T2}}}$$

Perez-Ramon and Renk, arXiv:1411.1983

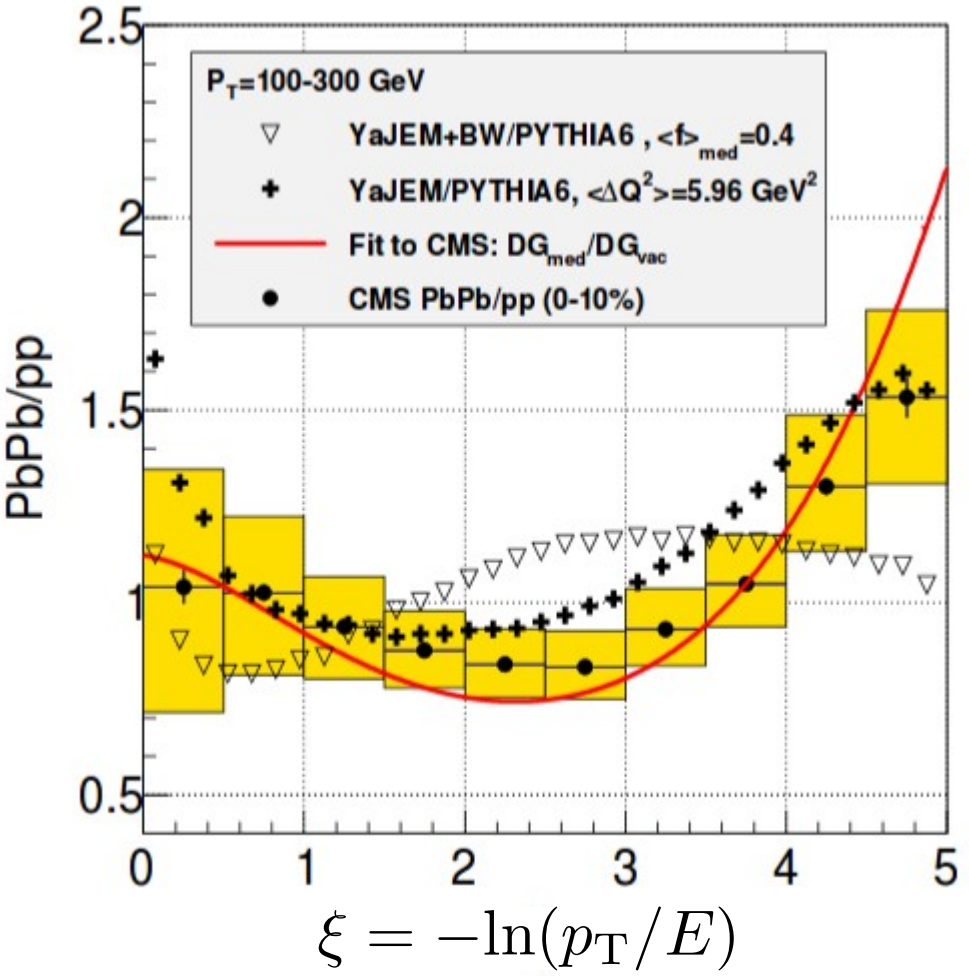

$$\xi = -\ln(p_{\mathrm{T}}/E)$$

Data described by “pQCD with appropriate medium modifications”

ATLAS, PRL 105 (2010) 252303

CMS, PRC 90 (2014) 024908

28 Quark-mass dependence

Andronic et al., arXiv:1506.03981

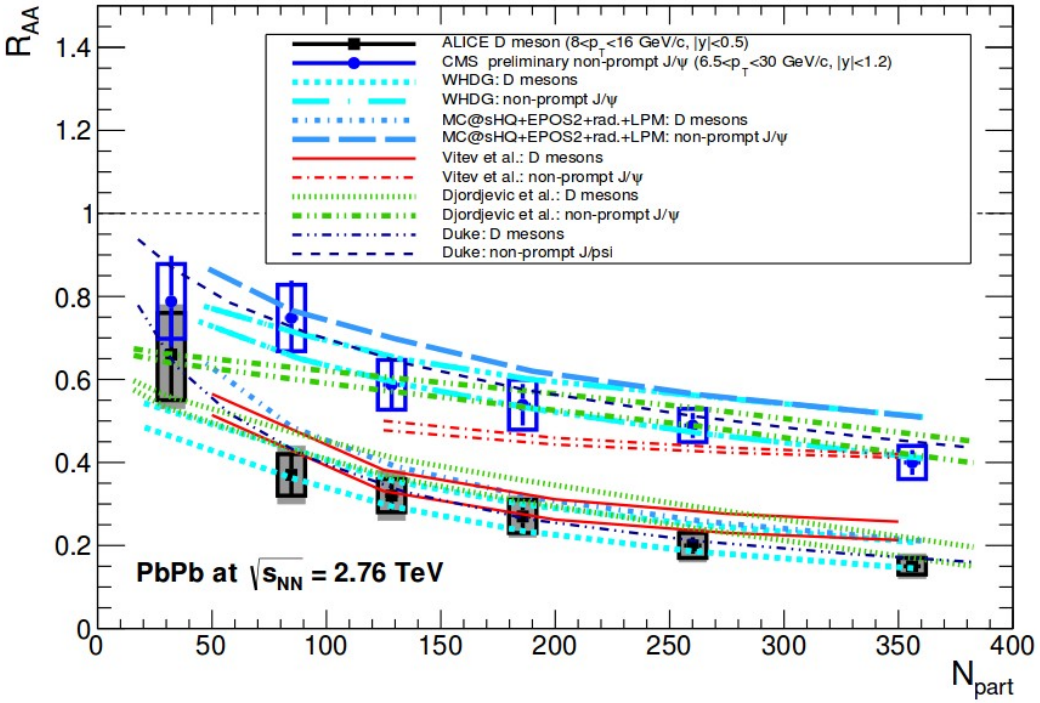

Seen for B vs D, and described by models

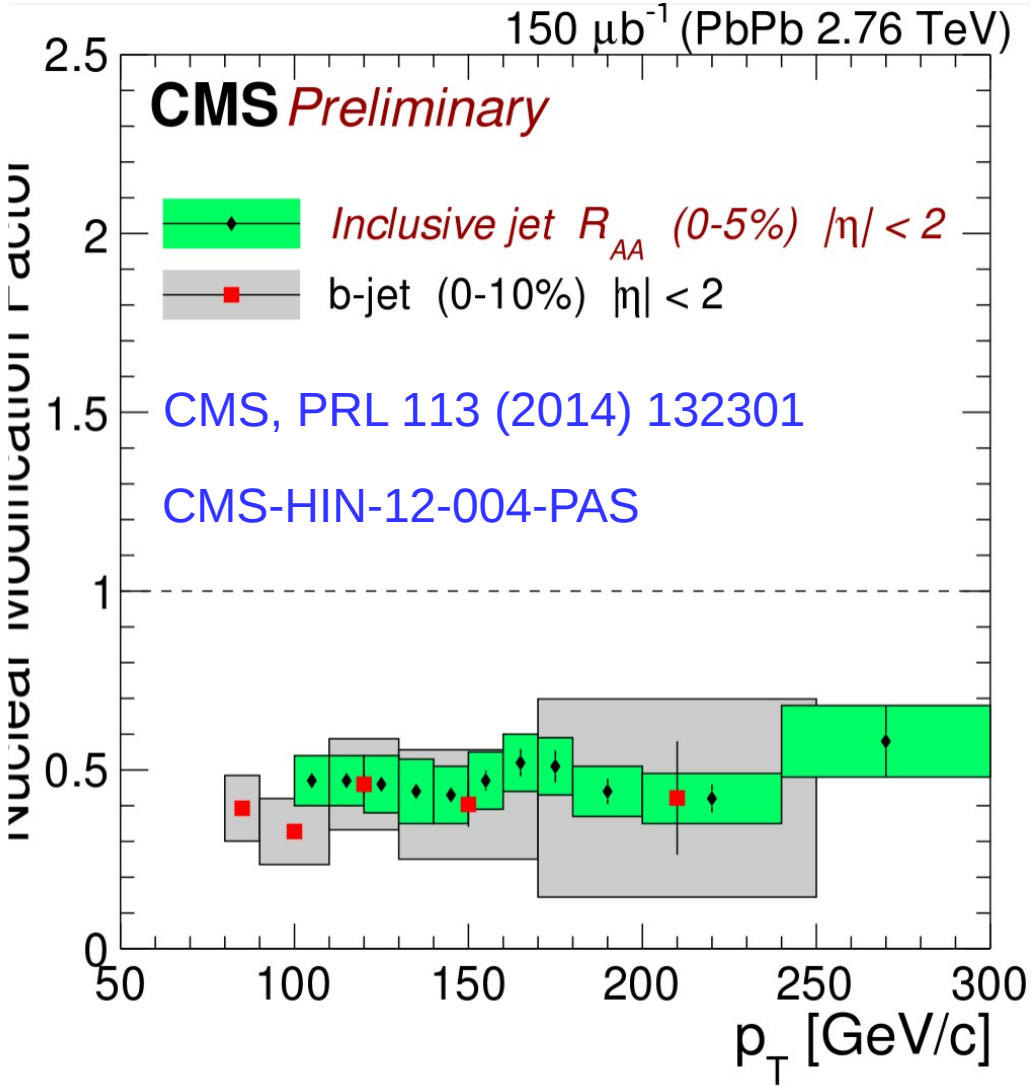

Not seen for b-jets (m<<jet p_T)

"Deadcone effect"

(Radiation suppressed for $\theta < M_Q/E_Q$)

Expect R_{AA}(light hadrons) < R_{AA}(D) < R_{AA}(B)

Charmonia

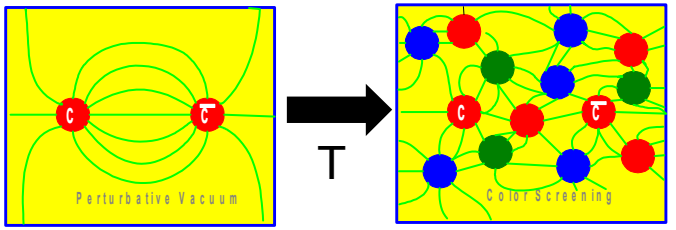

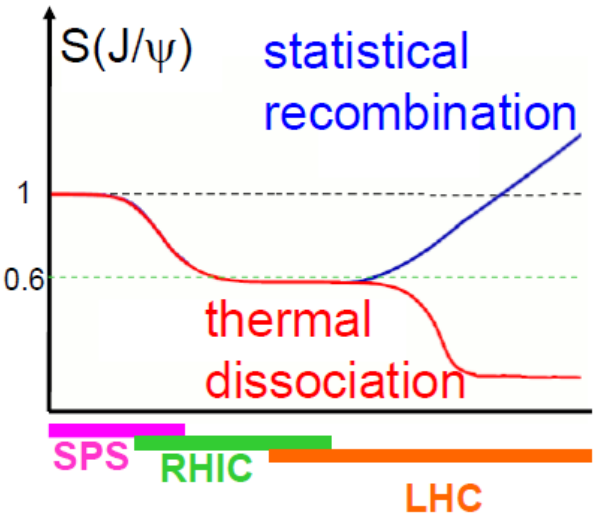

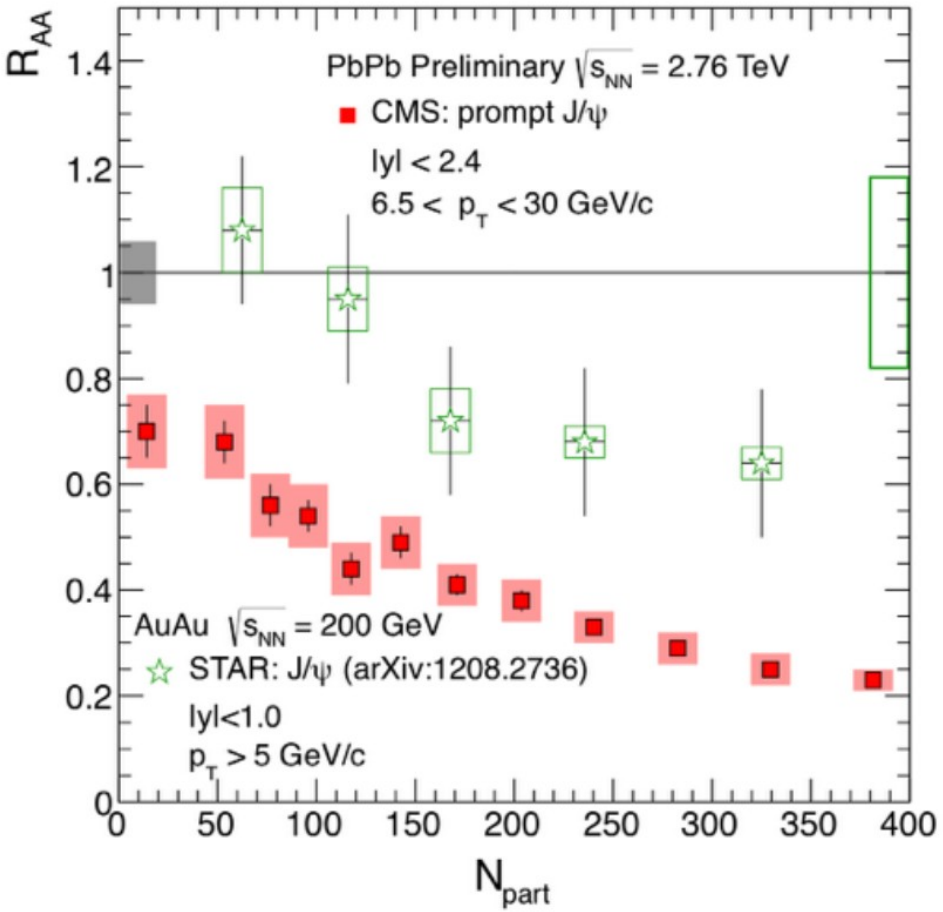

Temperature dependence at high p_T

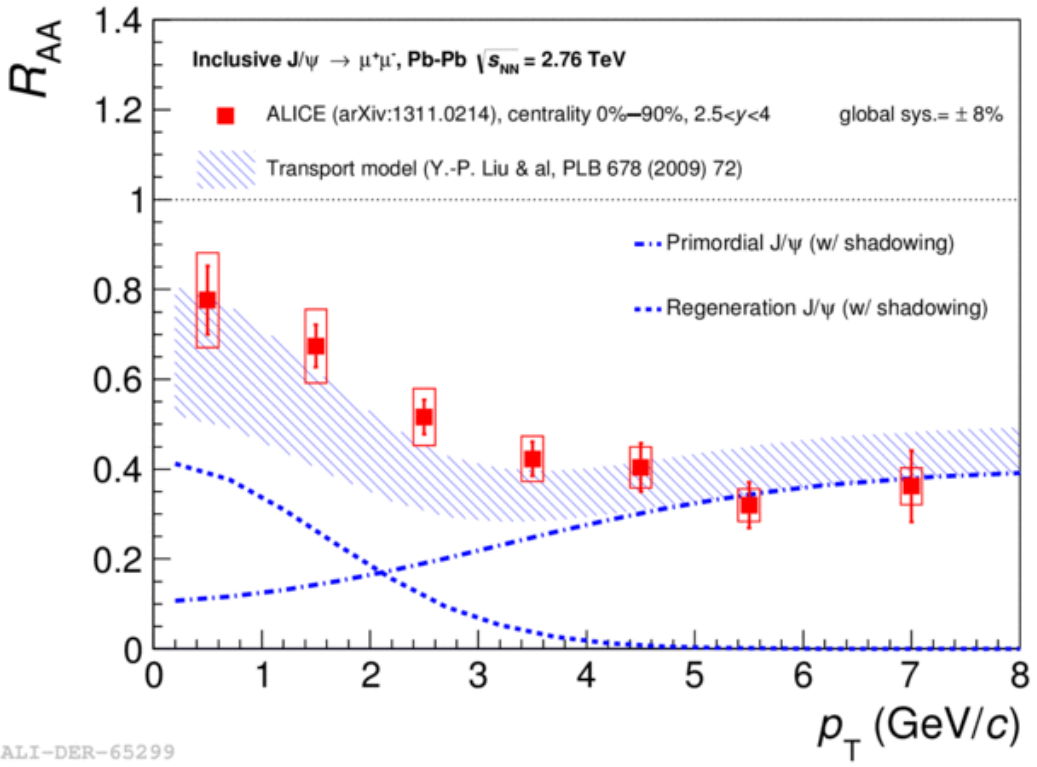

Recombination at low p_T
(where charm density is small)

30 Bottomonia

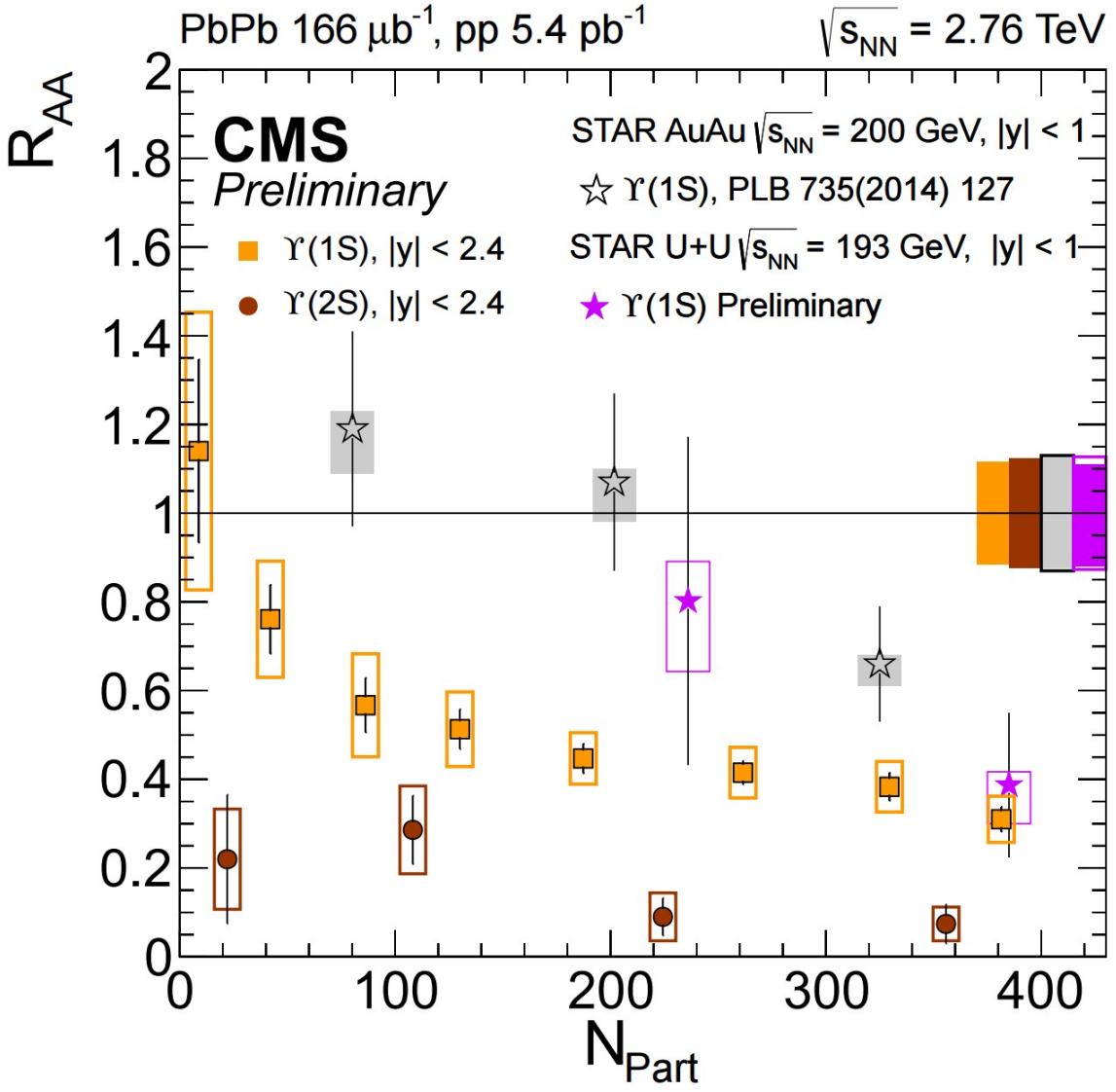

Sequential suppression with binding energy and temperature

Collectivity in small systems

32 NS ridge structures in angular correlations

ATLAS-CONF-2015-027

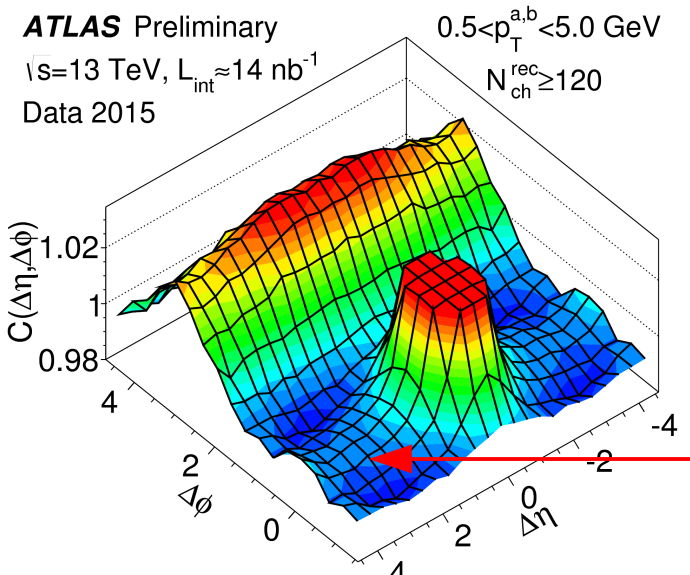

(see B.Wynne, Wed 9:15)

Near-side (NS) ridges in high multiplicity events at LHC energies

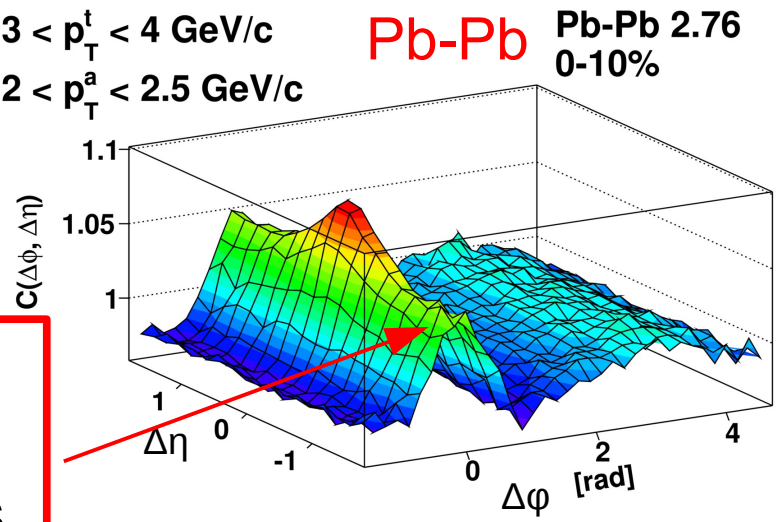

ALICE, PLB 708 (2012) 249

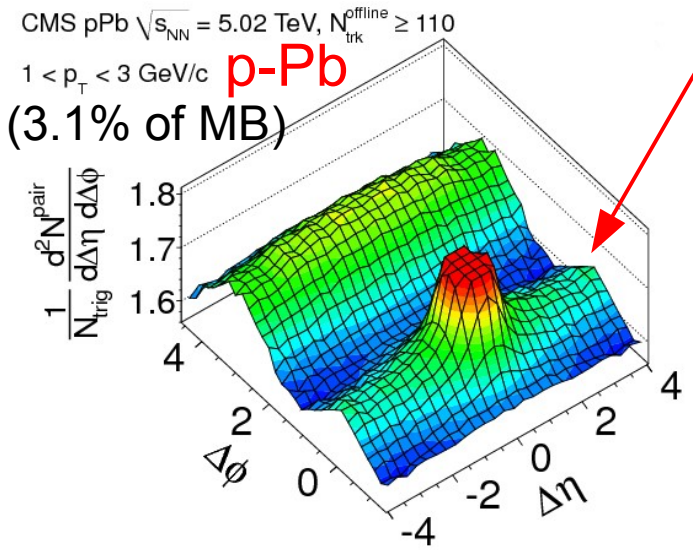

CMS, PLB 718 (2012) 795

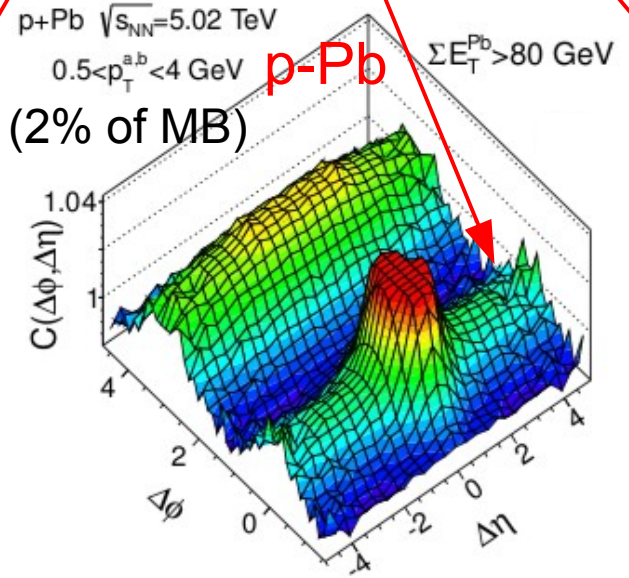

ATLAS, PRL 110 (2013) 182302

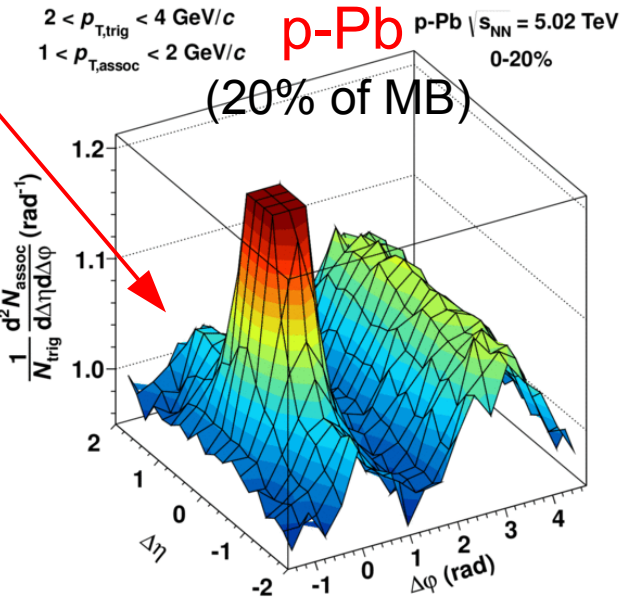

ALICE, PLB 719 (2013) 29

33 Observation of double ridge

ALICE, PLB 719 (2013) 29

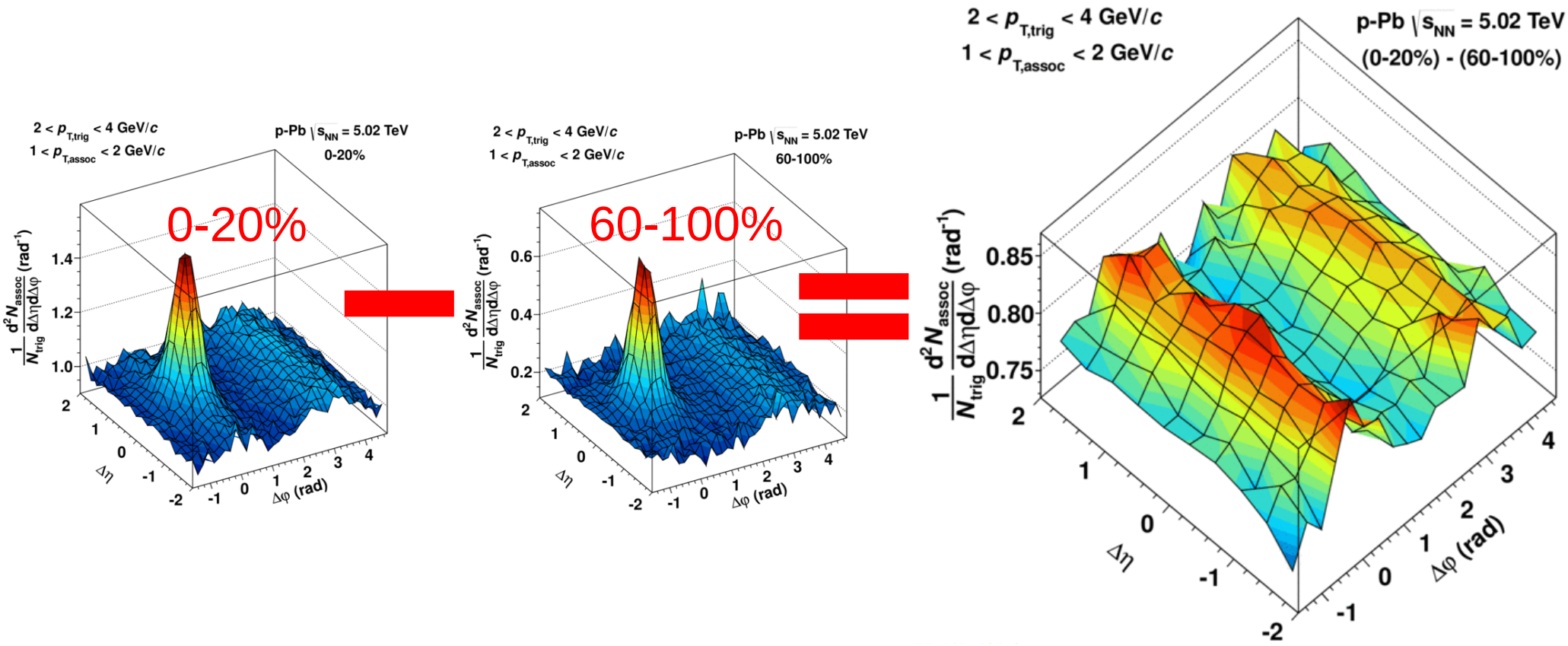

- Extract double ridge structure by subtracting the jet-like correlations from 60-100% low multiplicity class
  - Checked that correlations in 60-100% are similar to pp (at 2.76 and 7 TeV)

Analysis of double ridge

- v_n coefficients
  - Significant for n=2 to 5
  - Substantial to even high p_T
- Multi-particle correlations
  - At least 8 particles correlate(
  - $v_2\{4\} \approx v_2\{6\} \approx v_2\{8\}$
- Particle species dependence
  - Cross of v_2(proton) with v_2(pion) at about 2 GeV/c for p_T<2 GeV/c
  - Similar for $v_3(\Lambda)$

Features qualitatively similar to those seen in Pb-Pb collisions. Suggests same physics at place?
(Note: no direct evidence of jet quenching)

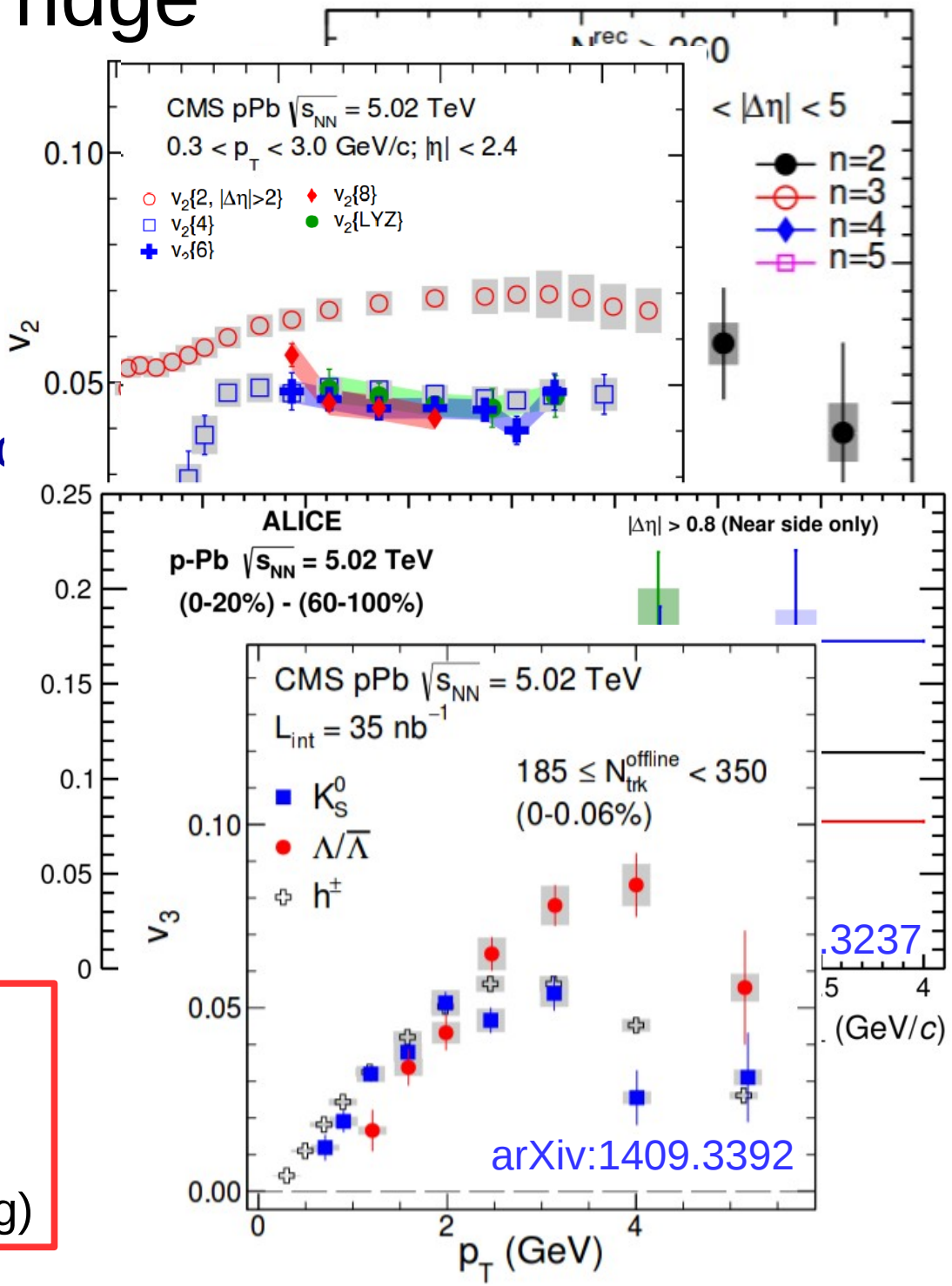

Interpretation: Hydrodynamics

arXiv:1307.5060

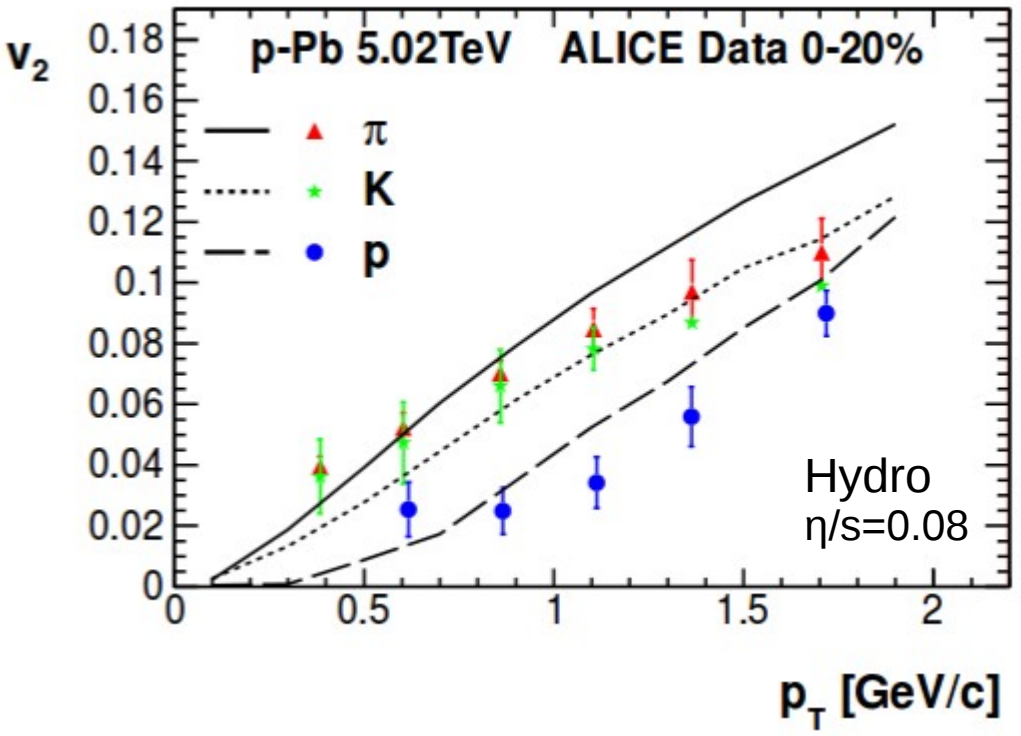

arXiv:1404.7327

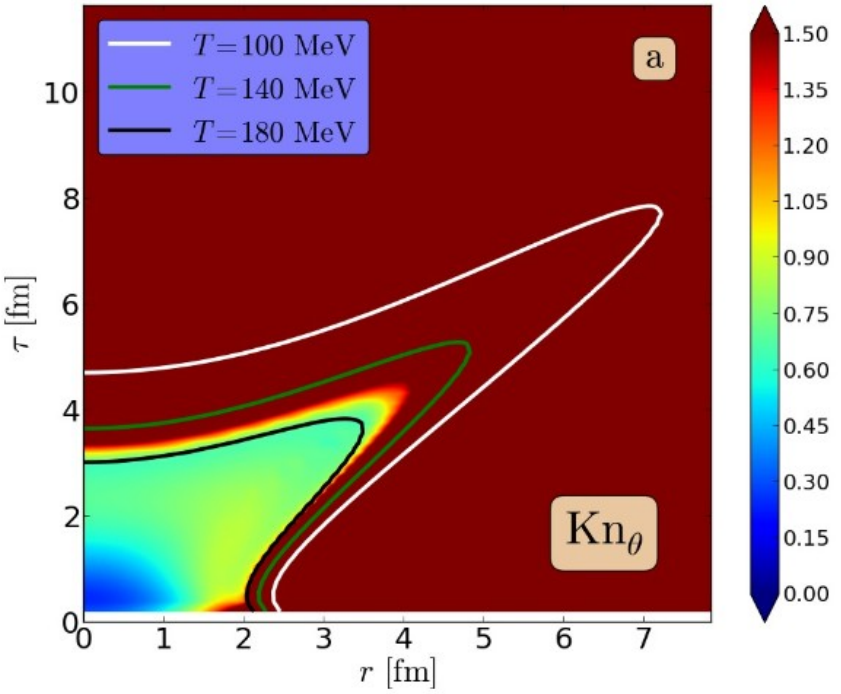

- Formation of mini-QGP with hydrodynamical evolution
  - Obvious conclusion, since features in data similar to Pb-Pb
- Debate if hydro can be applied, and gives with meaningful parameters (eg. η/s~0.08 smaller than in PbPb)?
- Macro- and microscopic length/time scales separable?

36 Interpretation: Glasma graphs in initial state

- Two symmetric ridges predicted by CGC glasma graphs found to describe the ridge yields and shape
  - Already applied at RHIC and in 7 TeV pp
- However, not obvious how to explain multi-particle cumulants and PID dependence

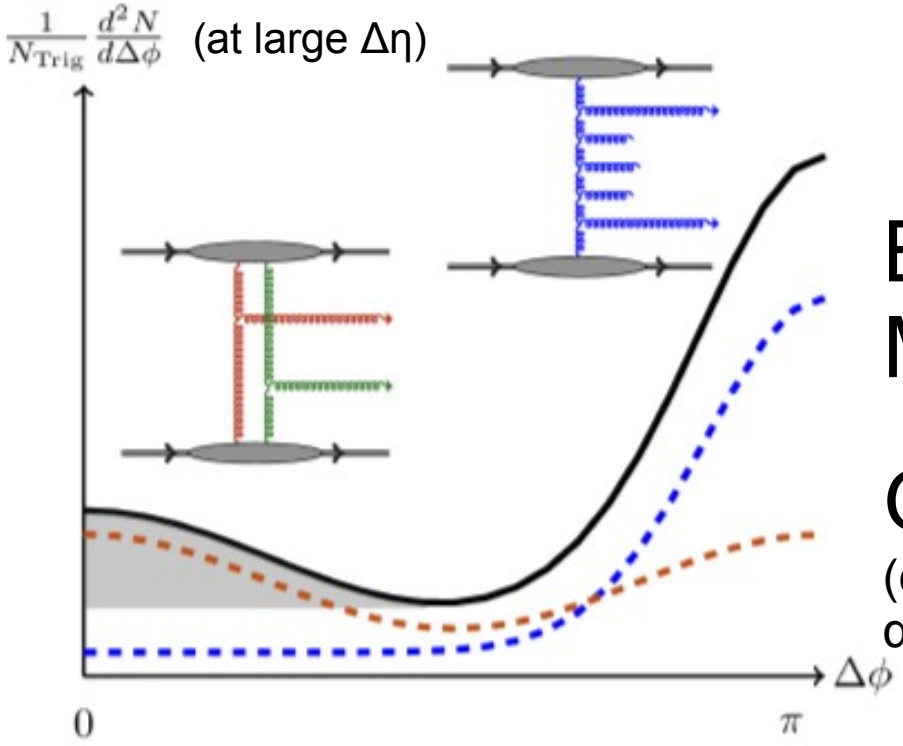

BFKL-Minijets

Glasma
(enhanced by α_s^{-8} for $k_T < Q_s$)

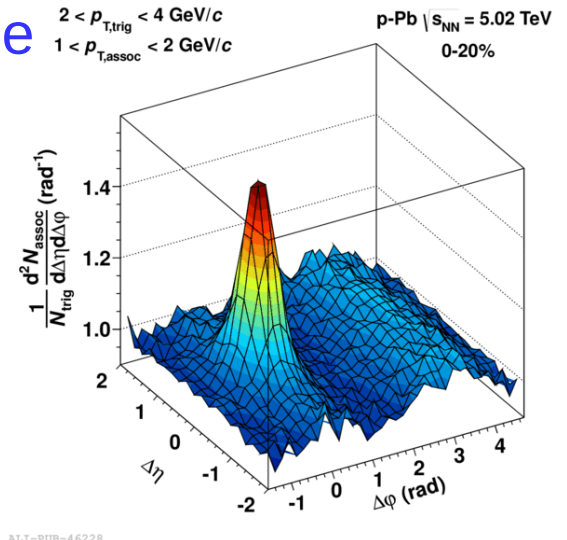

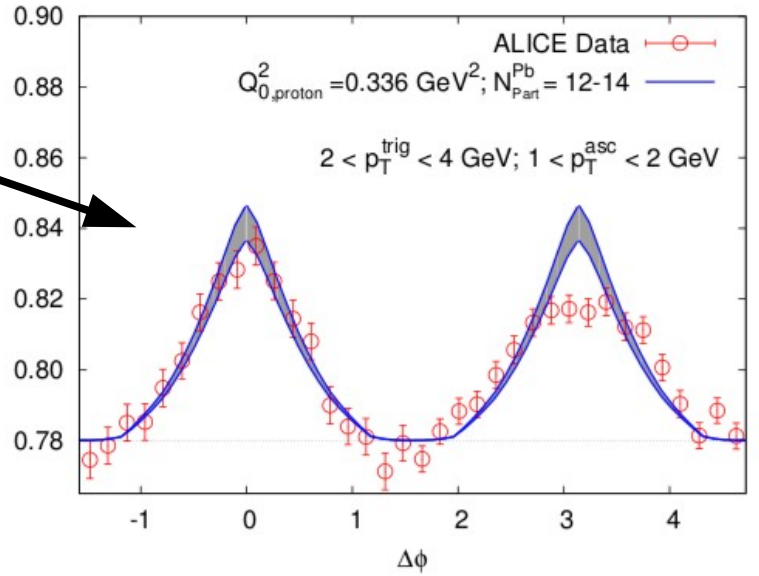

Dusling and Venugopalan, PRD 87 (2013) 094034

Saturation vs multiplicity effect?

Pb-going side

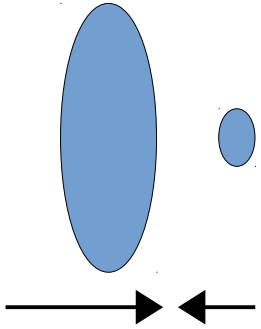

Large-x gluons in Pb
Small-x effects suppressed

p-going side

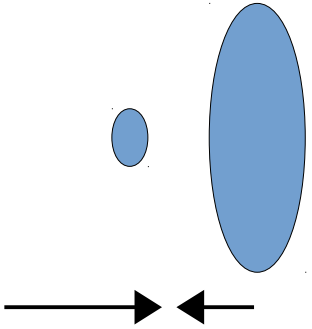

Small-x gluons in Pb
Small-x effects enhanced

arXiv:1412.6828

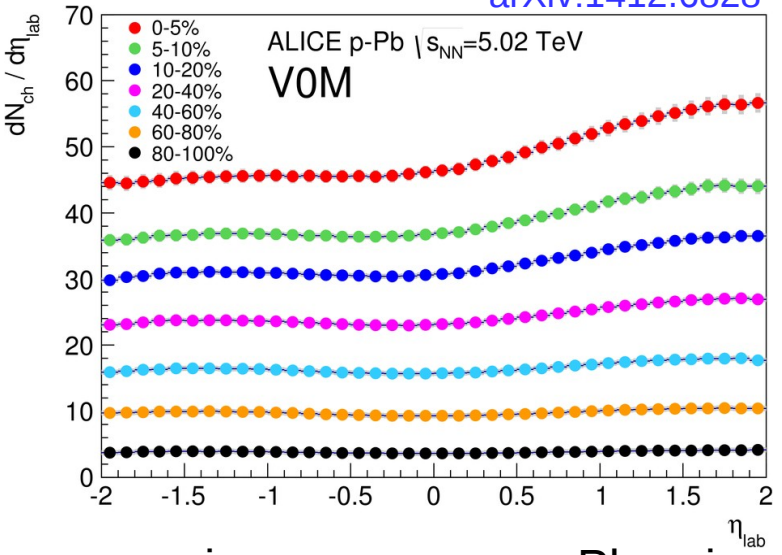

p-going Pb-going

$$v_2 \propto \varepsilon \frac{\mathrm{d}N/\mathrm{d}y}{S}$$

38 v_2 coefficients at 2.5<|η|<4.0

ALICE, arXiv:1506.08032

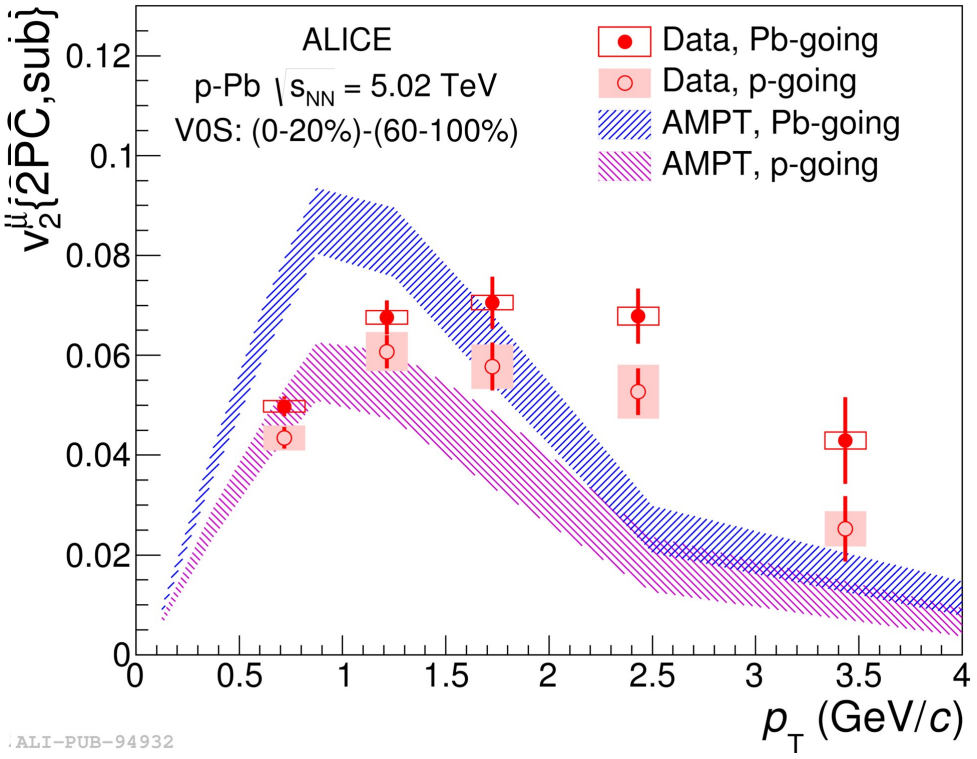

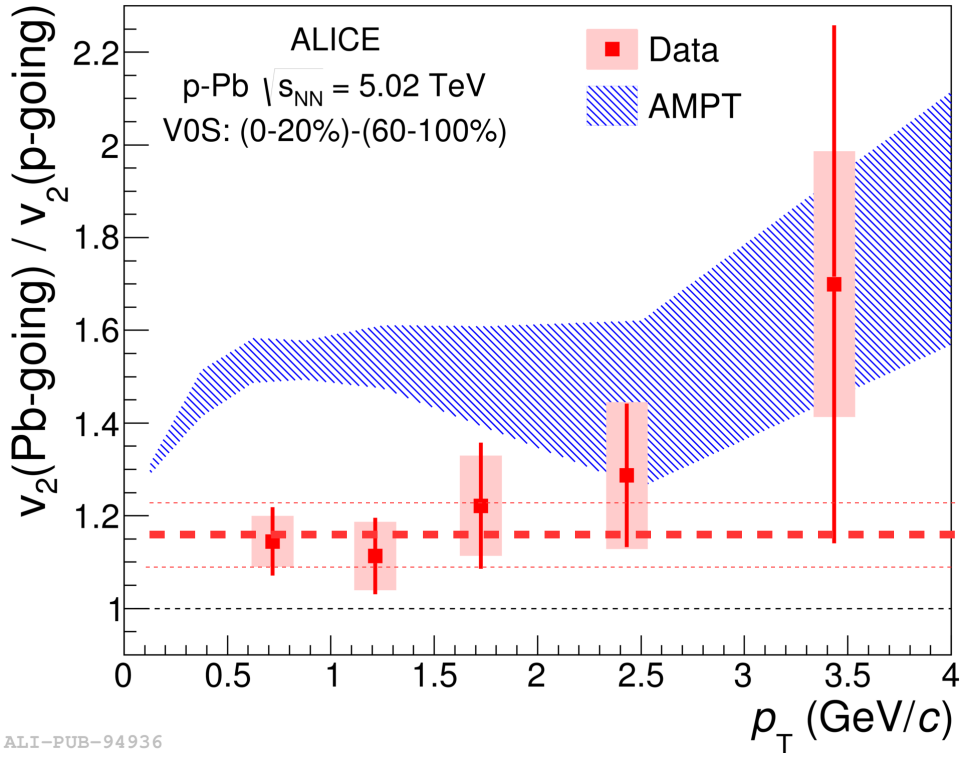

- Sizable inclusive muon v_2 with Pb-going larger than p-going
- Ratio from constant fit
  - 1.16±0.06 with χ^2/NDF=0.4

- Parton cascade model (which describes a variety of data in p/AA) only qualitatively agrees
- Vastly different particle composition or finite v_2 for HF muons (as in PbPb)?

Prel. LHCb result

LHCb-CONF-2015-004

$2<\eta_{lab}<4.9$

p+Pb configuration

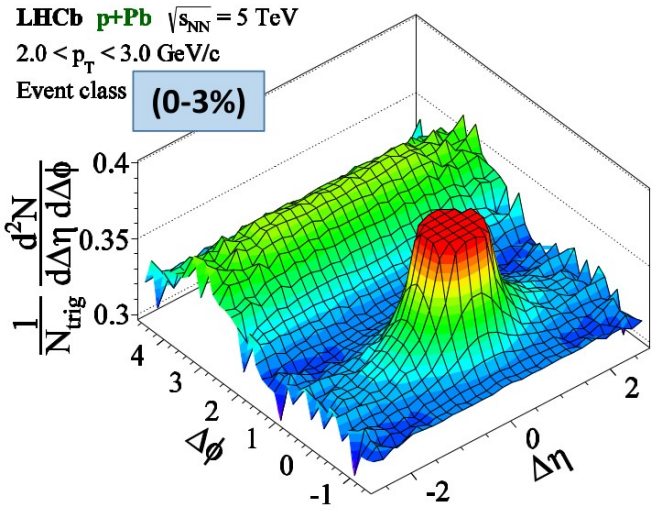

Pb+*p* configuration

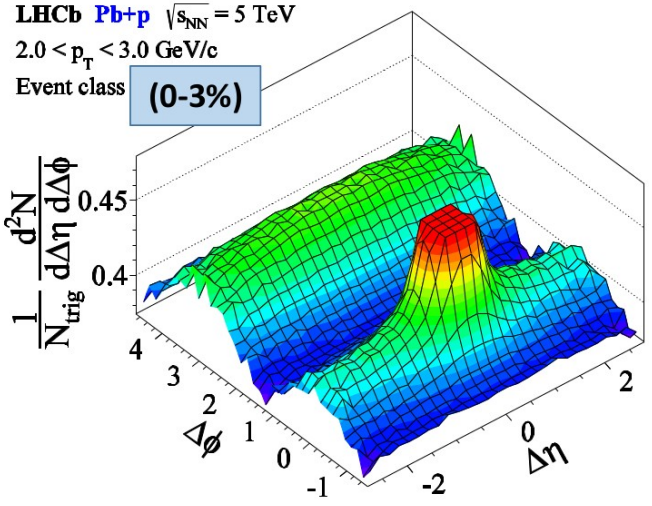

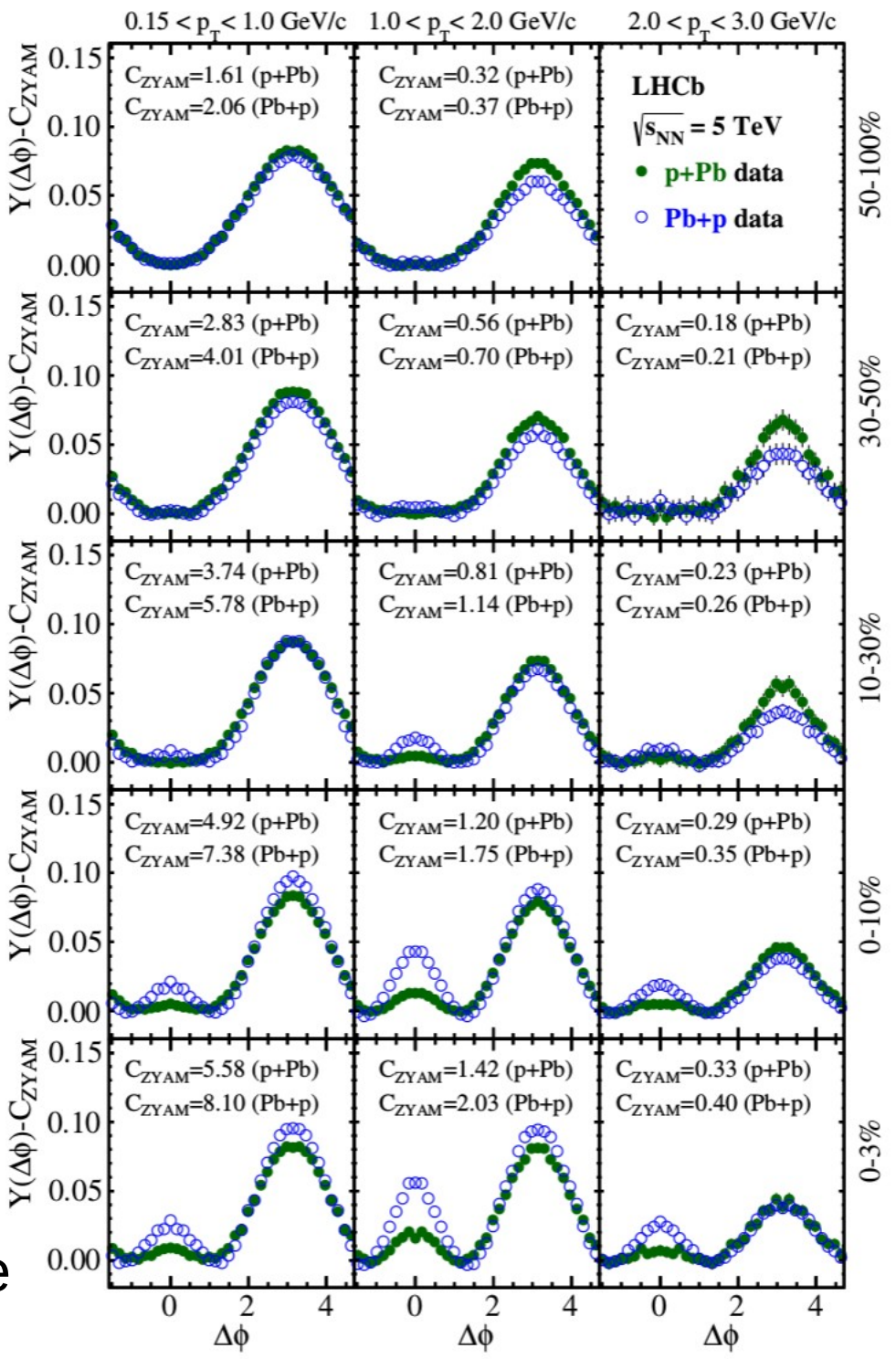

NS ridge is stronger in Pb-going case

Saturation vs multiplicity effect?

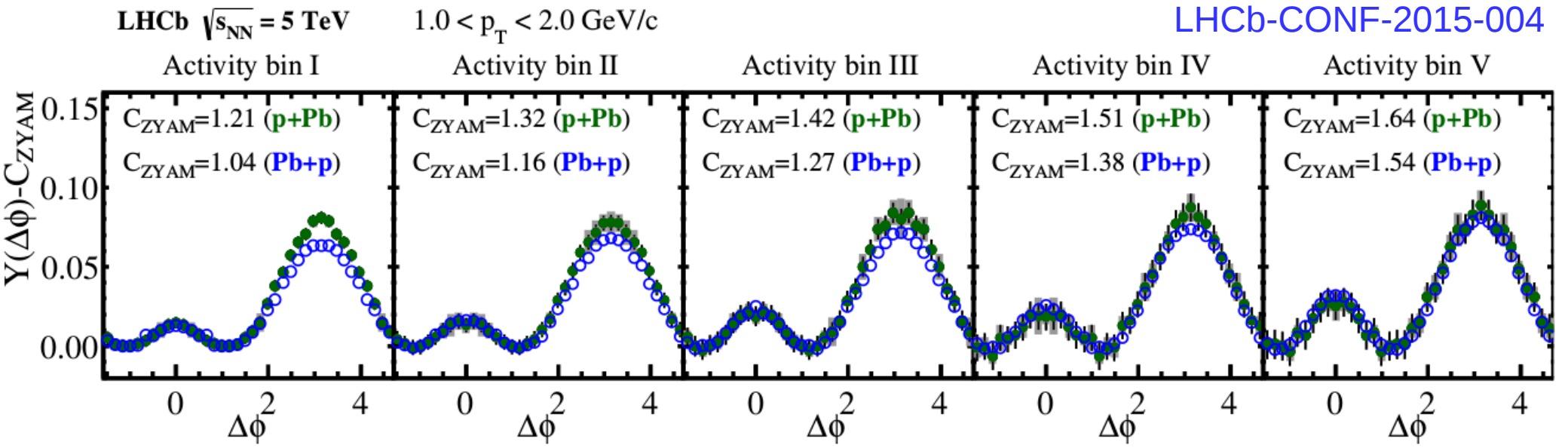

LHCb-CONF-2015-004

- v_2 (or NS rigde yields) larger on Pb-going than on p-going side
- For same multiplicity (in 2<η<4.9) LHCb finds the same NS rigde yields
- Suggests that multiplicity (density) matters

Common absolute activity bins	
	$\mathcal{N}^{\rm hit}_{\rm VELO}$-range in Pb+$p$
Bin I	2200 – 2400
Bin II	2400 – 2600
Bin III	2600 – 2800
Bin IV	2800 – 3000
Bin V	3000 – 3500

(p-Pb activity scaled by ~0.77 for backward VELO acceptance)

41 v_2 and v_3 in dAu at RHIC

PHENIX, PRL 111 (2013) 212301

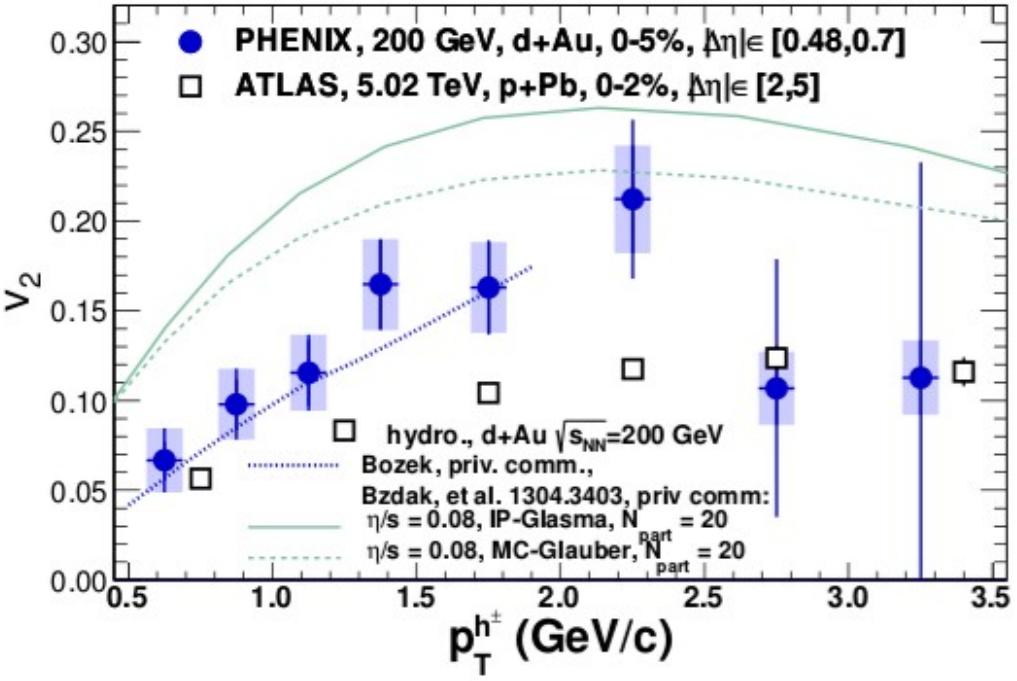

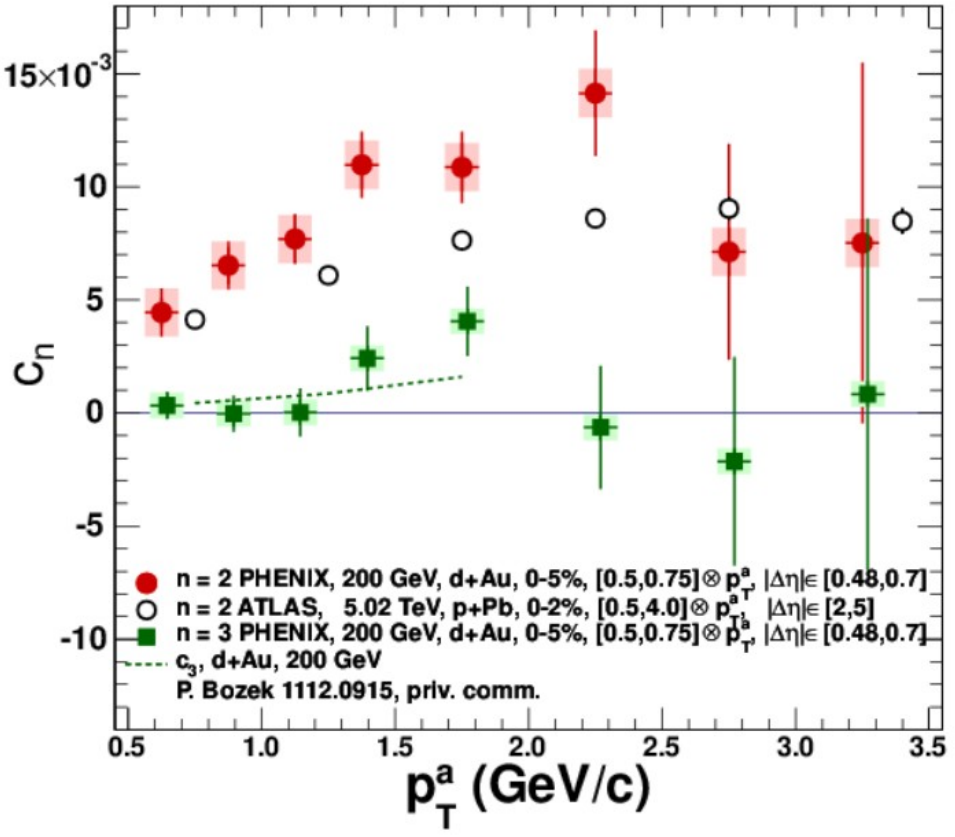

Large v_2 (about twice as much as that of pPb) and negligible v_3 found in dAu, as expect from initial state eccentricities.

Geometric engineering

Nagle et al., PRL 113 (2014) 112301

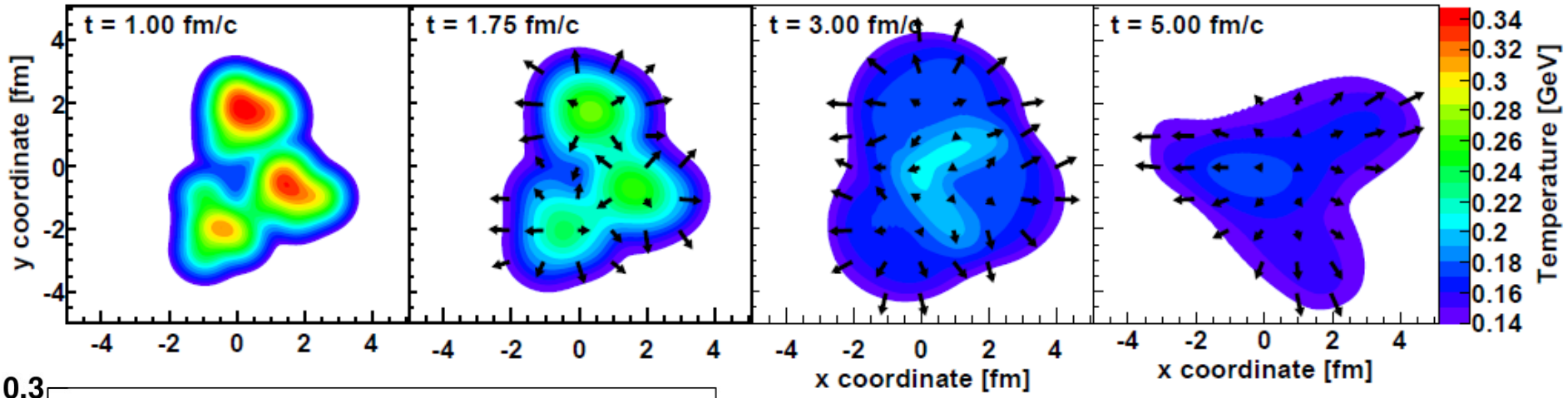

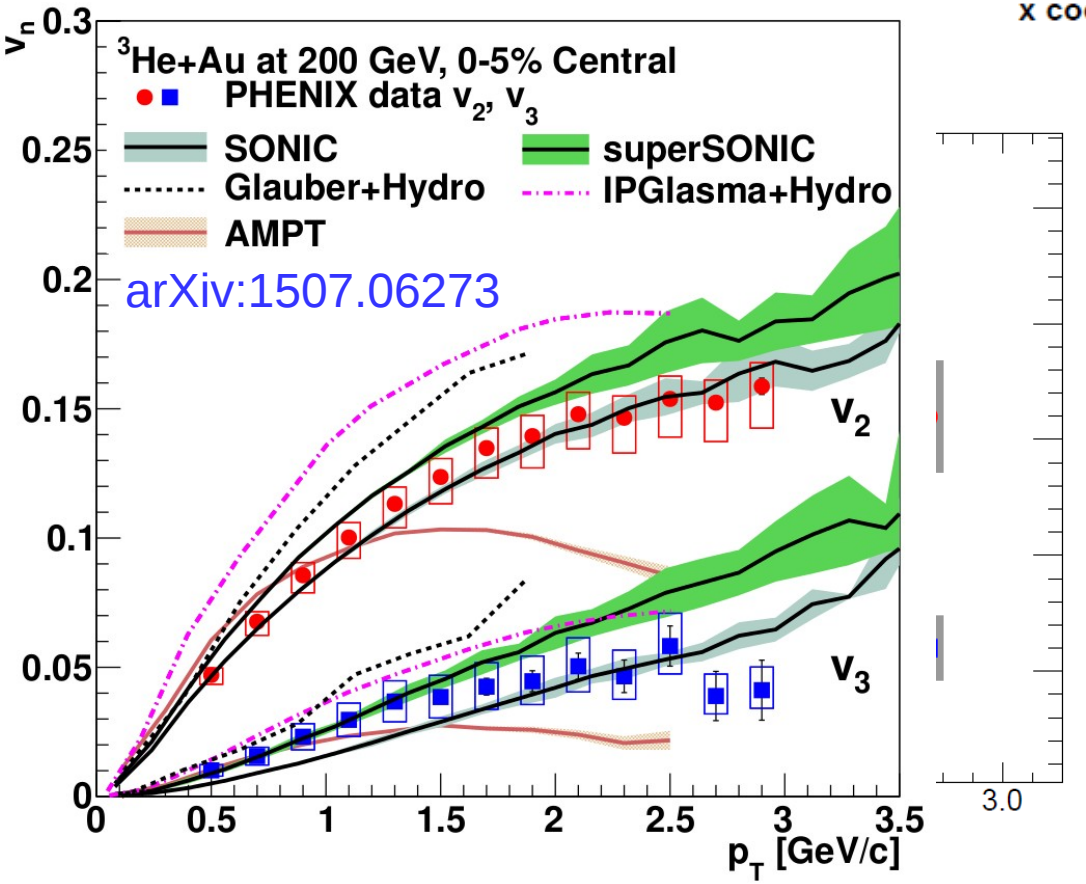

Expectation from IS:

- ^{3}He+Au (0-5%) N_{part}=25.0
  ε_2=0.504 ε_3=0.283
- d+Au (0-5%) N_{part}=17.8
  ε_2=0.540 ε_3=0.190

Measurement:

- The v_2 of ^{3}He+Au is similar to that of d+Au
- A clear v_3 signal observed in 0-5% ^{3}He+Au collisions

43 Summary

- Significant advances in recent years in the understanding of QGP
  - Nearly perfect liquid
    - η/s close to minimum, and larger at LHC than at RHIC energies
    - Variety of observables to further constrain models
  - Jets are weakly coupled to the medium
    - Medium modified pQCD models can describe features of data
    - Coherent energy loss at high, b vs c-quark mass ordering at low p_T
  - Sequential melting and recombination
- Collective effects in small systems
  - Not any longer just simple control systems
    - Challenge understanding of initial and final state effects
  - May provide a window into non-equilibrium dynamics

Stay tuned as results from pAu at RHIC, and more from run 2 at LHC will come soon!

44 Long-range elliptic anisotropy

arXiv:1509.04776

(today)

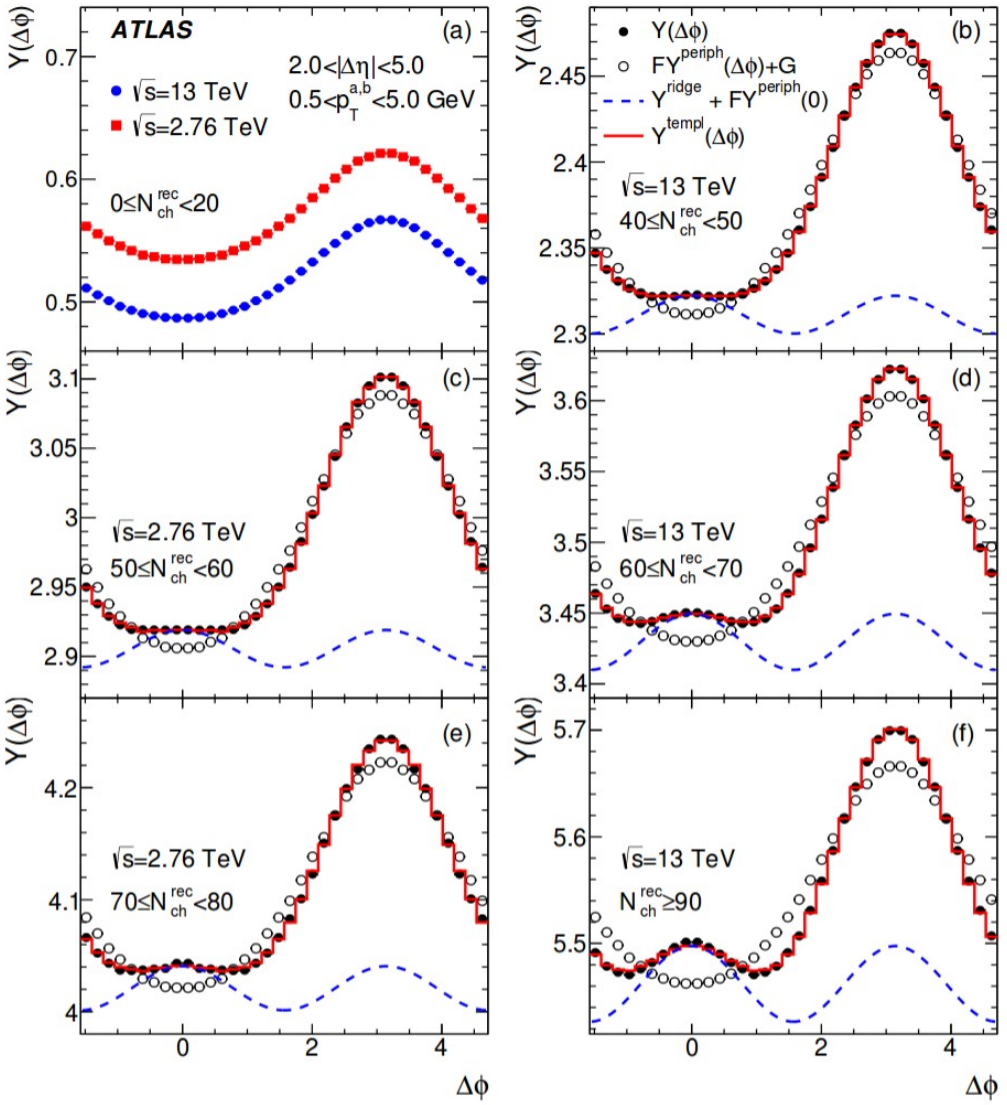

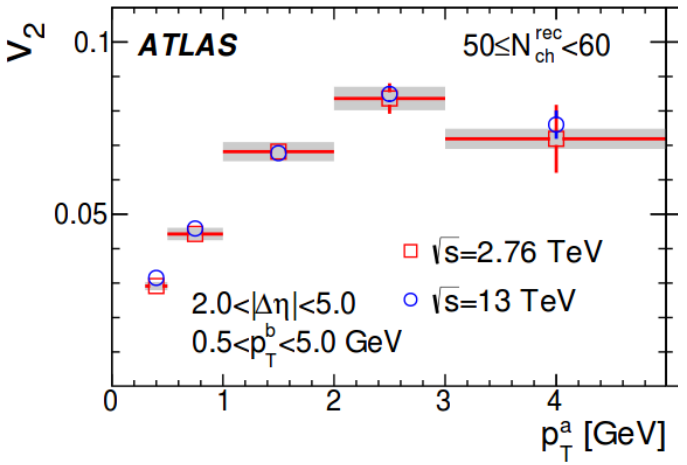

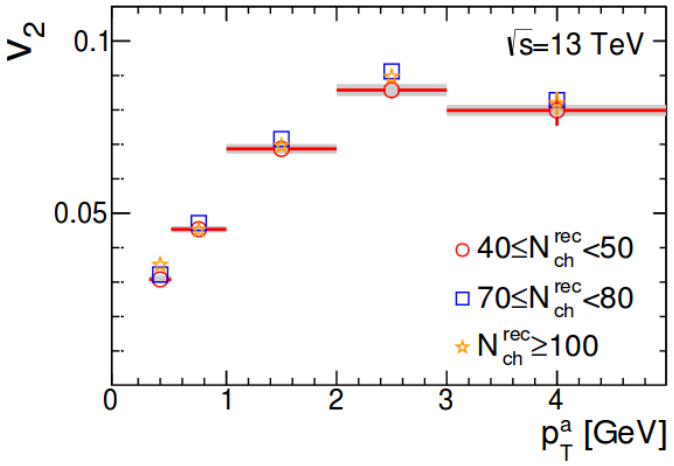

$$Y^{\mathrm{temp}}(\Delta\Phi) = F\,Y^{\mathrm{periph}} + Y^{\mathrm{ridge}}$$

$$Y^{\mathrm{ridge}}(\Delta\Phi) = G(1 + v_{2,2}\cos(2\Delta\Phi))$$

Energy + multiplicity independent v_2

(p_T shape similar to that seen in p+Pb and Pb+Pb)

Long-range elliptic anisotropy

arXiv:1509.04776

(today)

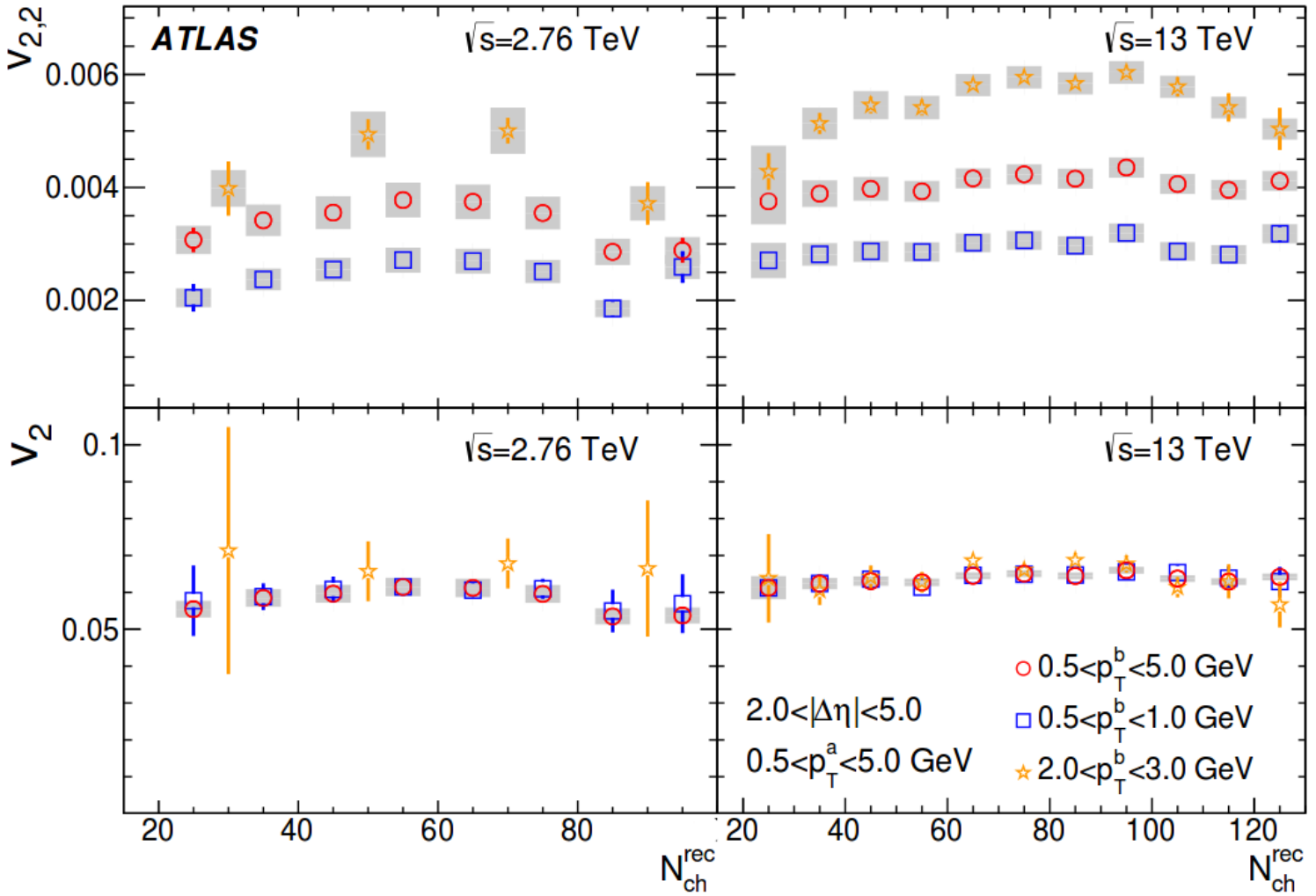

46 Extra

47 Chemical and thermal freezeout

$$N_i = V \frac{g_i}{2\pi^2} \int \frac{p^2 \, \mathrm{d}p}{e^{(E_i - \mu_B B_i)/T} \pm 1}$$

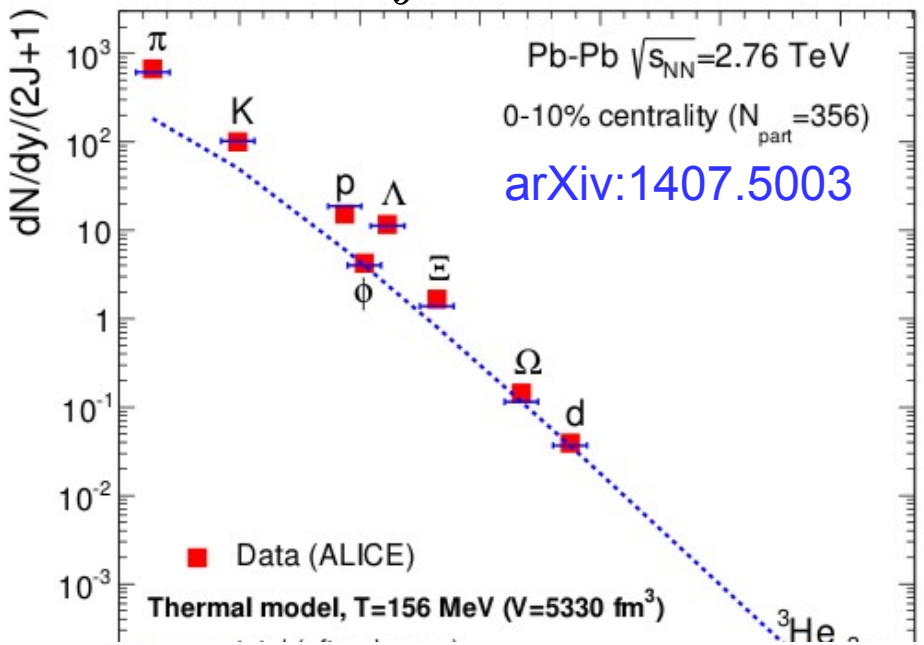

PRL 109 (2012) 252301

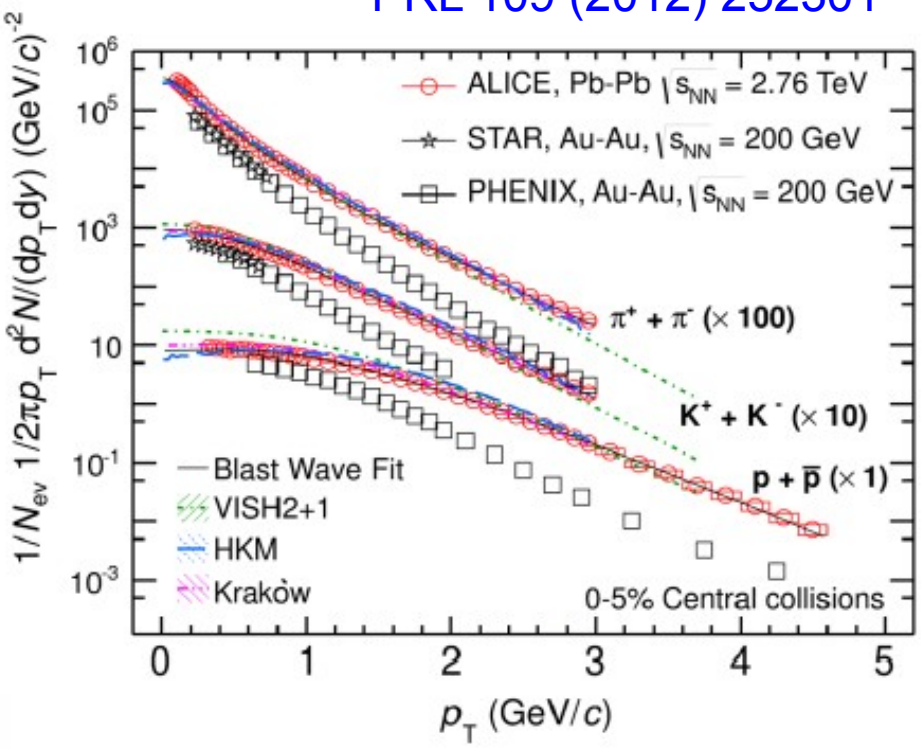

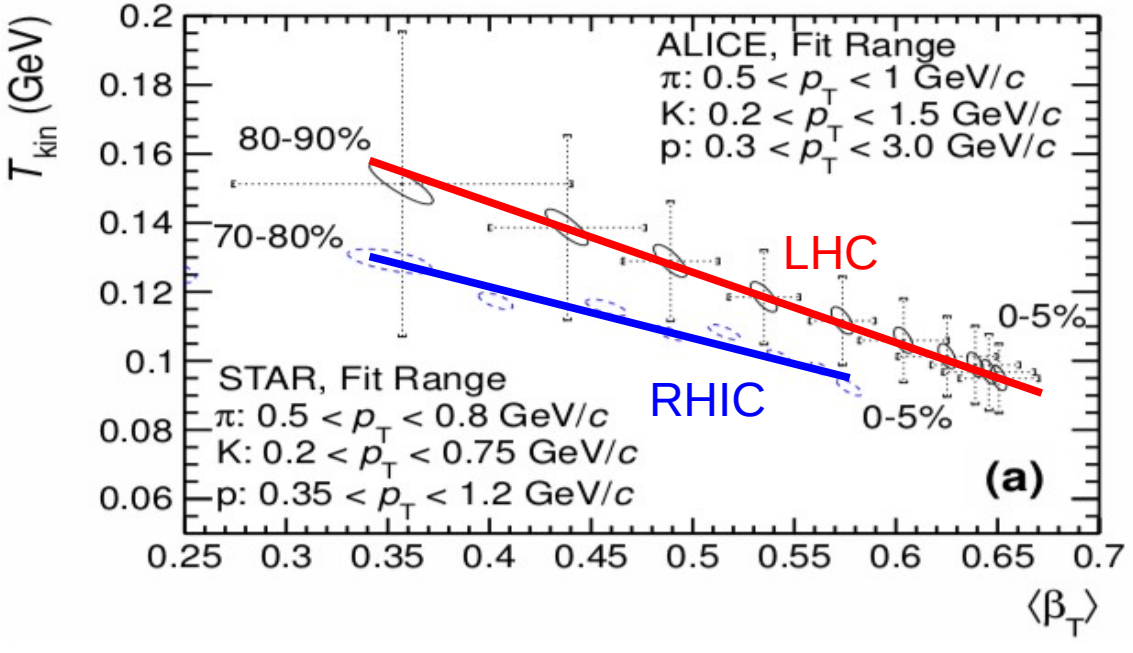

Radial flow

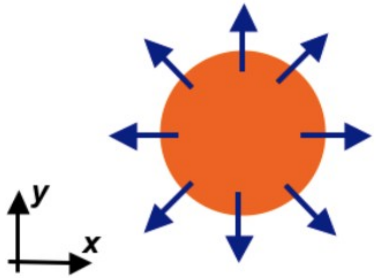

$$p_T^{flow} = p_T + m\beta_T^{flow}\gamma_T^{flow}$$

Shuryak and Zhirov, PLB 89 (1979) 253

48 Measured v_2 vs centrality at LHC

Two-particle methods

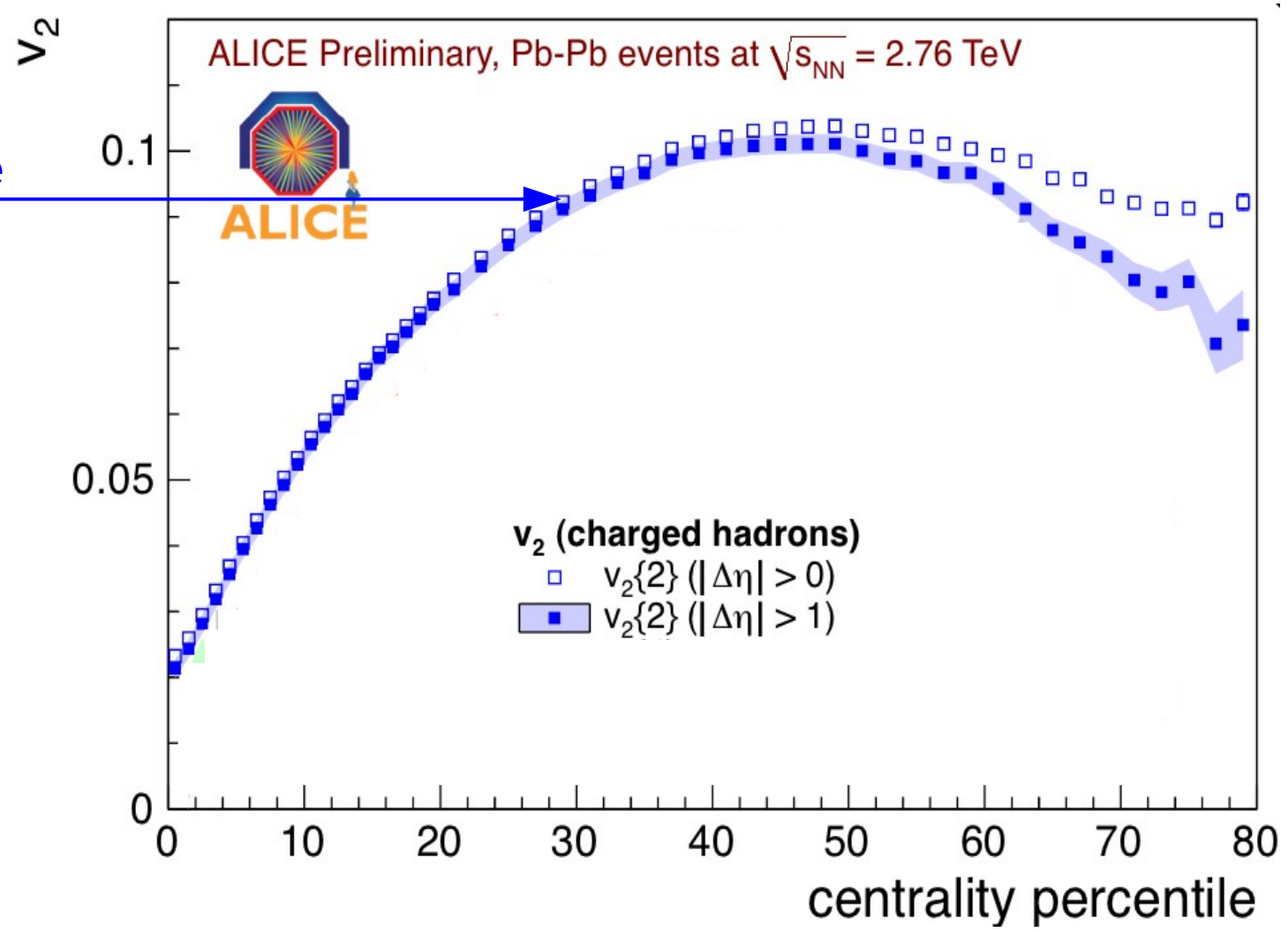

Multi-particle correlations: $v_2\{4\}$ and higher

(From S. Tuo)

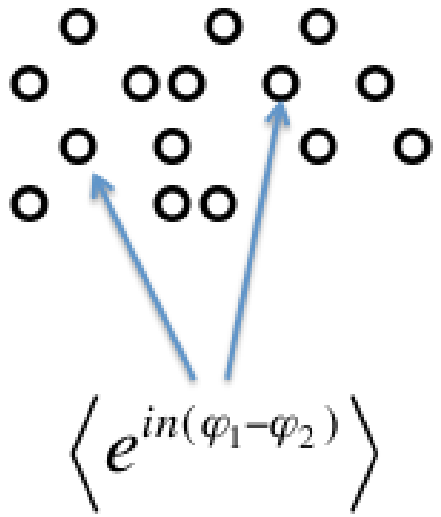

$$\left\langle e^{in(\varphi_1-\varphi_2)} \right\rangle$$

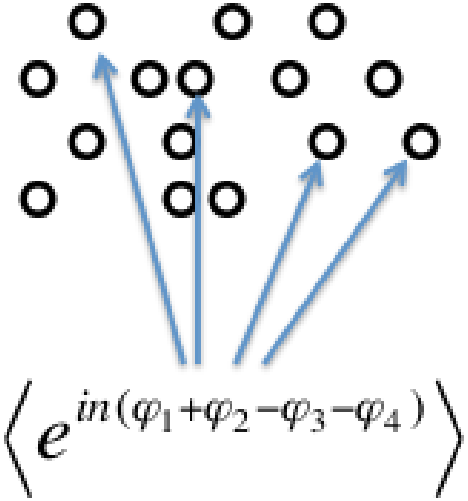

$$\left\langle e^{in(\varphi_1+\varphi_2-\varphi_3-\varphi_4)} \right\rangle$$

Four particle correlations (Q-cumulant method):

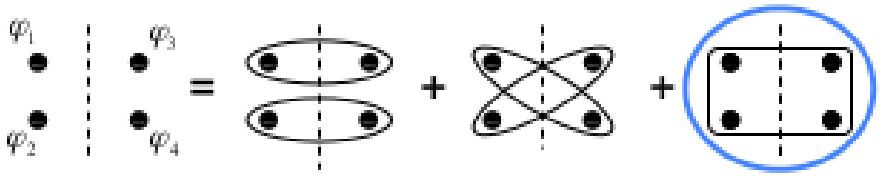

$$c_n\{4\} = \langle\langle 4\rangle\rangle - 2 \cdot \langle\langle 2\rangle\rangle^2$$

$$v_2\{4\} = \sqrt[4]{-c_n\{4\}}$$

$$\left\langle e^{in(\varphi_1+\varphi_2-\varphi_3-\varphi_4)} \right\rangle - \left\langle e^{in(\varphi_1-\varphi_3)} \right\rangle \left\langle e^{in(\varphi_2-\varphi_4)} \right\rangle - \left\langle e^{in(\varphi_1-\varphi_4)} \right\rangle \left\langle e^{in(\varphi_2-\varphi_3)} \right\rangle$$

Multi-particle correlations (cumulant) studies extract the genuine multi-particle correlation

Multi-particle correlations: $v_2\{4\}$ and higher

Two-particle methods

Multi-particle methods

(difference between multi- and two particle correlations originates from non-flow and flow fluctuations)

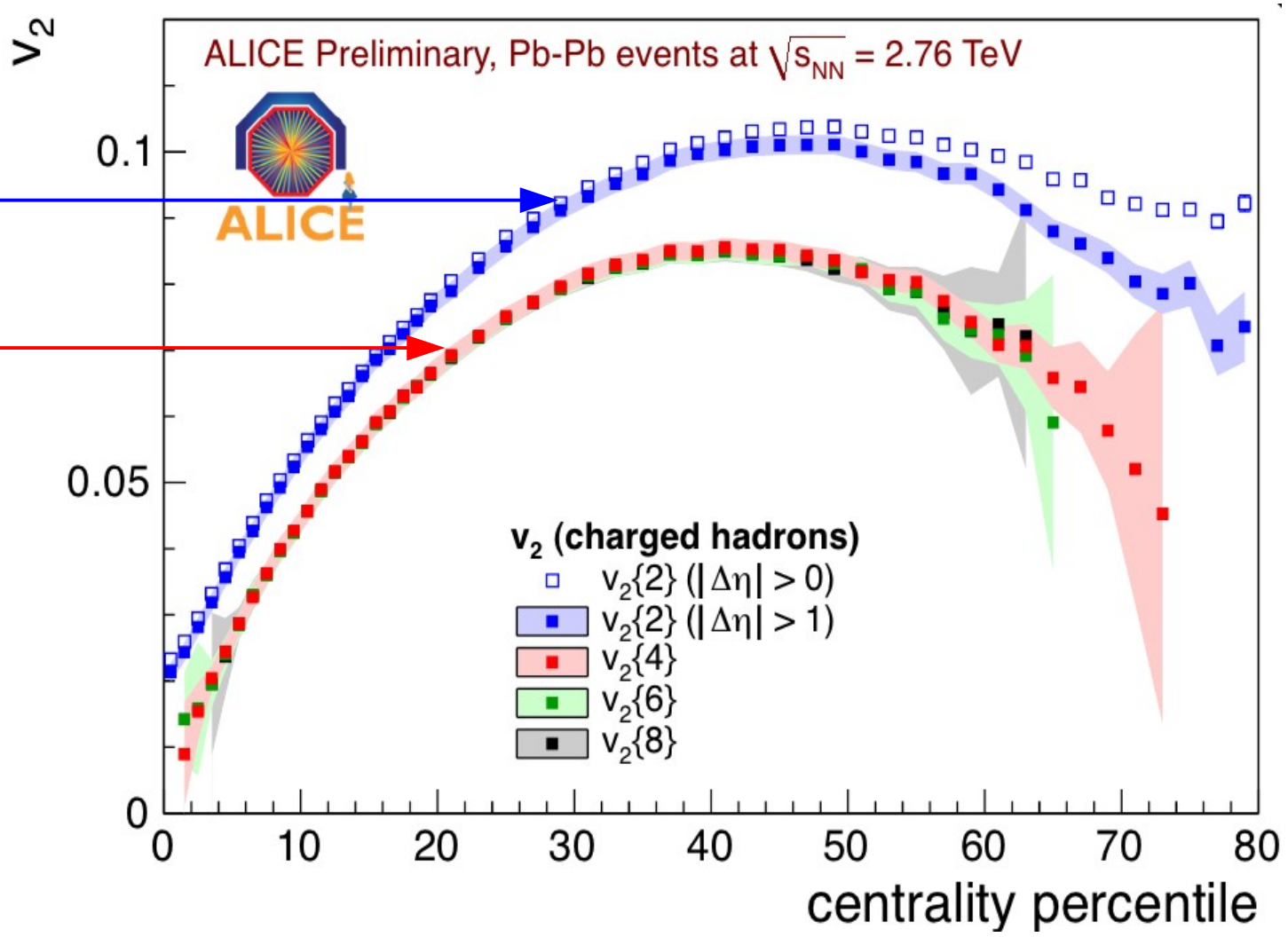

Multi-particle correlation v2{n} results converge for n≥4, indicating that non-flow contribution is negligible for n≥4

Beam energy scan at RHIC

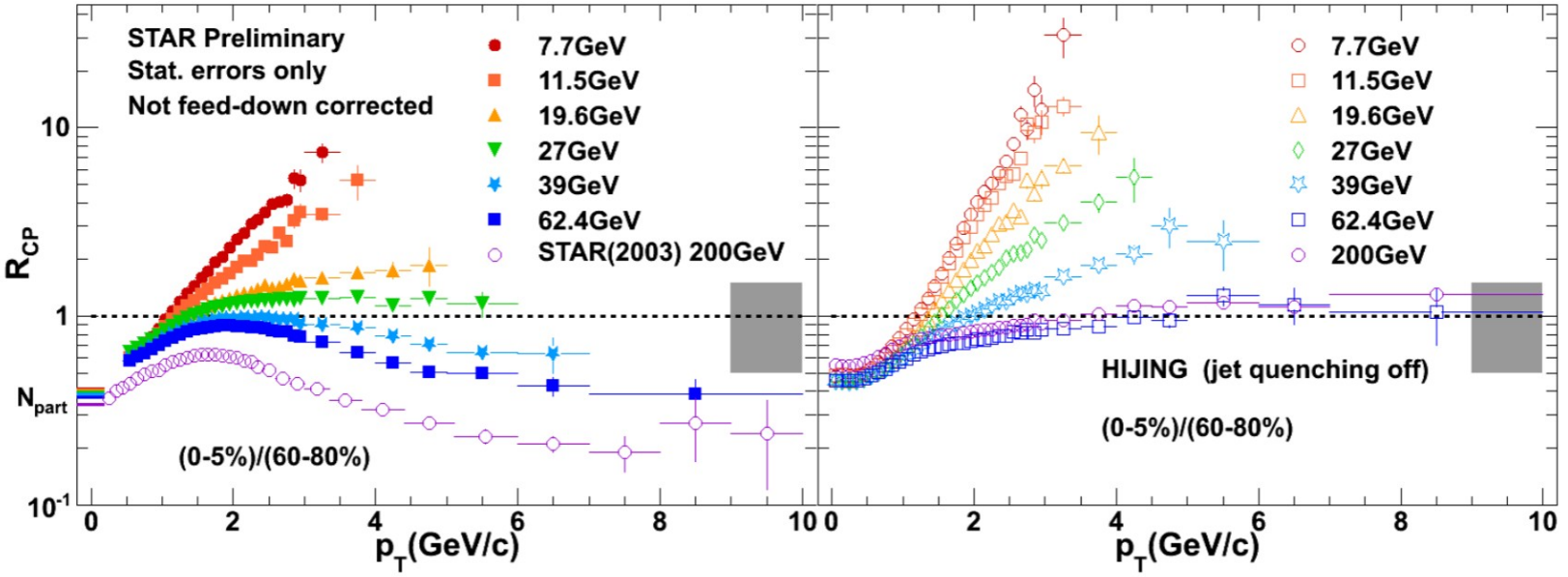

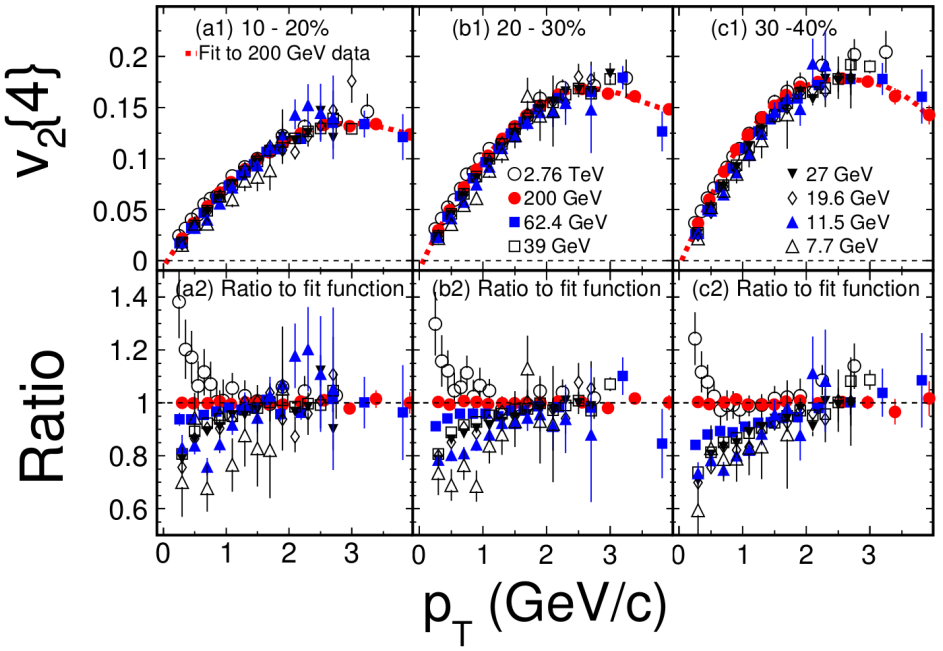

Ultra-central collisions

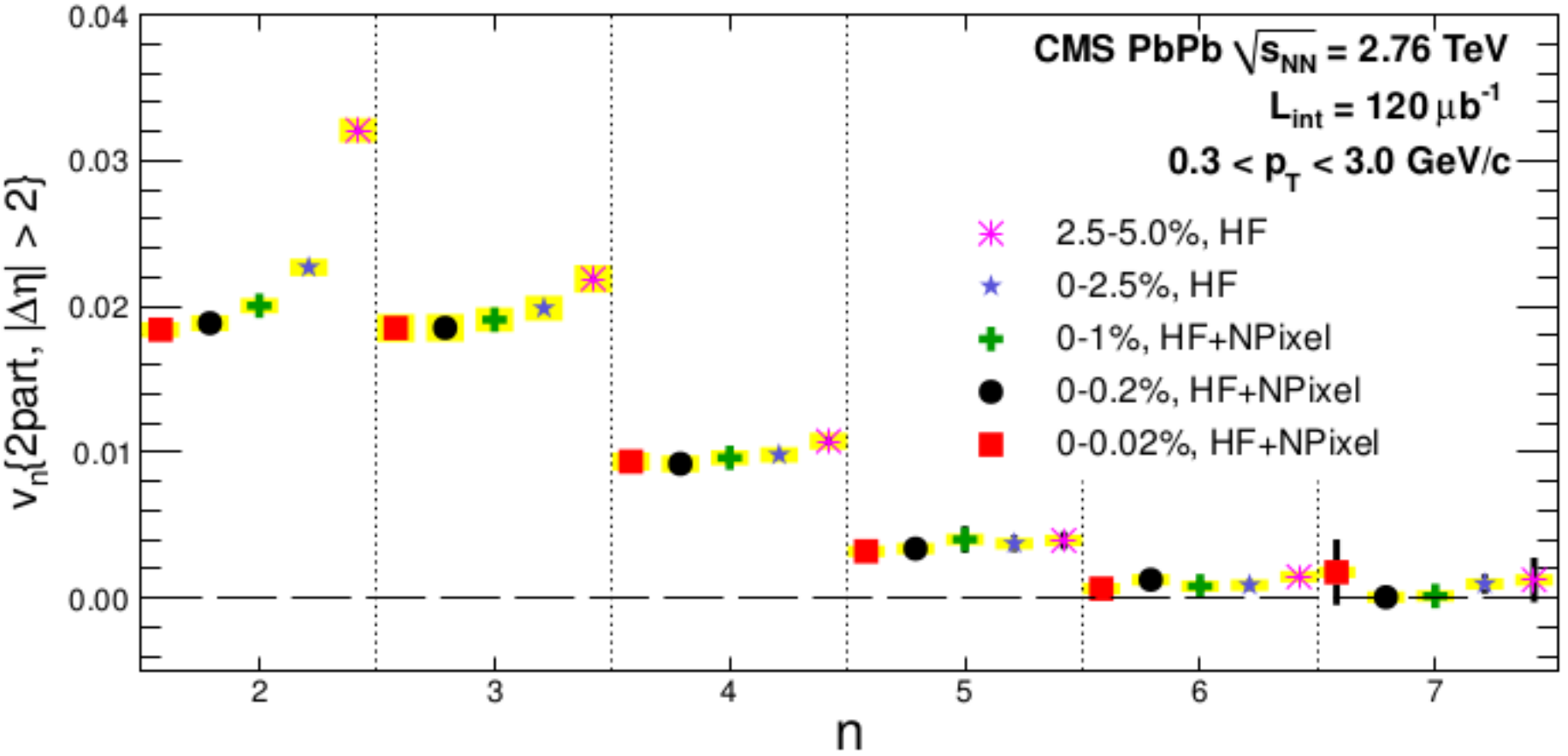

JHEP 02 (2014) 088

Comparison data and models

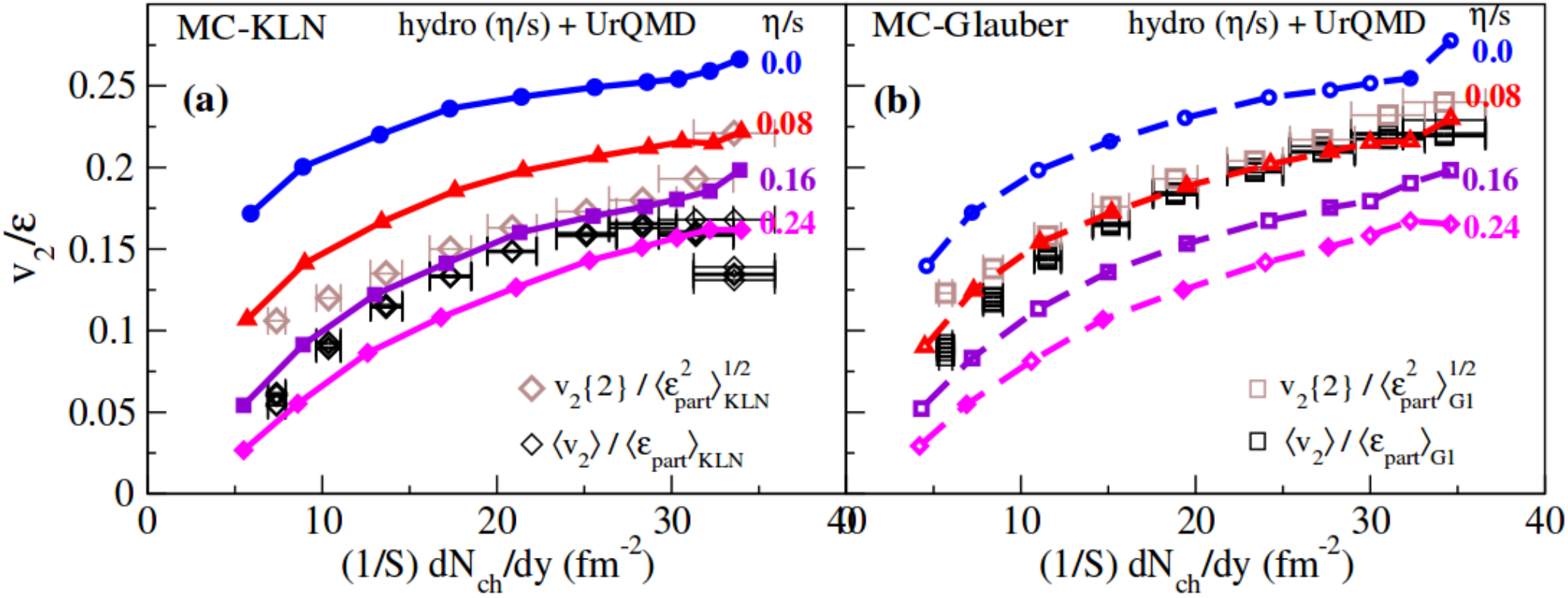

$$\frac{1}{4\pi} \leq \left[\frac{\eta}{s}\right]_{QGP} \leq 2.5 \times \frac{1}{4\pi}$$

(uncertainty dominated by assumptions about initial state)

Importance of initial state fluctuations

Standard Eccentricity

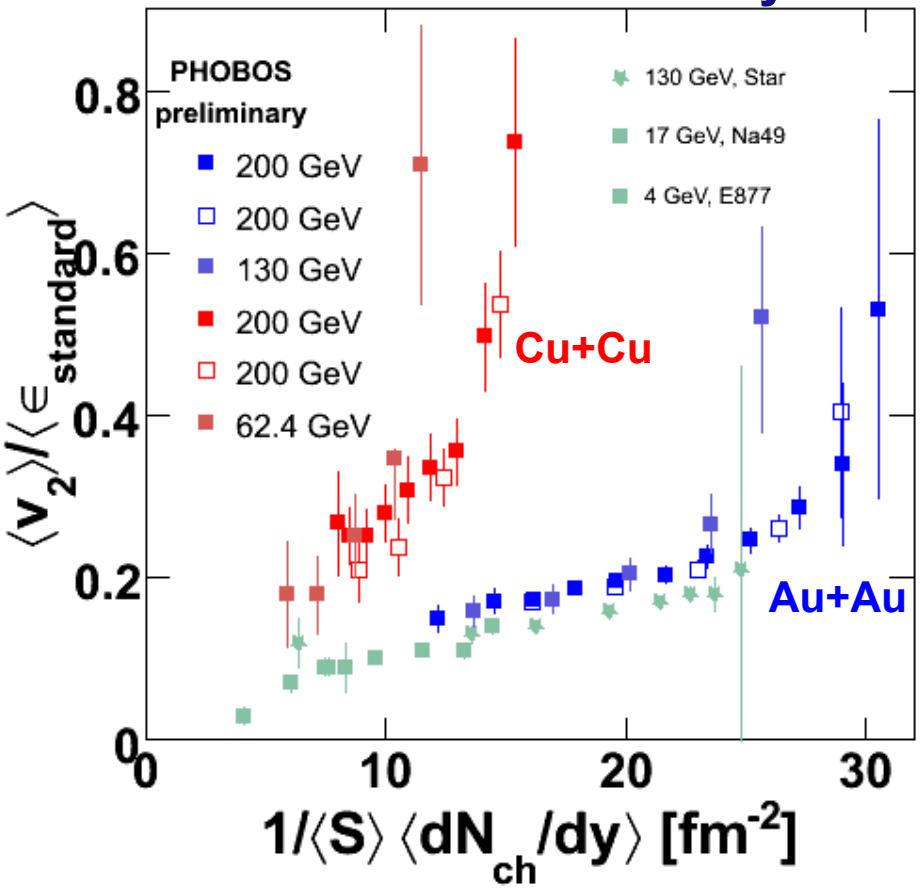

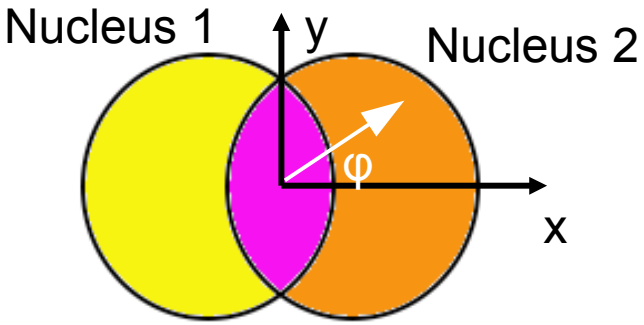

Participant Eccentricity

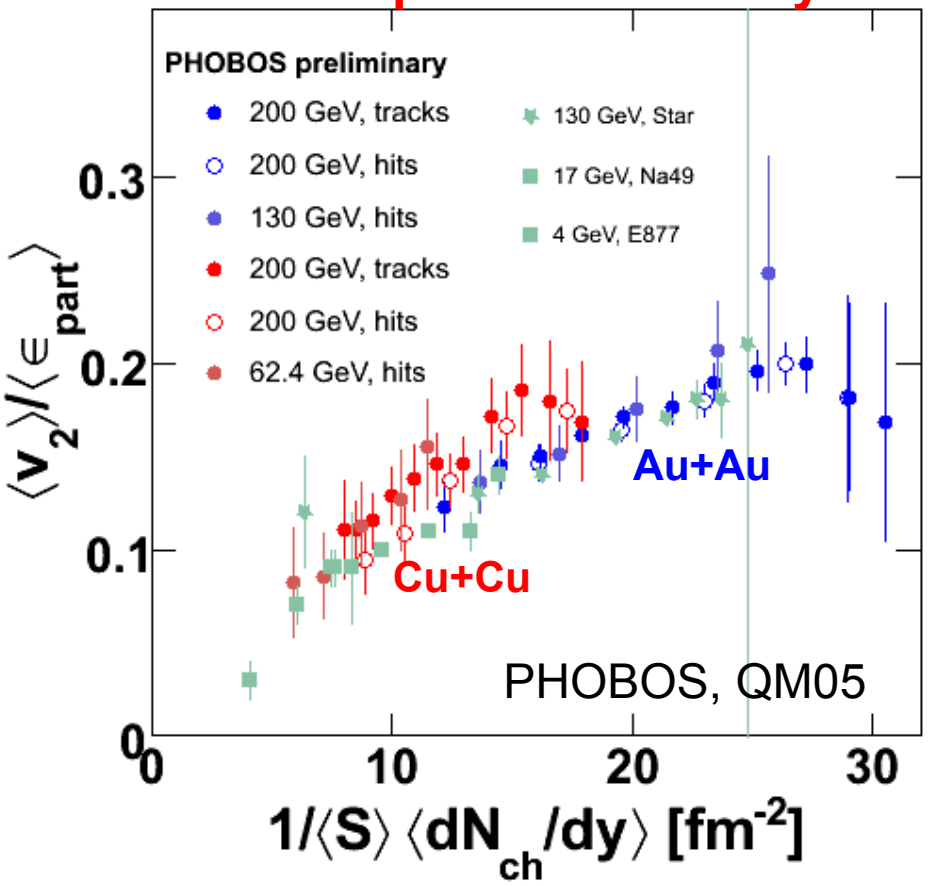

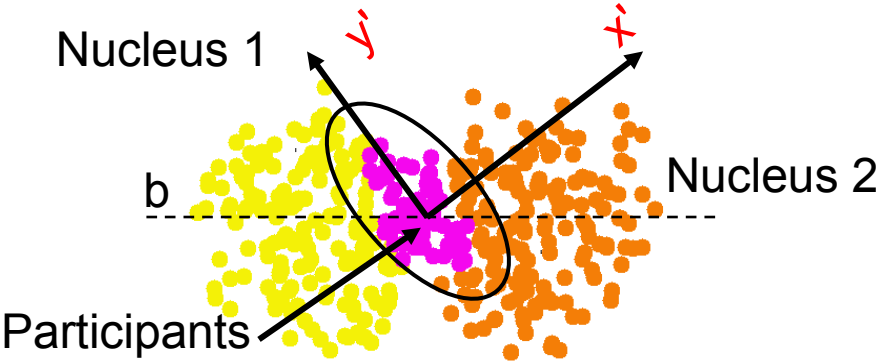

PHOBOS, PRL 98 (2007) 242302

Chemical freeze-out at LHC

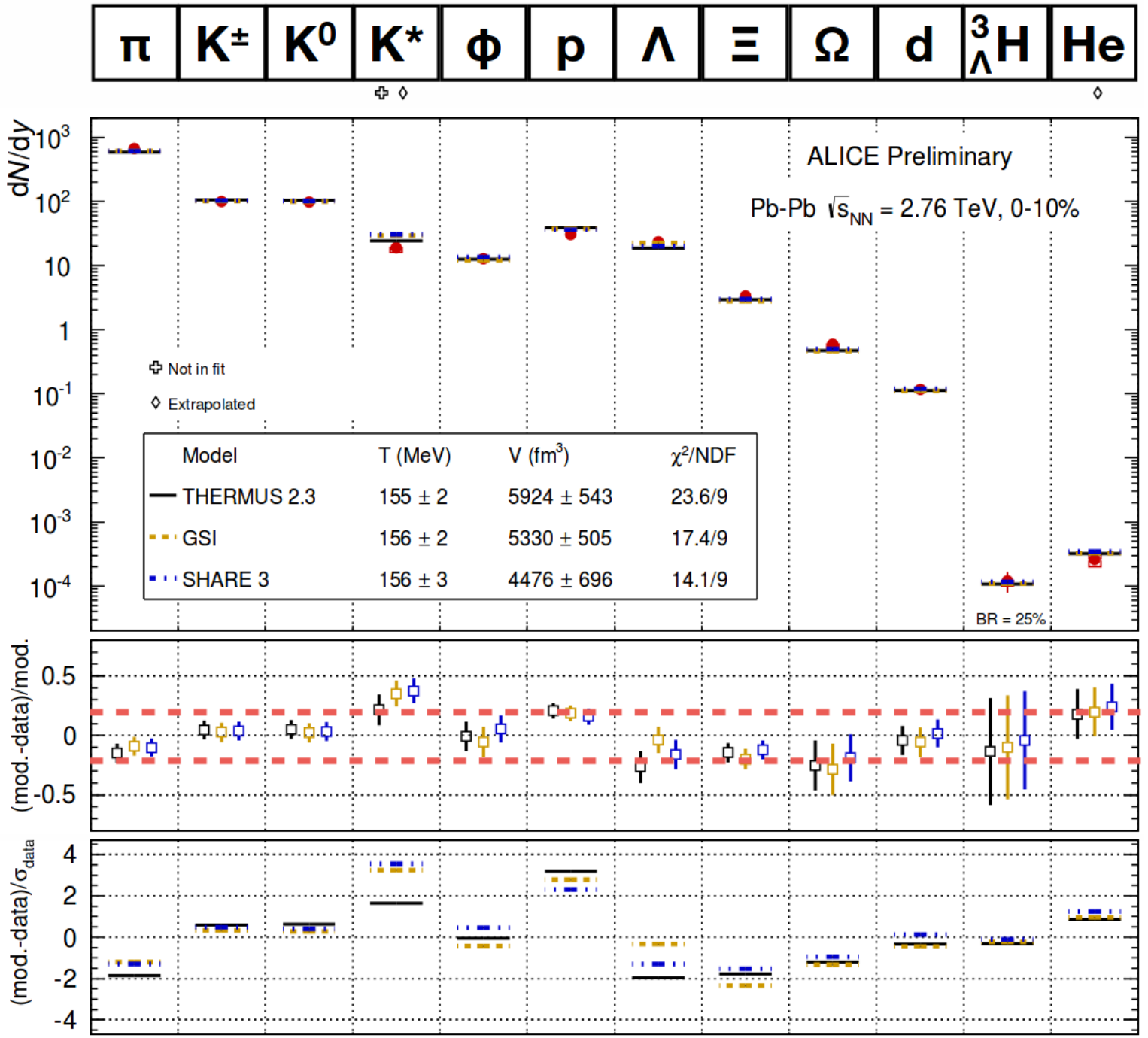

Transport parameter

PRC 90 (2014) 014909

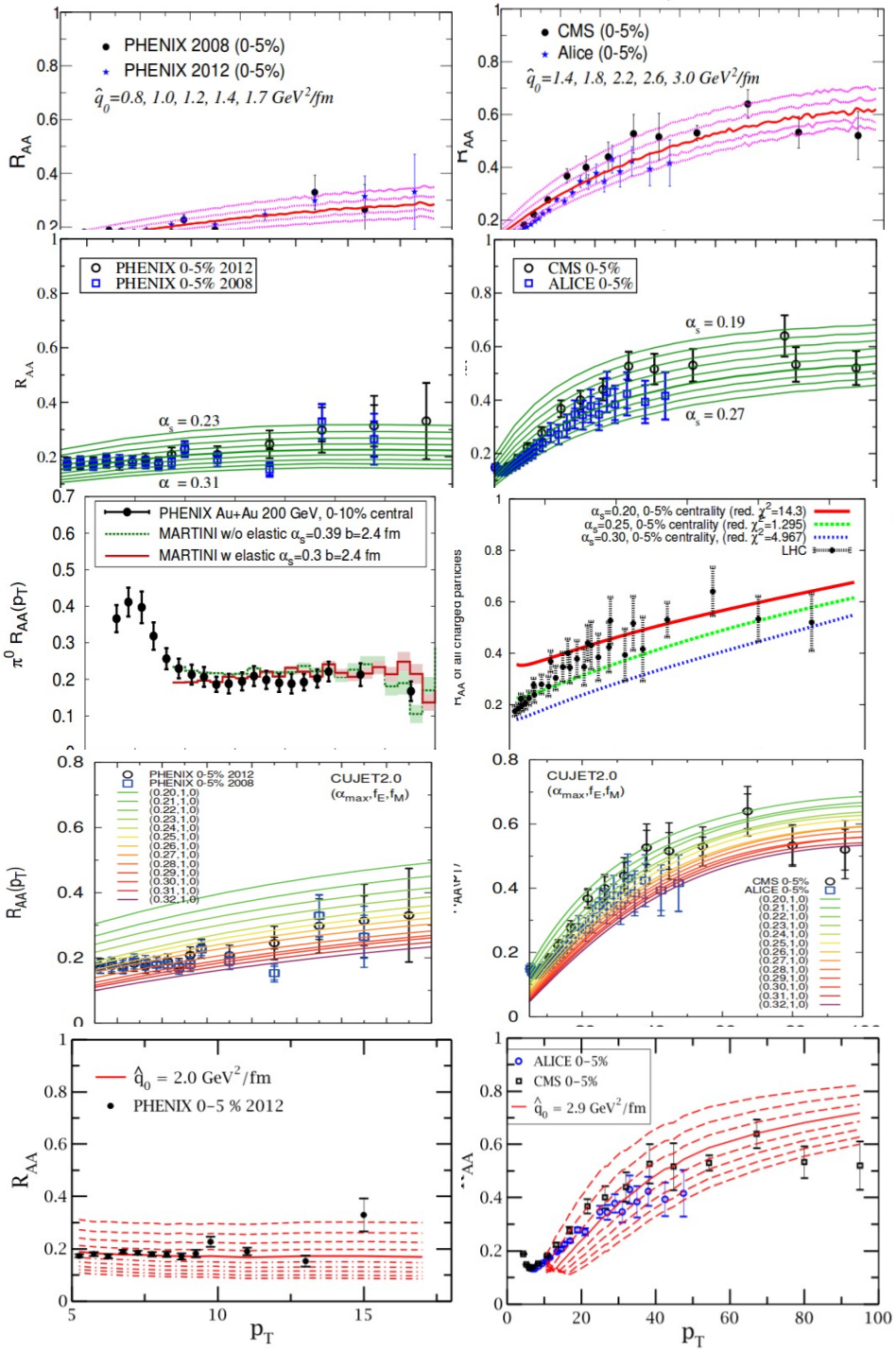

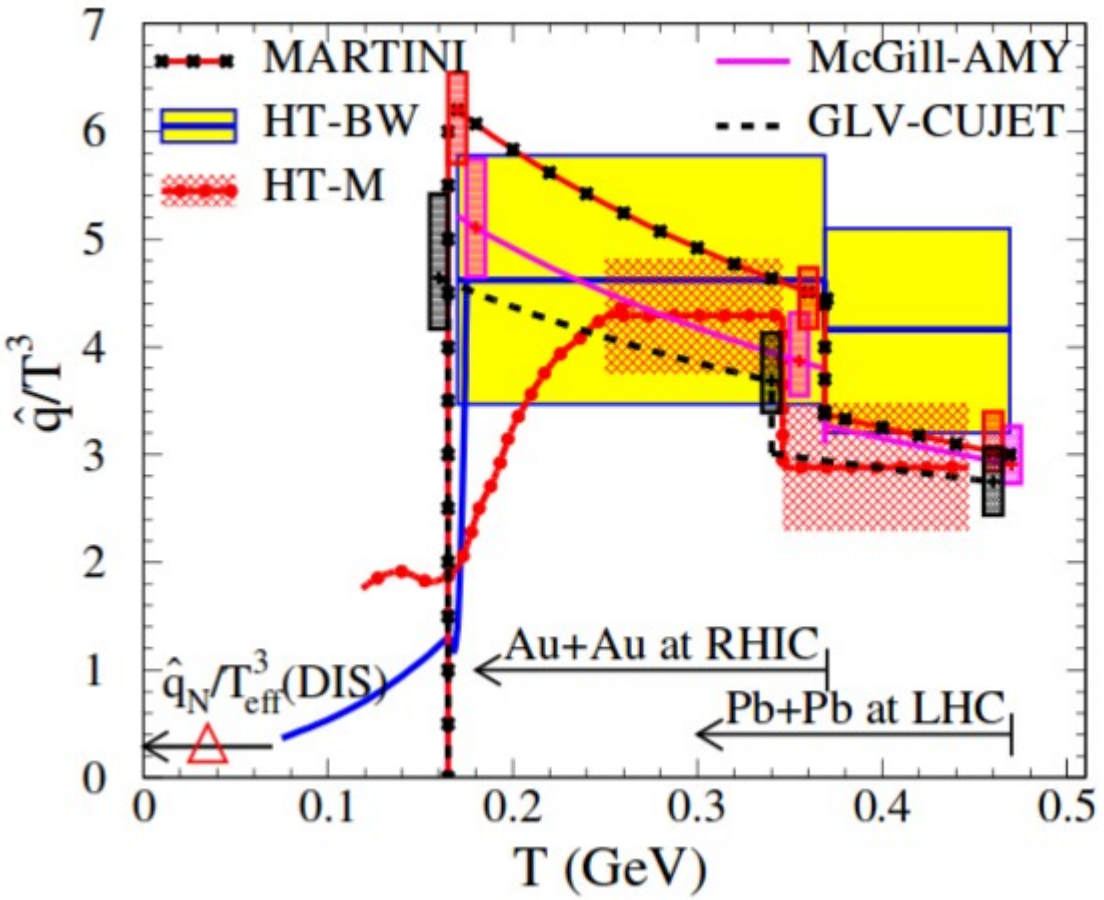

$$\frac{\hat{q}}{T^3} \approx \begin{cases} 4.6 \pm 1.2 & \text{at RHIC} \\ 3.7 \pm 1.4 & \text{at LHC} \end{cases}$$

$$\hat{q} \approx \begin{cases} 1.2 \pm 0.3 \\ 1.9 \pm 0.7 \end{cases} \text{GeV}^2/\text{fm at} \quad \begin{matrix} T = 370 \text{ MeV} \\ T = 470 \text{ MeV} \end{matrix}$$

(for quark jet with E=10 GeV initially)

Jet quenching: Dijet imbalance

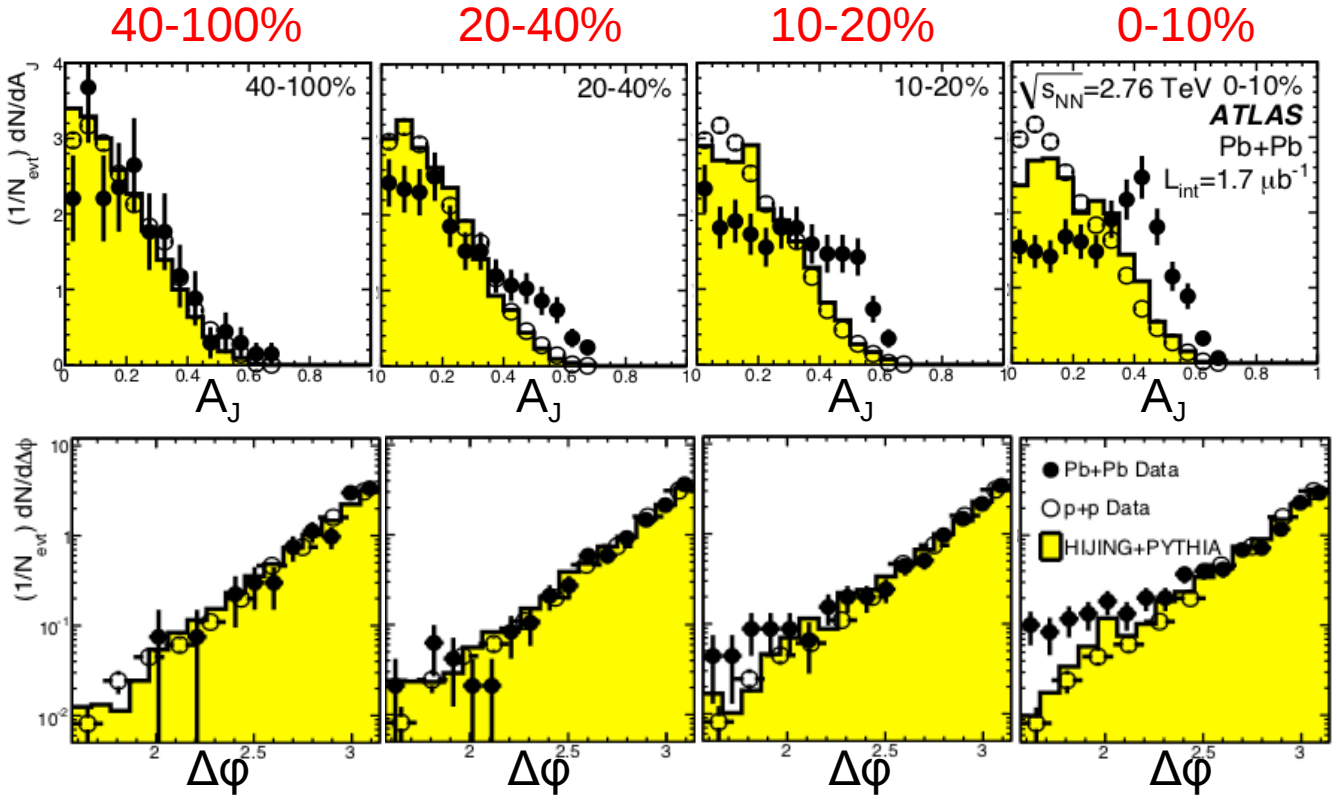

Momentum imbalance wrt to MC (pp) reference increases with increasing centrality.
No (or very little) azimuthal decorrelation.

ATLAS, PRL 105 (2010) 252303
CMS, PRC 84 (2011) 024906

$$A_{\mathrm{J}} = \frac{E_{\mathrm{T1}} - E_{\mathrm{T2}}}{E_{\mathrm{T1}} + E_{\mathrm{T2}}}, \quad \Delta\varphi_{12} > \frac{\pi}{2}$$

58 Track spectrum inside jets

CMS, PRC 90 (2014) 024908

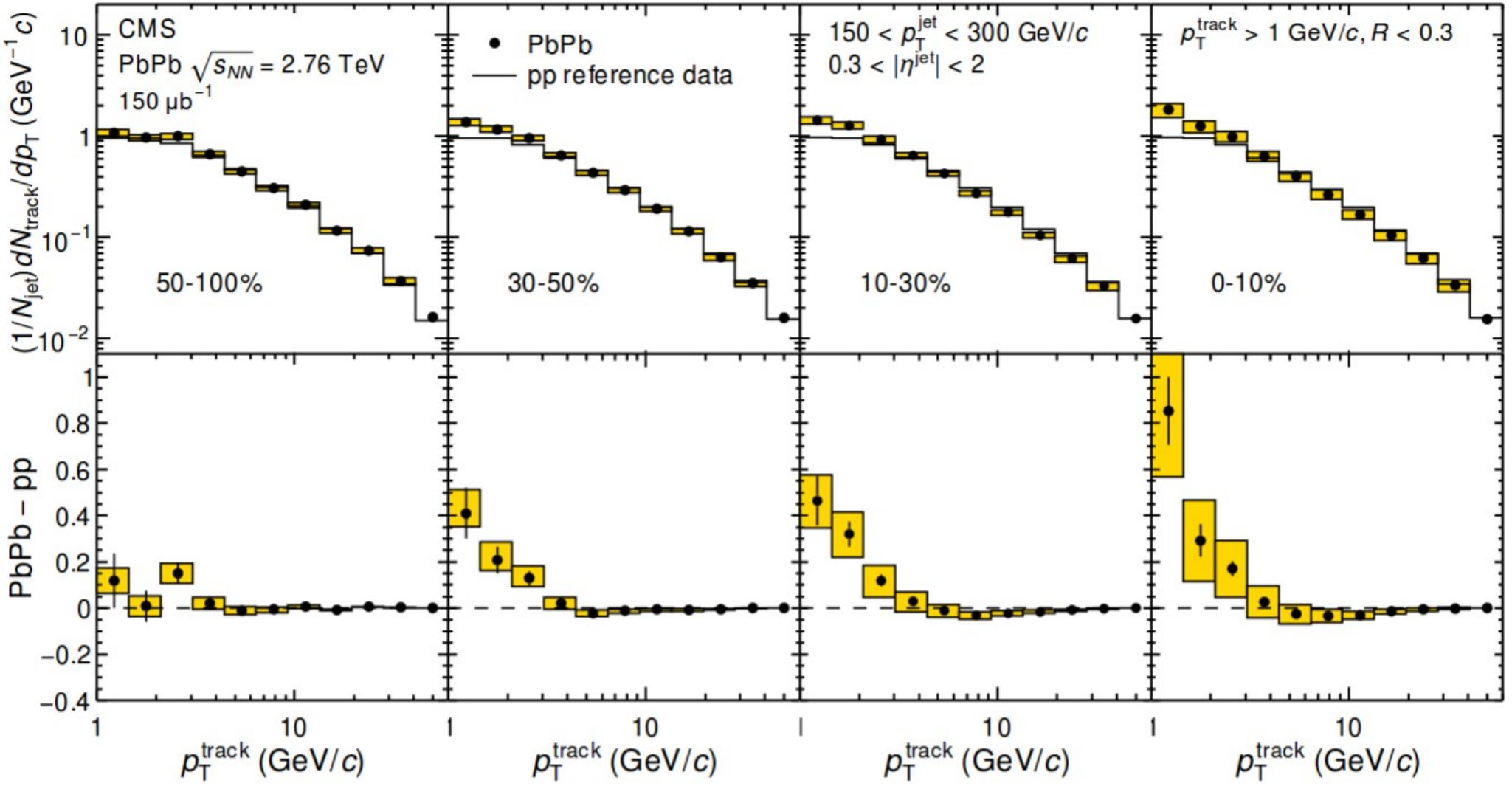

Comparison to prel. CMS

CMS-HIN-14-000

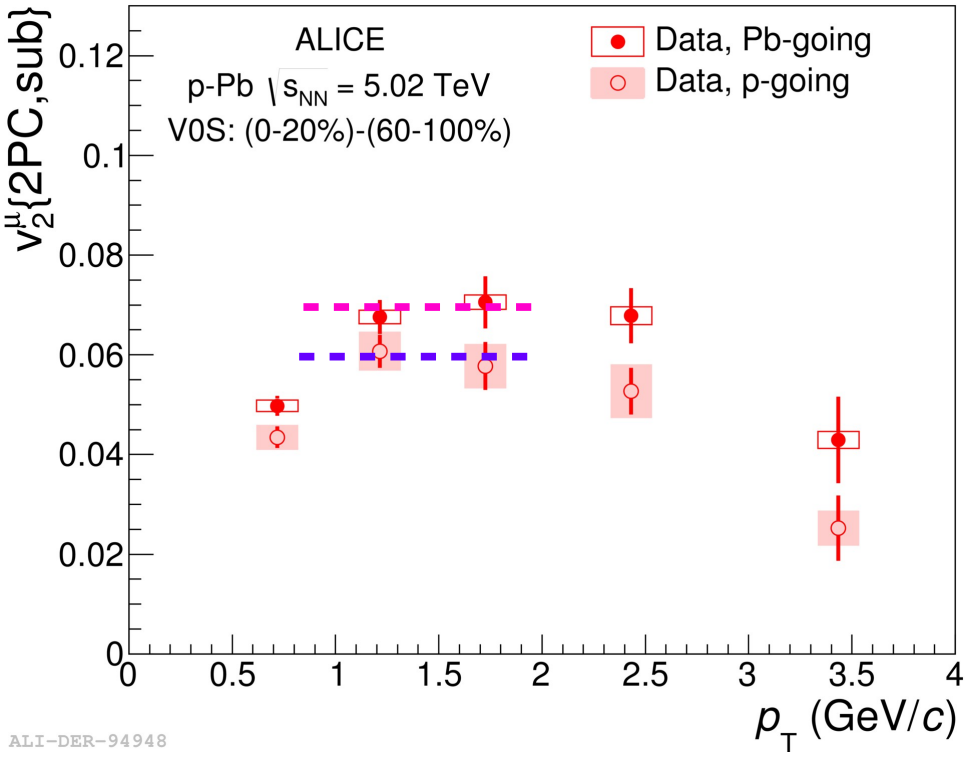

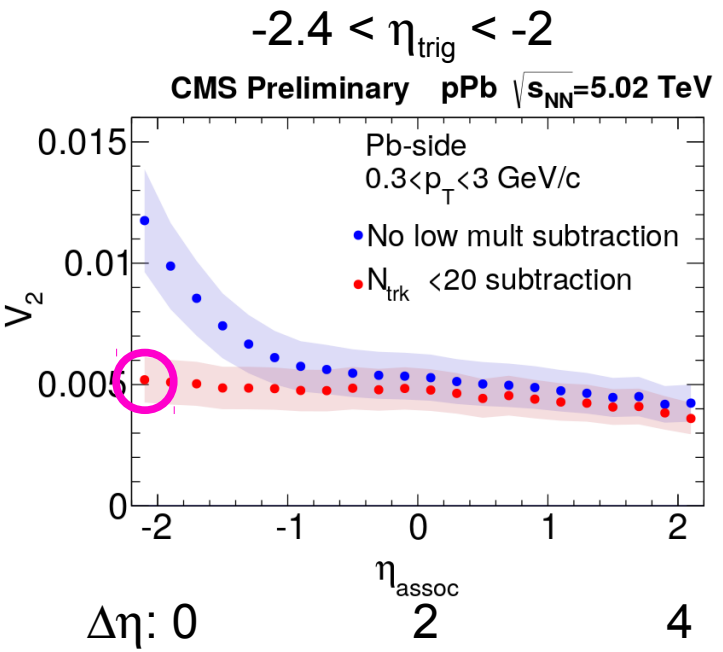

V_2=0.005

↓

v_2=0.07

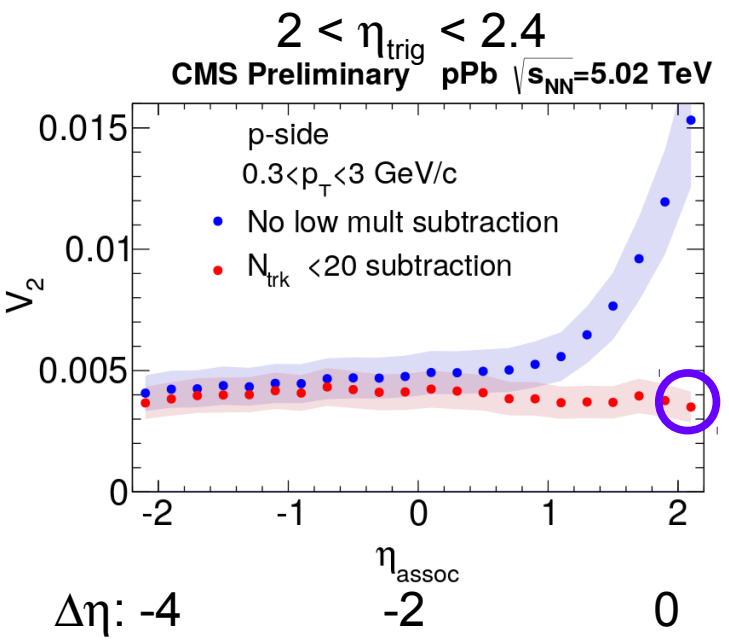

V_2=0.0035

↓

v_2=0.06

- Resulting coefficients
  - of similar magnitude
  - with same asymmetry
- Not apples-to-apples comparison
  - Muons vs charged particles
  - Kinematic ranges + event selection

Comparison with AMPT

ALICE, arXiv:1506.08032

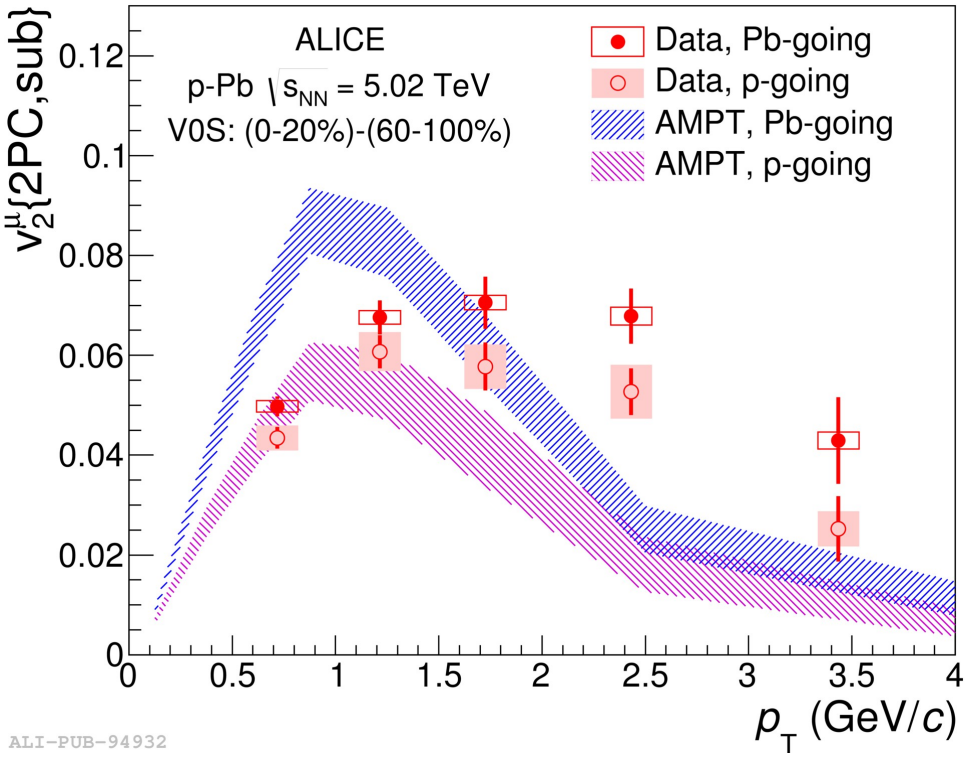

- AMPT (σ=3mb) at generator level, decay particles to muons, apply rel. efficiencies
- Mimic every aspect of the analysis as closely as possible
  - Event selection
  - Subtraction method
    - AMPT shows larger sensitivity than data to low-multiplicity class scaling (up to f=2)
- Find HF muon v_2 to be 0 in AMPT (using 5M events with HF muon in acceptance for each beam direction)
  - Set it to 0 in the final results to reduce statistical fluctuations

Comparison with Pb-Pb

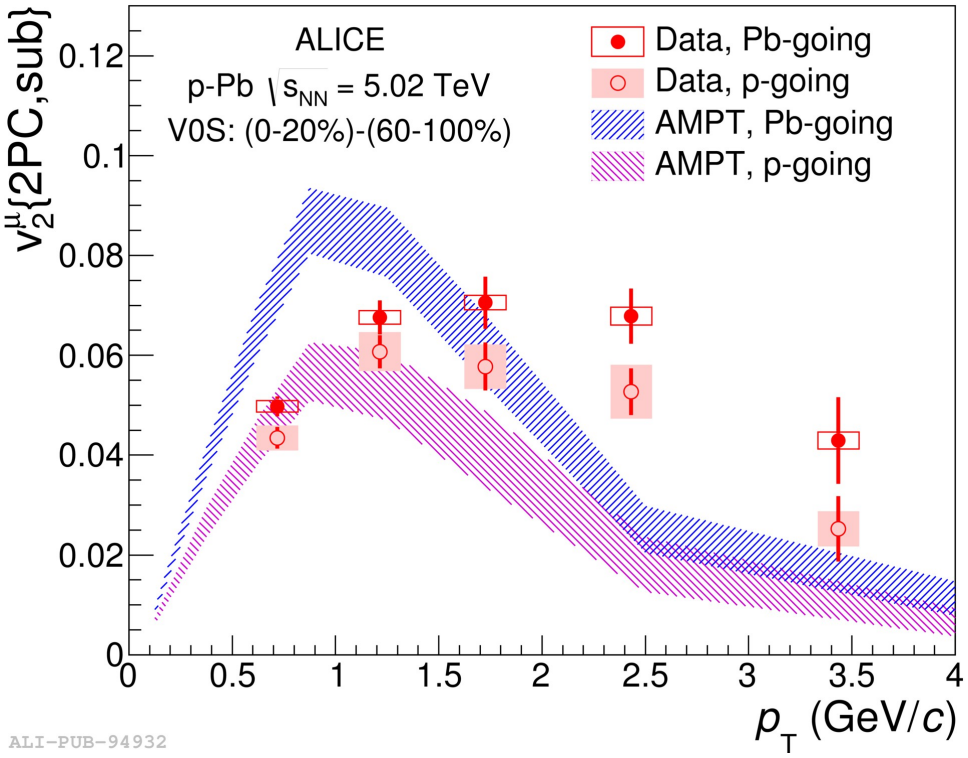

ALICE, arXiv:1507.03134

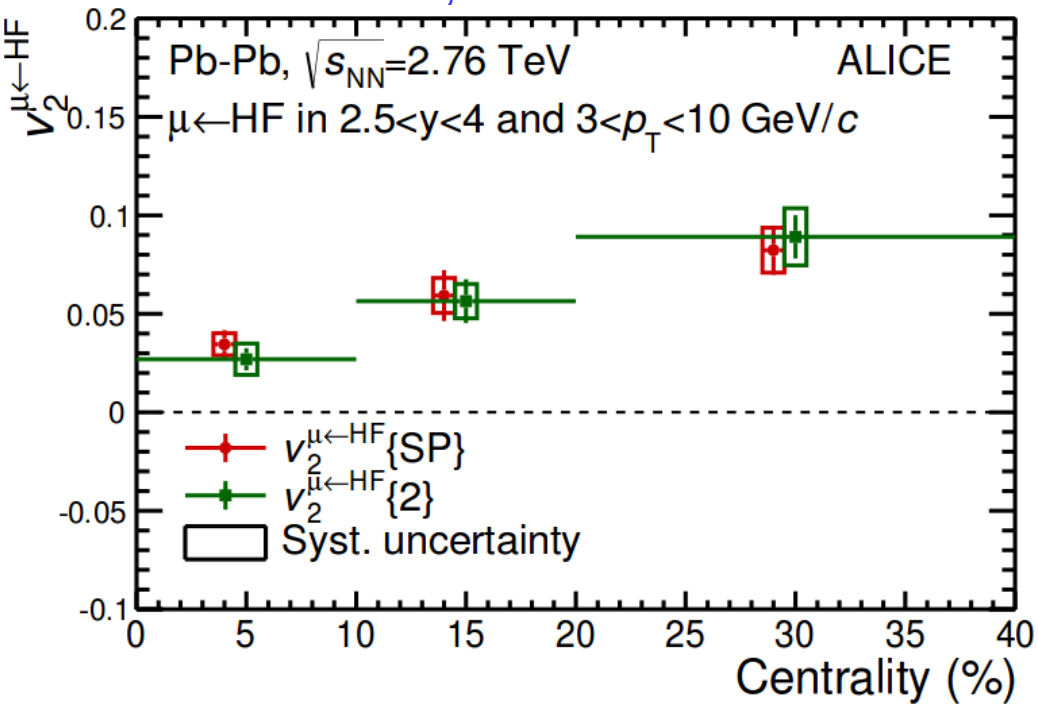

- At low p_T (<1.5 GeV/c), the calculation roughly describes the p-going, but overpredicts the Pb-going case
- At higher p_T, different trends for both beam directions
- Possible scenario
  - Drastically different relative parent composition in AMPT vs data
  - Finite value of v_2 for muons from HF decay (observed in Pb-Pb)

Factorization of v_2 in p-Pb

CMS, arXiv:1503.01692

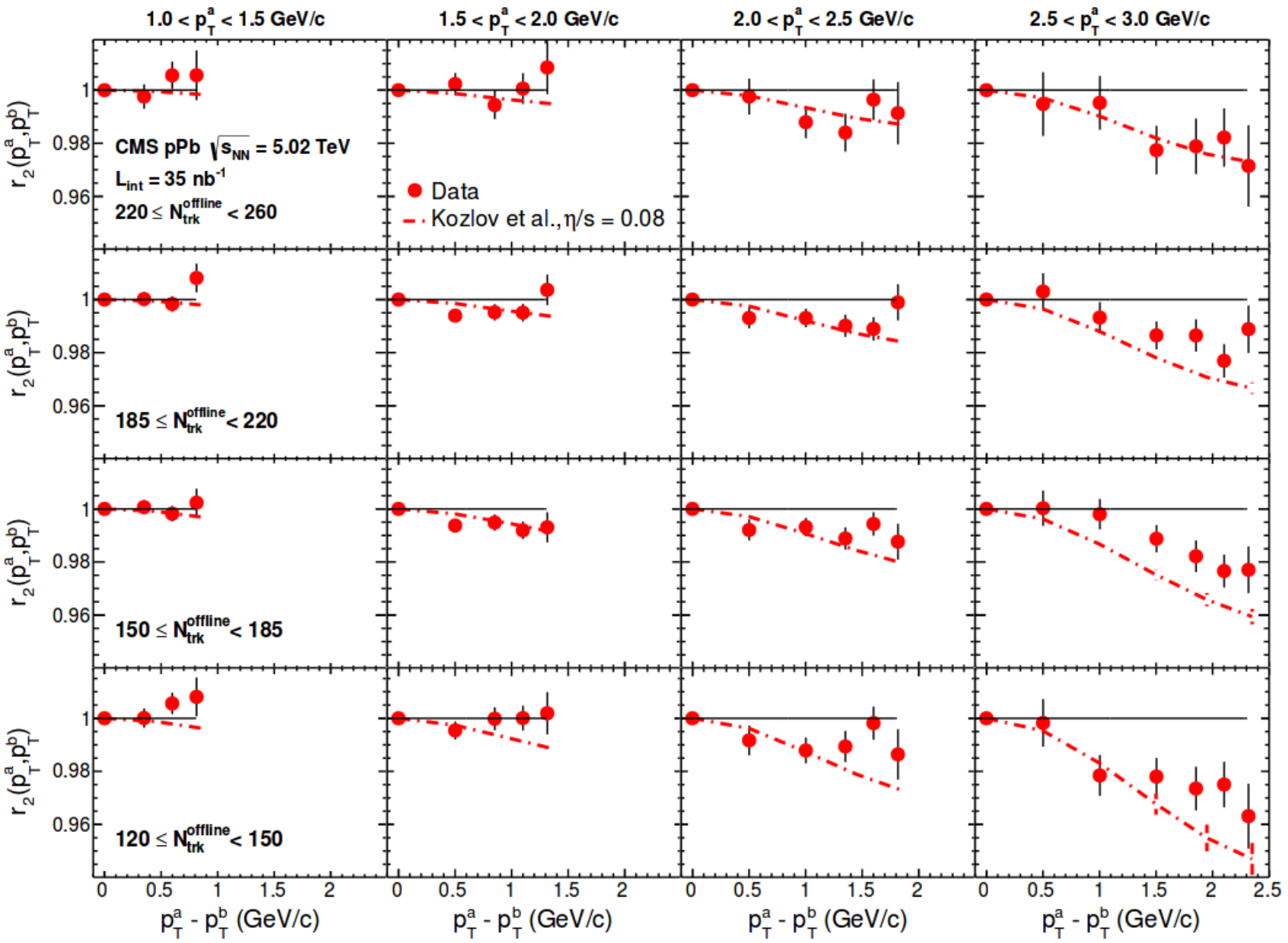

Associated yields

ALICE, arXiv:1406.5463

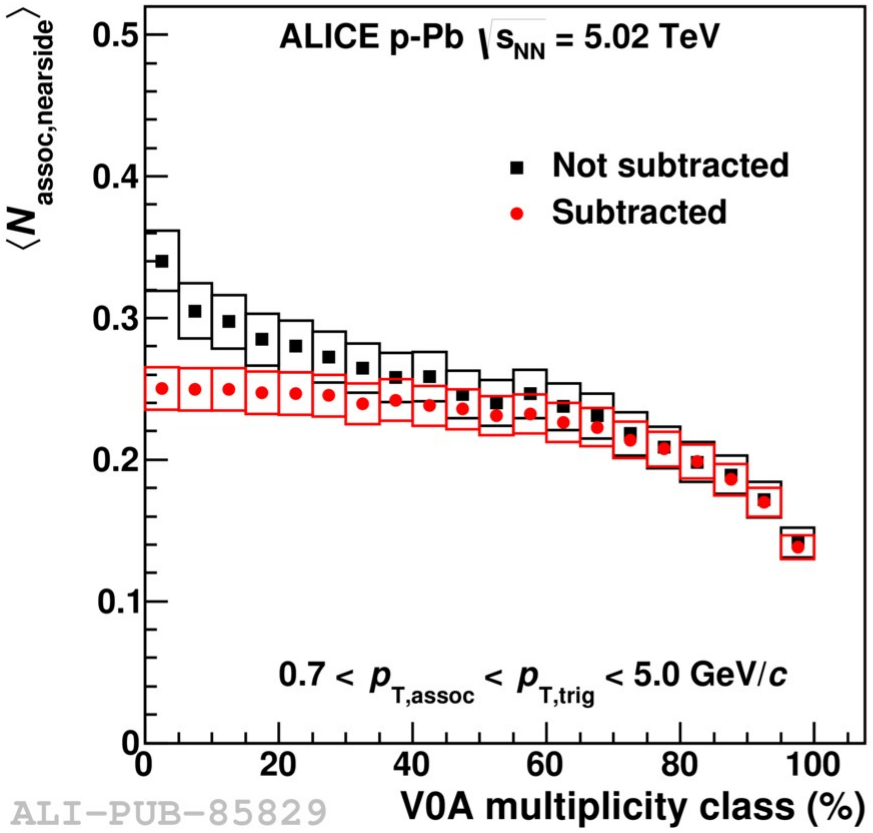

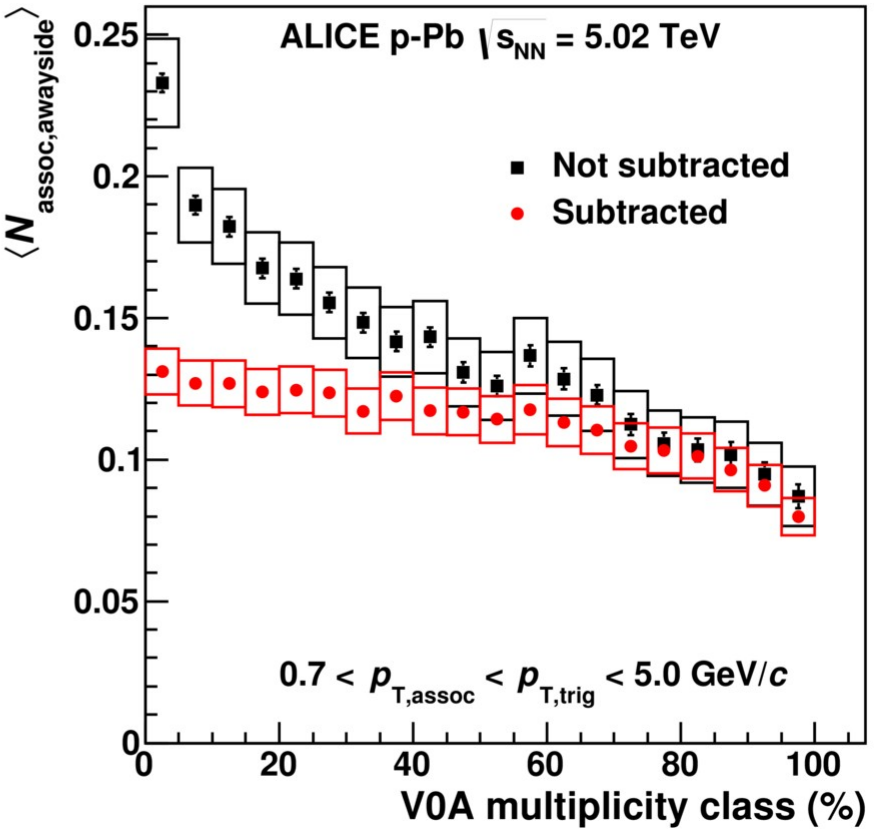

Associated yields after long range subtraction are smaller for lower multiplicity classes

64 Charged particle R_{pPb}

$$R_{AB} = \frac{\mathrm{d}N_{AB}/\mathrm{d}p_{\mathrm{T}}}{\langle N_{\mathrm{coll}}\rangle \mathrm{d}N_{\mathrm{pp}}/\mathrm{d}p_{\mathrm{T}}}$$

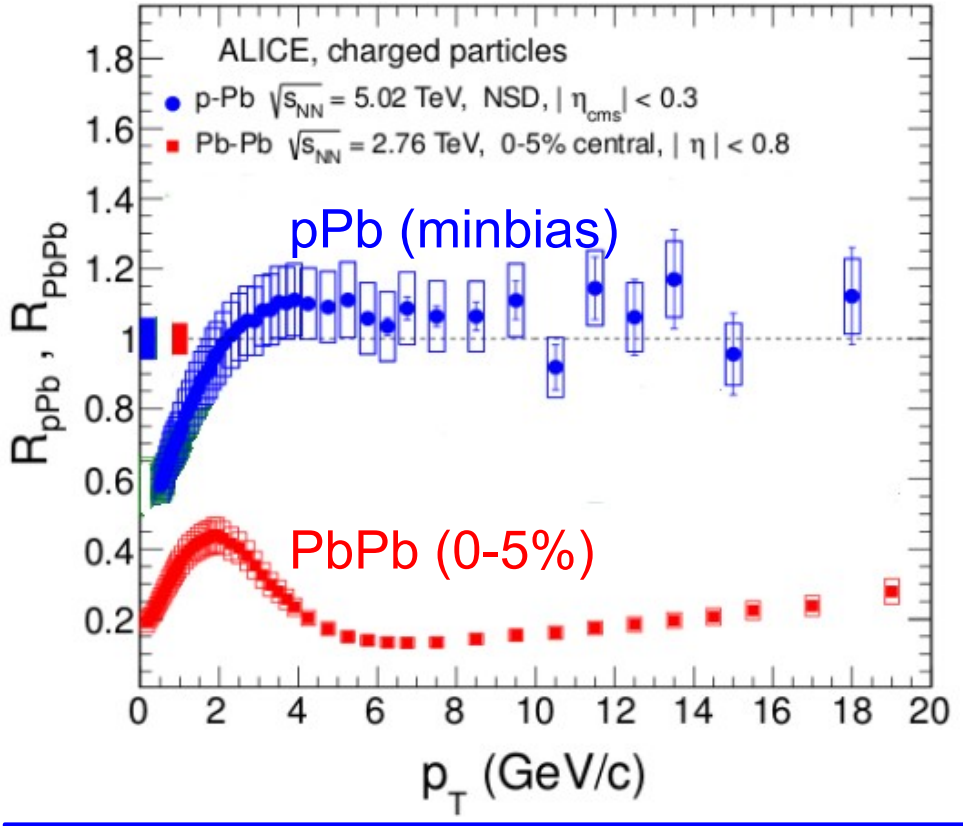

ALICE, PRL 110 (2013) 082302

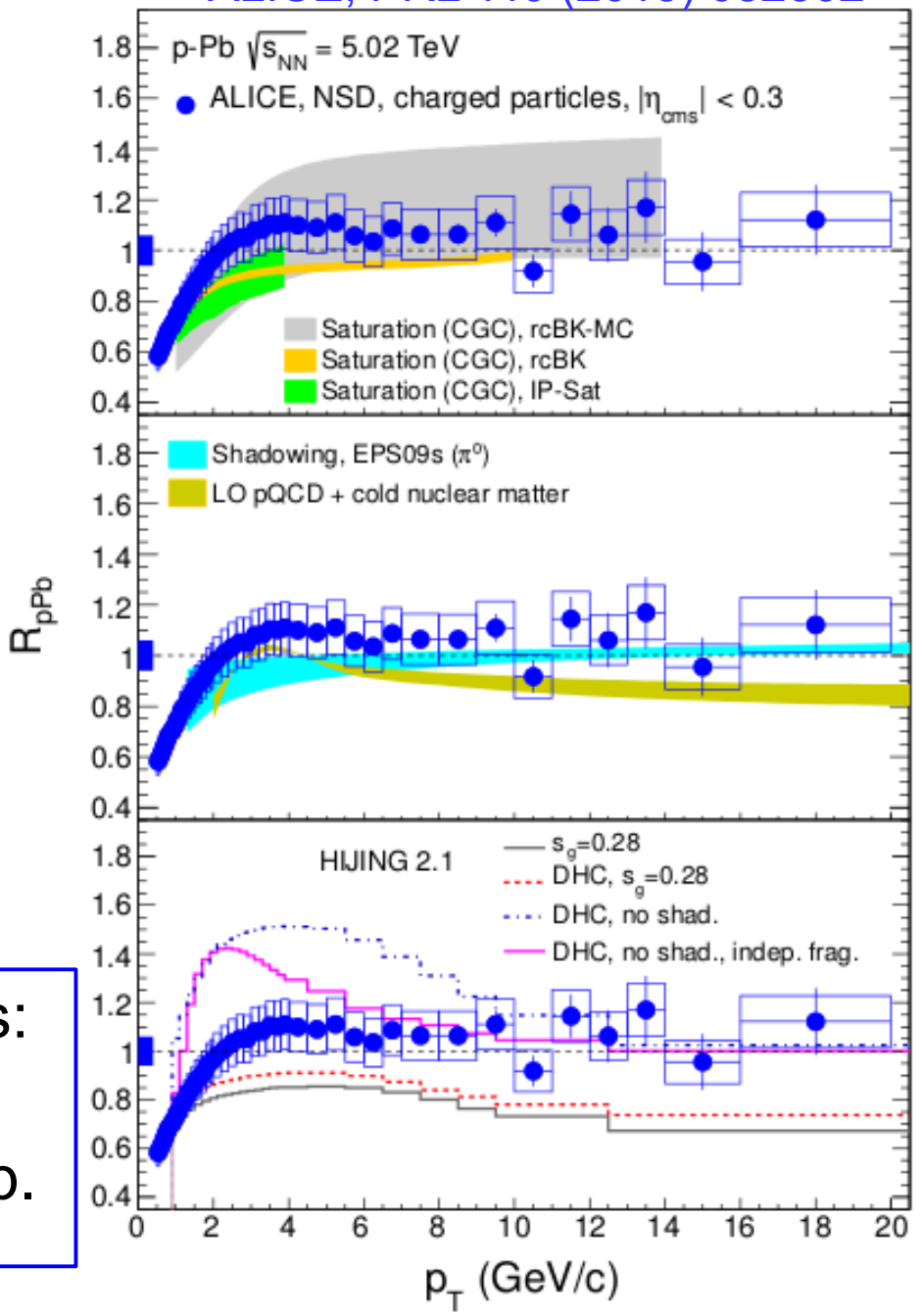

No surprises at high p_T in first results:

Supports existence of strong final state effects (at mid-rapidity) in PbPb.

65 QpPb

arXiv:1412.6828

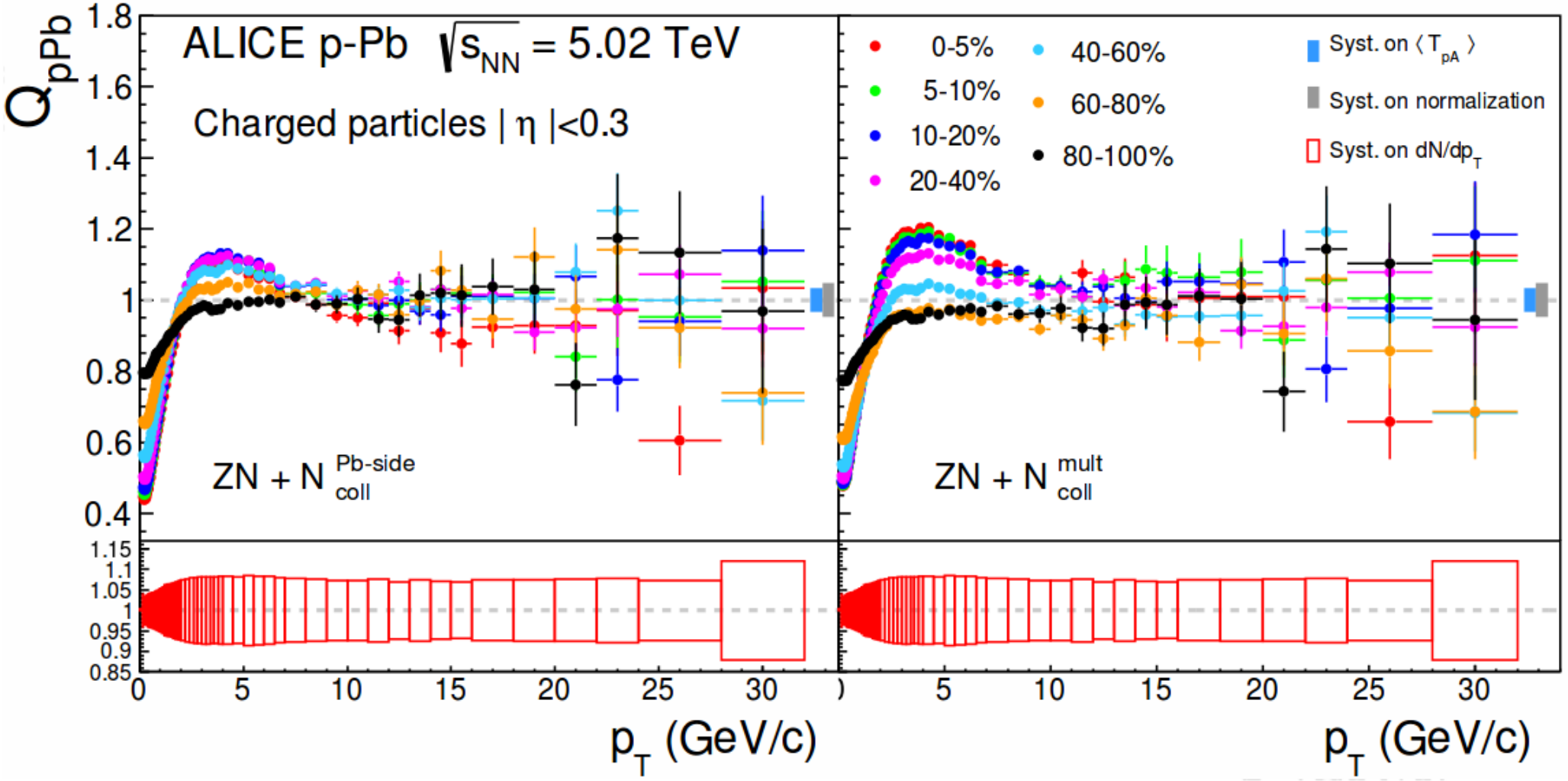

66 QpPb

arXiv:1412.6828

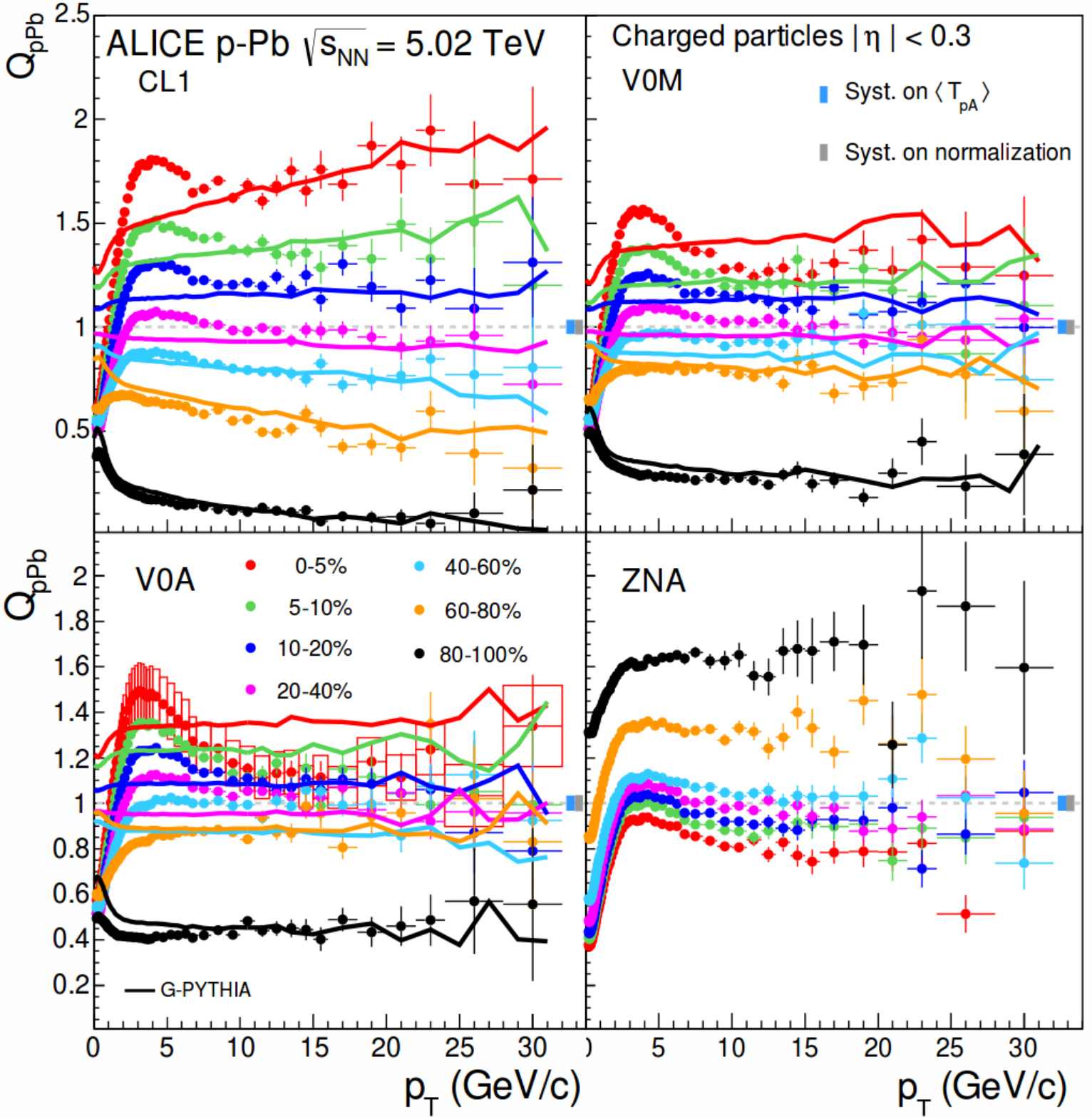

Heavy-flavor electron ridge

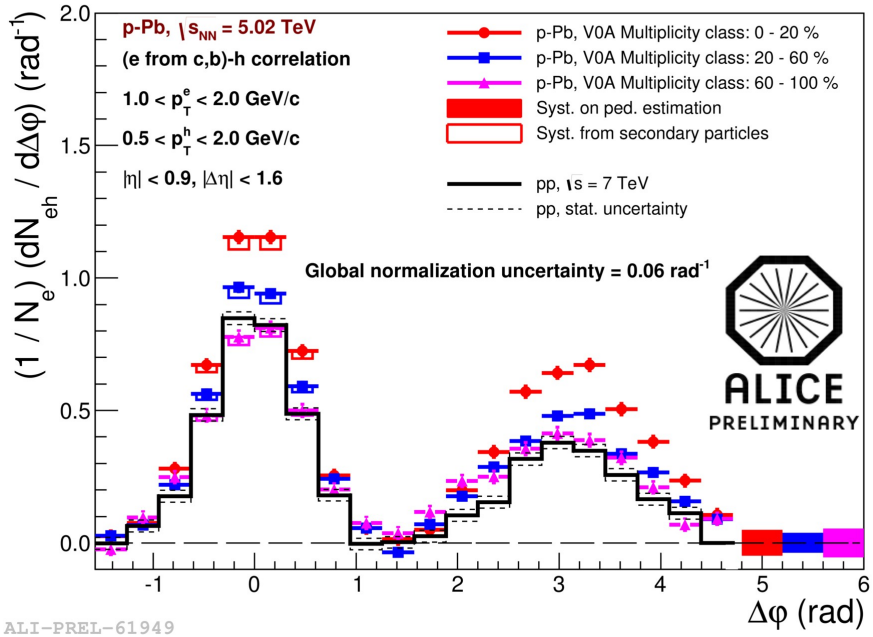

ALI-PREL-61949

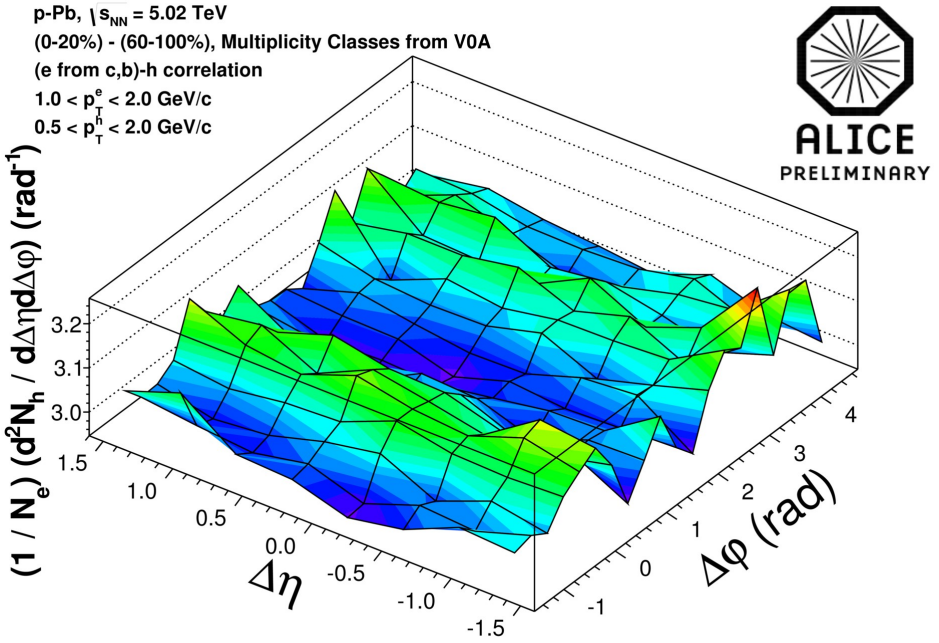

ALI-PREL-62026

At mid-rapidity, double ridge for electrons from HF decays observed

AMPT describes data quite well (example)

arXiv:1406.2804